

3 1293 10421 9310



This is to certify that the

thesis entitled

STUDY OF DIFFUSION OF POLYDISPERSE POLYSTYRENE AND STYRENE-ACRYLONITRILE COPOLYMERS IN SOLUTION BY LIGHT BEATING SPECTROSCOPY AND INTERFEROMETRY

presented by

P. V. S. R. Krishnam Raju

has been accepted towards fulfillment of the requirements for

Ph. D. __degree in _____ Chemical Engineering

Major professor

Date May 10, 1978

O-7639

STUDY OF DIFFUSION OF POLYDISPERSE POLYSTYRENE AND STYRENE-ACRYLONITRILE COPOLYMERS IN SOLUTION BY LIGHT BEATING SPECTROSCOPY AND INTERFEROMETRY

Ву

P. V. S. R. Krishnam Raju

A DISSERTATION

Submitted to
Michigan State University
in partial fulfillment of the requirements
for the degree of

DOCTOR OF PHILOSOPHY

Department of Chemical Engineering

ABSTRACT

STUDY OF DIFFUSION OF POLYDISPERSE POLYSTYRENE AND STYRENE-ACRYLONITRILE COPOLYMERS IN SOLUTION BY LIGHT BEATING SPECTROSCOPY AND INTERFEROMETRY

Bv

P. V. S. R. Krishnam Raju

A systematic study was made of diffusion in dilute and moderately concentrated solutions of polystyrene in benzene and decalin, and styrene-acrylonitrile copolymer in dimethyl formamide, methyl ethyl ketone and benzene. Diffusion data were obtained at ambient temperature in the concentration range of 0.01 to 10% by weight of polymer. Studies were made with polydisperse polystyrene samples having weight average molecular weights in the range of 38,000 to 350,000 and for polydisperse styrene-acrylonitrile copolymer samples having weight average molecular weights in the range of 200,000 to 800,000. The styrene-acrylonitrile copolymers of azeotropic composition, 24% by weight of acrylonitrile, were synthesized by free radical polymerization. Translational diffusion coefficients were obtained using a laser homodyne spectrometer in dilute polymer solutions and using an interferometric method in moderately concentrated polymer solutions. An expression was derived for the relationship between the experimental average diffusion coefficient obtained from the interferometer and the

distribution of diffusion coefficients for the individual species of a polydisperse polymer.

The concentration dependence of the diffusion coefficient is linear over the entire concentration range investigated by both these experimental methods. The data are fit with an equation of the form $D = D_o(1 + k_dc)$. The value of k_d is always positive in good solvents. In other solvents the value of k_d is negative at low molecular weights and positive at high molecular weights. Observed values of D_o are 1 to $7x10^{-7}$ cm²/sec.

Data obtained in this work are compared with available theoretical treatments for diffusion in monodisperse homopolymer solutions. A semi-empirical relation, based upon a modification of the Kirkwood-Riseman approach, is proposed for describing diffusion in infinitely dilute polymer solutions, and is tested against data from this work and from the literature. The observed diffusional behavior can be explained for all the polymer-solvent pairs investigated in this work using the modified Kirkwood-Riseman expression for $\mathbf{D}_{\mathbf{O}}$ and a method of Duda and Vrentas for evaluating $\mathbf{k}_{\mathbf{d}}$. The difference in the numerical values of the diffusion coefficients obtained for a polydisperse polymer-solvent pair from interferometry and from light beating spectroscopy, in the concentration range where the two methods overlap, can be explained by the influence of polydispersity on the results of each method.

Dedicated to my parents.

ACKNOWLEDGMENTS

The author would like to express his deep appreciation to his major professor, Dr. Robert F. Blanks, for his constant guidance and assistance throughout the course of this work, and also for his painstaking review of the manuscript. Gratitude is expressed to Dr. Jack B. Kinsinger and Dr. Donald K. Anderson for their generous guidance and active help in performing the experiments. Thanks are also due to Dr. Martin C. Hawley for his participation in this work. Special thanks are due to Dr. Thomas V. Atkinson for help with the computer interfacing.

The author is greatly indebted to the Department of Chemical Engineering and the Division of Engineering Research for providing financial support during his graduate work.

Sincere gratitude is due to my parents for their moral support and encouragement throughout my graduate studies. Special thanks are expressed to my wife, Udaya, for providing encouragement and for her patience while I spent countless hours on this work.

TABLE OF CONTENTS

		Page
LIST OF	TABLES	. vii
LIST OF	FIGURES	. ix
Chapter		
I.	INTRODUCTION	. 1
II.	SCOPE	. 4
	Objectives of the Research	. 4 . 4 . 7 . 8
III.	THEORY OF DIFFUSION IN POLYMER SOLUTIONS	. 16
	Diffusion in Infinitely Dilute Polymer Solutions Kirkwood-Riseman Theory	. 17 . 19 . 25 . 31
	Polymer Solutions	. 35 . 40 . 43
IV.	POLYMERIZATION AND FRACTIONATION	. 52
	Copolymerization Theory Rate of Copolymerization Chemically-Controlled Termination Diffusion-Controlled Termination Synthesis of Copolymers Initiator Monomers	. 52 . 54 . 55 . 56 . 56 . 57 . 58
	Polymerizations	. 59

Chapter	Р	age
	Fractionation of Copolymers	59
	Small-Scale Fractionations	62
	Large-Scale Fractionations	64
٧.	EXPERIMENTAL METHODS FOR MEASURING DIFFUSION	67
	COEFFICIENTS	67
	Light Beating Spectroscopy	67
	Background	67
	Theory	73
	Beat Frequency	73
	Theory of Brownian Motion	75
	Application to Polymer Solutions	77
	Evnonimental Apparatus	84
	Experimental Apparatus	88
	Computer Interfacing of the Averager	
	Procedure for Experimental Run	99
		101
	Calibration	105
	Calibration	107
	Error Analysis	110
		111
		111
		112
		119
		123
	Extension to Polymer Solutions	129
		133
	Error Analysis	134
VI.	PRESENTATION OF EXPERIMENTAL DATA	137
	Light Donting Chapturesony	137
	= 1 J. 1 = 0	144
	Interferometry	144
VII.	DISCUSSION OF THE RESULTS AND COMPARISON WITH THEORY .	153
	Comparison of Light Beating Data for Polystyrene	
	in Methyl Ethyl Ketone	154
	Comparison of Light Beating Data for Polystyrene	
	in Tetrahydrofuran	161
	in Tetrahydrofuran	
	in Toluene	164
	Comparison of Data Obtained from Interferometry	107
	with the Data Obtained from Light Posting for	
	with the Data Obtained from Light Beating for	166
		166
	Discussion of the Results Obtained from Light	167
	Beating Spectroscopy	167

Chapter	Page
Polystyrene in Various Solvents	169
Solvents	175
Interferometry	179 179 182
Styrene-Acrylonitrile Copolymer in Various Solvents Comparison of Light Beating and Interferometry	186
Data	192 194
VIII. CONCLUSIONS AND RECOMMENDATIONS	196
NOMENCLATURE	201
Appendix	
A. SAMPLE CALCULATION	208
B. MARK-HOUWINK CONSTANTS	215
D. LIGHT BEATING DATA	217
E. DATA FROM INTERFEROMETRY	220
G. CARDS USED IN COMPUTER INTERFACING	223
H. PROGRAM FOR DATA TRANSFER	231
J. DERIVATION FOR FUNCTION I (m,n)	234
RTRI TOGRAPHY	238

LIST OF TABLES

Table		Page
2-1.	Molecular weights and molecular weight distributions for polystyrene	6
4-1.	Details of bulk polymerization at 60°C using AIBN .	60
4-2.	Molecular weight and molecular weight distribution of copolymers by GPC	61
4-3.	Results of small-scale fractionations	63
4-4.	Results of large-scale fractionations	65
5-1.	Comparison of half widths obtained from the recorder and computer	100
5-2.	Ratios of $D_{av}/D(M_w)$	106
5-3.	Results of calibration runs for polystyrene spheres in water	108
5-4.	Results of the calibration runs on the interferometer	135
6-1.	Values of D and k calculated from light beating data	143
6-2.	Values of D_0 and k_d obtained from interferometric	
	data for monodisperse polystyrenes and their mixtures	151
7-1.	Comparison of King, et al. and Ford, et al. data for polystyrene in methyl ethyl ketone at 25°C, obtained by light beating spectroscopy	156
7-2.	Comparison of Mendema, et al. and Jamieson, et al. data for polystyrene in tetrahydrofuran	163
7-3.	Comparison of experimental and theoretical values of D_0	170

Table		P	age
7-5.	Comparisons for the values of B for polystyrene .	•	174
7-6.	Comparisons of experimental and theoretical values of $\mathbf{D}_{\mathbf{O}}$ for the copolymers	•	177
7-7.	Comparisons of experimental and theoretical values of $k_{\mbox{\scriptsize d}}$ for the copolymer		178
7-8.	Concentration dependence of D, for monodisperse polystyrenes and their mixtures obtained from interferometry		181
7-9.	Comparison of experimental and theoretical values of ${\bf D}_{\bf 0}$ for the monodisperse polystyrenes and their mixtures obtained by interferometry		183
7-10.	Comparison of experimental and theoretical values of D for polydisperse polystyrene (PS-2)		104
7-11.	obtained from interferometry	•	184
7-12.	obtained from interferometry Comparison of experimental and theoretical values of \mathbf{k}_{d} for polystyrene (PS-2) in benzene using	•	184
	higher values of B	•	186
7-13.	Comparison of experimental and theoretical values of D _O for the copolymers obtained from interferometry		188
7-14.	Comparisons of experimental and theoretical values of k _d for copolymers obtained from interferometry	•	189
7-15.	Comparison of experimental and theoretical values of $\mathbf{k}_{\mathbf{d}}$ for copolymers obtained from interferometry		
	with higher values of B	•	191
7-16.	Comparison of experimental and theoretical values of the thermodynamic parameters		195

LIST OF FIGURES

Figure		Page
3-1A.	A free-draining molecule during translation through solvent	21
3 - 1B.	Translation of a chain molecule with perturbation of solvent flow relative to the molecule	22
3-1.	Molecular weight dependence of D for polystyrene in cyclohexane at 35°C	24
3-2.	Molecular weight dependence of D $_{\rm O}$ for polystyrene in cyclohexane at 35°C	27
3-3.	Molecular weight dependence of D for polystyrene in methyl ethyl ketone at $25^{\circ}\text{C}^{\circ}$	28
3-4.	Molecular weight dependence of D for polystyrene in toluene at 20°C	29
3-5.	Molecular weight dependence of D for polystyrene in benzene at 25°C	30
3-6.	Molecular weight dependence of D for polystyrene in methyl ethyl ketone at 25°C°	36
3-7.	Molecular weight dependence of D $_0$ for polystyrene in toluene at 20°C	37
3-8.	Molecular weight dependence of D for polystyrene in benzene at 25°C	38
3-9.	Comparisons of theoretical predictions for k_d (cm ³ /g) with experimental data for 10^4 <m<sub>w<10^6 and 0<bx<math>10^{27}<1</bx<math></m<sub>	47
3-10.	Comparisons of theoretical predictions for k_d (cm ³ /g) with experimental data for $10^6 < M_W < 7 \times 10^6$	
	and $0 < B \times 10^{27} < 1.0$	48

3-11. Comparison of theoretical predictions for k _d (cm ³ /g) with experimental data for 2x10 ⁴ <m<sub>w<10⁶ and 1.0<bx10<sup>27<10.0 5-1. Spectrum of scattered light for polymer solutions . 5-2. Differences in heterodyne and homodyne methods 5-3. Lightbeating spectrometer</bx10<sup></m<sub>	age
5-1. Spectrum of scattered light for polymer solutions . 5-2. Differences in heterodyne and homodyne methods 5-3. Lightbeating spectrometer	49
5-2. Differences in heterodyne and homodyne methods 5-3. Lightbeating spectrometer	
5-3. Lightbeating spectrometer	69
5-4. Light collection optics	72
	85
5-5. Rasic timing diagram	86
o o. Dasie ciming dragium	90
5-6. Timing diagram for circulation pulse and one binary bit of digital data	92
5-7. Computer connections for programmed data transfer .	93
5-8. I/O instruction word	93
5-9. Flow of data from the averager to the computer	95
5-10. Interfacing circuit	96
5-11. Schematic diagram of interferometer showing position of mirrors	114
5-12. Photograph of Mach-Zehnder interferometer showing components	115
5-13. Photograph of diffusion cell for measurement of diffusion coefficients	117
5-14. Diagram of diffusion cell	118
5-15. Typical set of photographs taken during diffusion run (experimental run no. R18)	122
5-16. Diffusion cell coordinates	123
5-17. Fringe pattern	126
6-1. Concentration dependence of diffusion coefficients obtained from light beating for PS-1 in benzene and decalin at 25°C	1 38

Figure		Page
6-2.	Concentration dependence of diffusion coefficients obtained from light beating for PS-2 in benzene and decalin at 25°C	139
6-3.	Concentration dependence of diffusion coefficients obtained from light beating for SAN-1 in dimethyl formamide, methyl ethyl ketone and benzene at 25°C	140
6-4.	Concentration dependence of diffusion coefficients obtained from light beating for SAN-2 in dimethyl formamide, methyl ethyl ketone, and benzene at 25°C	141
6-5.	Concentration dependence of diffusion coefficients obtained from light beating for SAN-3 in benzene, methyl ethyl ketone, and dimethyl formamide at 25°C	142
6-6.	Concentration dependence of diffusion coefficients obtained from interferometry for PS-3, PS-4, PS-5 and PS-6 in benzene at 25°C	146
6-7.	Concentration dependence of diffusion coefficients obtained from interferometry for PS-2 in benzene at 25°C	147
6-8.	Concentration dependence of diffusion coefficients obtained from interferometry for SAN-1 in dimethyl formamide, and methyl ethyl ketone at 25°C	148
6-9.	Concentration dependence of diffusion coefficients obtained from interferometry for SAN-2 in dimethyl formamide, and methyl ethyl ketone at 25°C	149
6-10.	Concentration dependence of diffusion coefficients obtained from interferometry for SAN-3 in dimethyl formamide, and methyl ethyl ketone at 25°C	150
7-1A.	Comparisons of D versus M relationships obtained by Ford, et al. and King, et al. for polystyrene in methyl ethyl ketone at 25°C	157
7-1.	Comparison of concentration dependence of D for polystyrene in methyl ethyl ketone obtained by Ford, et al. and King, et al	160

Figure		Page
7-2.	Comparison of concentration dependence of D, for polystyrene in toluene obtained by Rehage, et al. and Chitrangad	165
7-3.	Comparison of concentration dependence of D, obtained from light beating by Pusey, et al., and from interferometry by Rehage, et al	168
A-1.	Calculation for experimental run R18	214

CHAPTER I

INTRODUCTION

Diffusion in polymer-solvent systems has been studied extensively both in the dilute range and very recently in the moderately concentrated range of polymer in solution. However, the behavior of such systems is still not well understood. Complexities arising when attempting to understand the diffusion phenomenon in polymer solutions may be attributed to several of the following factors which significantly influence the phenomenon: polymer molecular weight, molecular weight distribution of polymer, polymer-solvent thermodynamic interactions, polymer concentration, polymer structure, solvent viscosity and temperature.

Engineers require knowledge of transport processes and properties of polymer solutions for the design of processes for producing synthetic polymers. The transport properties are also of significant importance in refining, purification, and handling of a wide variety of macromolecular solutions. The above mentioned mass transfer operations involving polymer solutions are often controlled by molecular diffusion and values of the diffusion coefficient are usually lacking. Diffusion coefficients in polymer-solvent systems have been shown to be highly concentration dependent (1A-1). Therefore it is essential to include the concentration dependence in the

mathematical representation of the diffusion process. This requires experimental information, empirical correlations, and fundamental modeling concerning the diffusion process.

Most of the experimental effort in the last ten years to study diffusion in polymer-solvent systems in the dilute and intermediate concentration range have yielded very few accurate data. This lack of sufficient and accurate experimental data makes it difficult to verify the validity of existing theoretical expressions proposed by several investigators. Even for the cases where the existing data may be compared, serious disagreement often exists.

There is need, therefore, to systematically study diffusion in dilute, intermediate, and concentrated solutions of polymers of various molecular weight and structure in several thermodynamically different solvents. There is no single polymer-solvent system reported in the literature where the diffusion data are available from the infinitely dilute to the concentrated range. Duda and Vrentas (3A-6, 3B-2, 3B-3) are two of the most recently active researchers who are attempting to test the validity of existing theories in a systematic manner, from the very dilute polymer concentration to the diffusion of small molecules into polymers. On a long run their approach may be fruitful.

One of the big obstacles to obtaining diffusion data for polymer-solvent systems over the entire concentration range is the unavailability of a single experimental method. Investigators must use different experimental methods to study different concentration regions. Furthermore, if the polymer is polydisperse the results of

these different methods are often biased toward different sized species in the polymer sample. One solution to the polydispersity problem is to use monodisperse samples and this is frequently done. However, in the real world all the polymers that are used on a day-to-day basis are polydisperse.

In this work diffusion coefficients were obtained for polydisperse polymers in dilute and moderately concentrated polymer solutions. The influence of polydispersity on the diffusion data obtained by the two experimental methods used in this work is discussed. An effort is made to understand diffusion of copolymers in various solvents. Almost no data exist in the literature regarding diffusion measurements in copolymer systems.

CHAPTER II

SCOPE

Objectives of the Research

The subject of this thesis is the understanding of homopolymer and copolymer diffusional behavior. The specific work reported here was carried out with the following objectives in mind:

- 1. To study the manner in which polymer-solvent thermodynamic interactions influence the diffusional behavior of dilute and moderately concentrated solutions of polystyrene and styreneacrylonitrile copolymers in various "thermodynamically" good and poor solvents.
- 2. To compare the experimental results with theoretical equations describing diffusional behavior of polymers in solution and to extend homopolymer solution theories to copolymer solutions.
- 3. To compare the diffusion coefficients obtained from two experimental methods (light beating and interferometry) in the concentration range where they overlap each other.

Polymers and Solvents Used

To study the effect polymer-solvent thermodynamic interactions have on diffusional behavior, it was necessary to choose systems having a wide range of thermodynamic interactions. This could be accomplished by choosing thermodynamically "good" and "poor" solvents for

a given polymer. A poor solvent is one where polymer-polymer segment contacts are thermodynamically favored compared with polymer-solvent contacts. A good solvent is one where polymer-solvent contacts are more favored than polymer-polymer contacts. The characterization of a solvent as thermodynamically "good" or "poor" is discussed later in this section.

The homopolymer selected for this study was polystyrene. Two polystyrene homopolymer samples (PS-1 and PS-2) with about the same molecular weight distribution, and having different weight average molecular weights were obtained from Union Carbide Corporation. Two relatively monodisperse polystyrenes (PS-3 and PS-4) were obtained from Pressure Chemicals, Incorporated. The polymer molecular weights and the polydispersity of the samples are given in Table 2-1. The polymer PS-5 is an equal weight mixture of PS-3 and PS-4, and PS-6 is a mixture of 28% by weight of PS-3 and 72% of PS-4. The M_W and M_n for the polymers PS-5 and PS-6 are calculated using the standard relations (4A-1a). Polystyrene was chosen because its diffusional behavior has been studied in various solvents and it is commercially available in monodisperse form.

The styrene-acrylonitrile copolymers of three different molecular weights used in this study were prepared by bulk, free radical copolymerization. All the copolymers are of azeotropic composition (24 weight percent acrylonitrile). The polymerizations were carried out to only low conversions so as to produce copolymers having a uniform, randomly distributed, chemical composition. The

TABLE 2-1.--Molecular weights and molecular weight distributions for polystyrene.

Name given by the manufacturer	Name used in this work	Σ	Σ ³	M _Z	M/W
9436-52-010	PS-1	37,900	80,400	133,100	2.13
9436-52-040	PS-2	117,800	338,500	601,100	2.87
60917	PS-3	51,150	53,700	ı	1.05
36	PS-4	350,000	392,000	ı	1.12
	PS-5	89,581	223,675	ı	2.49
	PS-6	133,000	314,000	ı	2.36

molecular weights and polydispersity indicies of the copolymers obtained from Gel Permeation Chromatography are shown in Table 4-2.

The solvents used in this study were benzene, decalin (decahydro napthalene), methyl ethyl ketone and dimethyl formamide. All the solvents were purchased in high purity and distilled in glass. Benzene is non-polar and is an excellent solvent for polystyrene while decalin is a poor solvent. The copolymers were studied in three solvents: dimethyl formamide (polar) which is a good solvent for the copolymer and acrylonitrile homopolymer; methyl ethyl ketone (polar) which is an intermediate solvent both for the copolymer and the homopolymers; and benzene which is a poor solvent for the copolymer and acrylonitrile homopolymer. Thus, the choice of solvents gives a wide range of polymer-solvent thermodynamic interactions.

Experimental Methods

To achieve the objectives in this study, a wide variety of experimental work was involved. This consisted of:

- 1. Polymerization of the copolymers,
- 2. Fractionation and characterization of the copolymers,
- 3. Diffusion measurements in both dilute and moderately concentrated solutions.

This necessitated the use of the following equipment:

- Polymerization reactor with all the accessories for polymerization.
- b. Fractionation apparatus, for fractional precipitation.
- Light beating spectrometer for obtaining dilute solution diffusion coefficients.

d. Mach-Zehnder diffusiometer for obtaining diffusion coefficients in moderately concentrated solution.

The personnel at the analytical laboratory of Dow Chemical Company performed the measurements of molecular weight and molecular weight distribution of the copolymers.

Terminology in Polymer Solutions

The simplest form a polymer molecule can have is that of an unbranched chain. One speaks of "chain," because the polymer molecule consists of a large number of links, which result in a chain like structure. In solution or in bulk the the chain molecule is in general not stretched out lengthwise but, due to Brownian motion, assumes an almost limitless number of chain configurations. The particular form a polymer molecule will assume if it is completely free of outside influences may be considered in a simple way: the chain will always try to assume a condition of maximum possible entropy, which is the most irregular shape, the one for which there are the largest number of possible ways of attaining it, i.e. the largest number of configurations. A statistical chain model is one used to consider the most probable shape of a long molecule, and the shape predicted leads to a discussion of the molecular chain based upon random-flight statistics. This treatment gives the name "randomflight chain" to a statiscical model for real polymer molecules. The dimension of a chain molecule which is widely used in random-flight statistics to characterize its spatial or configurational character is the end-to-end distance, the distance from one chain-end group to the other in its randomly coiled form. Since for the chain, the

number of possible configurations is large, a time average value of the end-to-end distance is specified, the usual appropriate average being the root mean-square end-to-end distance, $\langle R_0^2 \rangle^{\frac{1}{2}}$. This quantity is also called the unperturbed dimension of the polymer, because the statistical analysis is based on the assumption that the polymer chain configuration is completely free of outside influences.

The configuration of the polymer molecule will also depend on its environment, which is often a solvent. In a good solvent, where the energy of interaction between a polymer molecular segment and a solvent molecule adjacent to its exceeds the mean of the energies of interaction between the polymer-polymer and solvent-solvent pairs, the molecule will tend to expand further compared with its unperturbed dimension so as to reduce the frequency of contacts between pairs of polymer segments. This expansion is characterized by a parameter, α , which is called the linear expansion factor, and is defined as

$$\langle R^2 \rangle^{\frac{1}{2}} = \langle R_0^2 \rangle^{\frac{1}{2}} \alpha$$
 (2-1)

where $\langle R^2 \rangle^{\frac{1}{2}}$ is the mean square end-to-end distance for the polymer in any particular environment. In a poor solvent, on the other hand, where the energy of interaction between polymer segment and solvent is more repulsive, smaller configurations in which polymer-polymer contacts occur more frequently will be favored. In the limit where the solvent is so poor that the polymer assumes its

minimum or unperturbed dimensions, the polymer chain is described as being in its "theta" state as will be discussed below.

It may be better understood to rank the thermodynamic quality of a solvent for a polymer (good solvent or bad solvent), based upon thermodynamic arguments using the Flory-Huggins equation (2A-1). This equation gives the free energy of mixing of polymer (2) with solvent (1) as

$$\frac{\Delta G_{m}}{RT} = n_{1} \ln \phi_{1} + n_{2} \ln \phi_{2} + \chi \phi_{1} \phi_{2} (n_{1} + m n_{2})$$
 (2-2)

where n_i is the moles of component i, ϕ_i is the volume fraction of component i, m is the ratio of molar volumes of polymer to solvent, and χ is the Flory-Huggins thermodynamic interaction parameter. In order for a given solvent to dissolve polymer the free energy of mixing should be negative. Since the first two terms in the above equation are always negative, this means the smaller the value of χ , the better the thermodynamic quality of the solvent for the polymer. The thermodynamic quality of a solvent for a polymer can be investigated experimentally.

The osmotic pressure of a dilute polymer solution (for which the partial molar volume of the solvent is indistinguishable from its molar volume) can be expressed as (2A-2)

$$\pi = (R T / M_2) c_2$$

where π is the osmotic pressure, R is the gas constant, T is the absolute temperature, M $_2$ and c $_2$ are the molecular weight and

concentration of polymer. At higher concentrations, where binary and higher order interactions of polymer segments are present

$$\pi = R T [(c_2 / M_2) + A_2 c_2^2 + A_3 c_2^3 + ----]$$

where A_2 , A_3 etc. are the second, third, and higher osmotic virial coefficients. According to Flory's theory the second virial coefficient A_2 , can be defined in terms of χ and α as

$$A_2 = (v_p^2 / v_s) (l_2 - \chi) F (x)$$
 (2-3)

where

$$F(x) = 1 - \frac{x}{2! \ 2^{\frac{3}{2}}} + \frac{x^2}{3! \ 3^{\frac{3}{2}}} - \frac{x^3}{4! \ 4^{\frac{3}{2}}} + ---$$

$$x = 2 (\alpha^2 - 1)$$

Here \mathbf{v}_p is the specific volume of polymer and \mathbf{v}_s is the molar volume of solvent. The second virial coefficient for polymer solutions can also be obtained from light scattering measurements. The linear expansion factor, α , may be measured by intrinsic viscosity both at theta and non-theta conditions. Alternatively the unperturbed dimension and the value of $< R^2 >^{\frac{1}{2}}$ may be measured by light scattering measurements. The values of $< R^2 >^{\frac{1}{2}}$ and $< R^2 >^{\frac{1}{2}}$ have been measured for many systems and are available in the literature (3A-9).

The osmotic swelling of the polymer by the polymer-solvent interactions in good solvents is often referred to as the "excluded volume effect." Two or more polymer segments remote from one another

along the chain cannot occupy the same volume element at the same time, because of their finite volumes. In other words repulsive forces will act between these segments when they are close to one another. In addition, this repulsive force will, to some extent, be altered by the presence of solvent molecules. Intermolecular interactions of this sort are associated with the "excluded volume effect."

The excluded volume effect vanishes under a special condition of temperature or solvent, which is known as the Flory "theta" temperature or theta solvent, and the condition is called the theta condition. The theta condition arises because of the apparent cancellation at this condition, of the effect of volume exclusion of segments which tend to enlarge the molecule, and the effect of Vander walls attraction between segments which contracts the molecule. At the theta condition, α must equal unity irrespective of the molecular weight of the polymer. When χ = 1/2, Flory defined this as the theta condition in terms of the interaction parameter χ . From equation 2-3, we can conclude that at the theta condition, A_2 , the second virial coefficient is zero.

This background material is provided as an aid in understanding the results and conclusions to be described in this work. In a thermodynamically good solvent, or at any condition other than the theta condition for a polymer solvent pair, excluded volume effects give rise to the linear expansion of the polymer molecule. It is only at the theta condition, when excluded volume effects are

absent, that the linear expansion factor is unity, and the second virial coefficient is numerically equal to zero.

Principles of Diffusion

Diffusion is the movement of an individual component through a mixture. Although the most common driving force for diffusion is a concentration gradient of the diffusing component, it can also be caused either by a pressure gradient or by a temperature gradient. In this section diffusion caused only by concentration gradients will be discussed. Diffusion may result from molecular motion only or by a combination of molecular and turbulent motion. In the absence of turbulence the rate of diffusion of component A is given by Fick's Law

$$J_{A} = -c D_{AB} \frac{dx_{a}}{dz}$$
 (2-4)

Where J_A is the molar flux for component A, c is the molar density of solution, D_{AB} is the diffusion coefficient of A in solution in B, x_A is the mole fraction of component A, and z is the direction of diffusion. The negative sign emphasizes that diffusion occurs in the direction of a drop in concentration. The flux J_A was defined with respect to molar average velocity. In engineering process calculations it is usually desirable to refer to a coordinate system fixed in the equipment. Therefore, Fick's first law in terms of N_A , the molar flux relative to stationary coordinates, becomes:

$$N_A = x_A (N_A + N_B) - c D_{AB} \frac{dx_A}{dz}$$
 (2-5)

This equation shows that the flux defined in terms of N_A is the result of two quantities: $x_A (N_A + N_B)$ which is the molar flux of a resulting bulk motion of fluid and - c $D_{AB} \frac{dx_A}{dz}$, which is the molar flux of A resulting from the diffusion superimposed on the bulk flow. For binary systems $D_{AB} = D_{BA}$.

All these relationships are based on the assumption that D_{AB} is not dependent on concentration. This may not be true for concentrated solutions. Dependence of D_{AB} on concentration is the result of change of mobility of the solute with concentration and deviations of the mixture from ideal behavior. For non ideal mixtures D_{AB} can be corrected by a factor of $\begin{pmatrix} \partial \ln a_A \\ \partial \ln x_A \end{pmatrix}$ where a_A is the activity coefficient of species A (2A - 2a). Therefore to evaluate the molar flux N_A , it is essential to know the concentration dependence of D_{AB} . In this work the concentration dependence of the diffusion coefficient for polymer molecules in solution is examined.

The equation of continuity for polymer molecules in solution is obtained by making a mass balance over an arbitrary differential fluid element. The diffusion equation (2-6) is obtained by the insertion of the expression for molar flux into equation of continuity with the assumptions of constant molar density, constant diffusivity and zero mass average velocity.

$$\frac{dc_A}{dt} = D_{AB} \nabla^2 c_A \tag{2-6}$$

The diffusion equation is called Fick's second law of diffusion. In multicomponent mixtures the diffusion contribution to the mass flux is seen to depend in a complicated way on the concentration gradients of the substances present. For multicomponent ideal-gas mixture a relation is known (2E-1) between D_{ij} (the diffusivity of pair i-j in the multicomponent mixture) and \mathcal{D}_{ij} (the diffusivity of pair i-j in the binary mixture). For ideal-gas multicomponent mixture the flux equations are known as Stefan-Maxwell equations (2E-1).

CHAPTER III

THEORY OF DIFFUSION IN POLYMER SOLUTIONS

Diffusion in binary systems of large polymer molecules and small solvent molecules exhibits markedly different behavior as the relative proportions of the two species are varied over the entire concentration range. Most of the research in this area leads to the conclusion that for diffusion in dilute polymer solutions in good solvents, the value of the diffusion coefficient, D, generally increases with polymer concentration in the region of low polymer concentration. On the other hand, it has been shown that for diffusion in polymer films or solids, in the region near undiluted polymer the value of D increases quite sharply with increasing diluent concentration. These facts lead to the idea that the D versus concentration curve for a polymer solvent system should exhibit a maximum at an intermediate concentration in the range from pure solvent to pure polymer. Although existing data for D covering a wide range of polymer concentrations are still quite few, this prediction is widely confirmed (3C-1, 3C-2) in thermodynamically good solvents.

For the purposes of this work, the total concentration range is considered in five sub-regions. They are: (1) infinitely dilute region, (2) dilute region (up to 1% by weight of polymer),

(3) intermediate concentration region (up to 10% by weight of polymer), (4) concentrated region (up to about 90% by weight of polymer) and (5) bulk polymer region. Only the first three ranges are studied in this work. Diffusion in the infinitely dilute range has been investigated most thoroughly and is best understood. This is discussed in the section on "Diffusion in Infinitely Dilute Polymer Solutions" in Chapter III. As the polymer concentration increases slightly from the limit of infinite dilution, the diffusion coefficient may be expected to vary as

$$D = D_0 [1 + k_d c]$$

 D_0 is the diffusion coefficient at the limit of zero polymer concentration, and c is the polymer mass concentration. The parameter k_d is a function of both thermodynamic and hydrodynamic factors. The section on "Modified Pyun and Fixman Theory" in Chapter III discusses the relations for obtaining k_d from the combination of two parameter theory, and a modified Pyun and Fixman (3B-3) theory. In the last section the value of k_d predicted by the above theories is compared with the experimentally available values in the literature for polymer-solvent systems.

Diffusion in Infinitely Dilute Polymer Solutions

The most important quantity obtained from a diffusion study in infinitely dilute polymer solutions is D_0 , the value of D at the limit of zero polymer concentration. For this quantity the well known Einstein formula (3A-1) is

$$D_0 = k T / f_0 \tag{3-1}$$

In this equation k is the Boltzman constant, T is the absolute temperature of the solution, and f_0 is the value of f at the limit of zero polymer concentration. Here f stands for the frictional coefficient of the polymer molecule, which is defined as the force experienced by the polymer molecule when it moves with a velocity of one centimeter per second relative to the solvent. The value of f_0 is influenced both by the size and shape of the polymer molecule as well as by the viscosity f_0 , of the solvent. For a rigid spherical molecule of radius f_0 , the Stokes formula is

$$f_0 = 6 \pi \eta_0 R_a$$

Most linear polymer molecules assume a randomly coiled form in solution. The derivation of an expression for f_0 for such molecules was first made by Kirkwood and Riseman (3A-2). They did not take into account the excluded volume effects between polymer segments. These effects were considered later by Flory (3A-3) and Johnston (3A-4), in two different approaches toward deriving relations for f_0 . The rest of this section contains a brief description of the theories of Kirkwood-Riseman, Flory, and Johnston. These theories are compared with the existing experimental data in the literature. This section concludes with the derivation of a semi-empirical model for predicting D_0 , based on Kirkwood-Riseman theory and proposed by the author.

Kirkwood-Riseman Theory

The Kirkwood-Riseman theory of transport processes in polymer solutions provides a convenient method for predicting the translational diffusion coefficient at infinite dilution. The theory is applicable under theta conditions only because excluded volume effects were not considered in the derivation. The frictional coefficient at infinite dilution of the polymer is developed on the basis of a random coil model with hindered internal rotation. The theory is based on the notion that the peripheral elements of the polymer chain perturb the flow in the neighborhood of the interior elements in such a manner that they are partially shielded from hydrodynamic interactions with the exterior fluid. At high molecular weights, the hydrodynamical shielding of the interior elements may become so effective that their contribution to the resistance offered by the molecule to the external fluid is negligibly small. Using this approach Kirkwood-Riseman derived the following equation for the translational diffusion coefficient of a chain-like molecule at infinite dilution (3A-5d, 3A-6)

$$D_{0} = \frac{kT}{n\zeta} (1 + \frac{8}{3} X)$$
 (3-2)

Where

$$\chi = \frac{\sqrt{2 \text{ n}}}{\eta_0 L \sqrt{12\pi^3}}$$

L is the effective bond length, n is the number of effective bonds or segments in a chain, ζ is the translational friction coefficient of a segment, and η_{α} is solvent viscosity. The parameter X is a measure of the hydrodynamic interactions between segments. The parameter ζ is not directly observable or predictable by a simple method for polymer solutions. In the limiting case of X >> 1, the parameter ζ drops out. The two limiting cases X = 0 and X >> 1, for the above equation, have special significance for polymer solutions. In the case X = 0, there is no hydrodynamic interaction between segments, and the velocity of the medium everywhere is approximately the same as though the polymer molecule were not present. The solvent streams through the molecule almost (but not entirely) unperturbed by it, hence this is called the free draining case. Figure 3-1A is illustrative of this case. The case X >> 1, is illustrated in Figure 3-1B. In this case the velocity of the solvent relative to the molecule increases from zero at the center to a value approaching its external value at some distance from the center. For this case the intrinsic viscosity is equivalent to that for a rigid sphere molecule, therefore, flexible polymer chains in this limit behave hydrodynamically as rigid sphere molecules. This limit corresponds to very large hydrodynamic interactions between segments, and the polymer molecule is treated as an hydrodynamically equivalent sphere. Thus the variable X represents the degree of drainage of the solvent through the polymer molecule domain, and is called the draining parameter. Yamakawa (3A-5d) compared the experimental intrinsic viscosity data for polyisobutylene in benzene

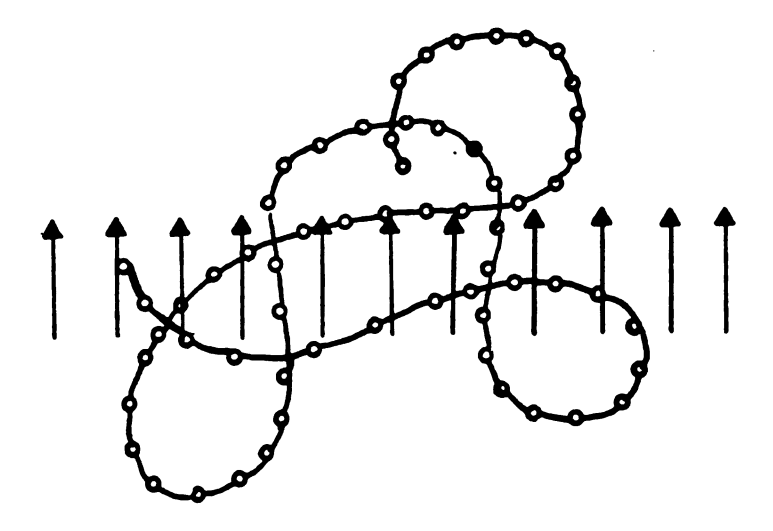


Figure 3-1A.--A free-draining molecule during translation through solvent.*

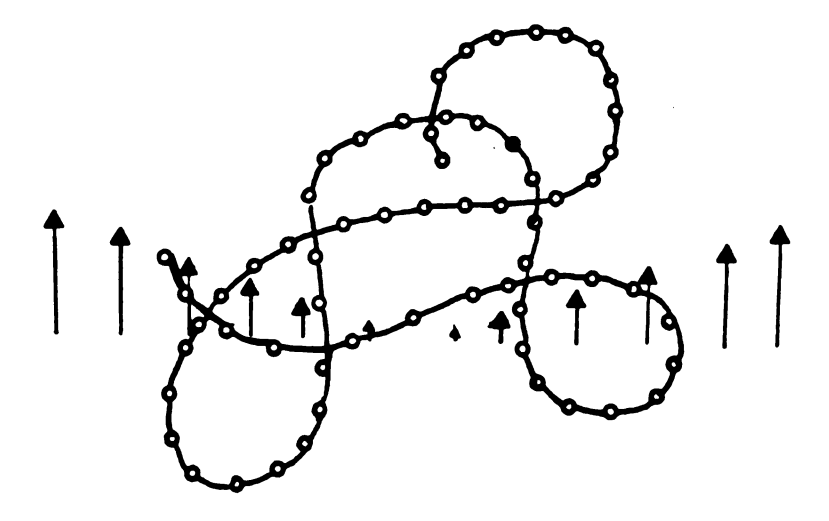


Figure 3-1B.--Translation of a chain molecule with perturbation of solvent flow relative to the molecule.*

*Arrows indicate flow vectors of the solvent relative to the polymer chain.

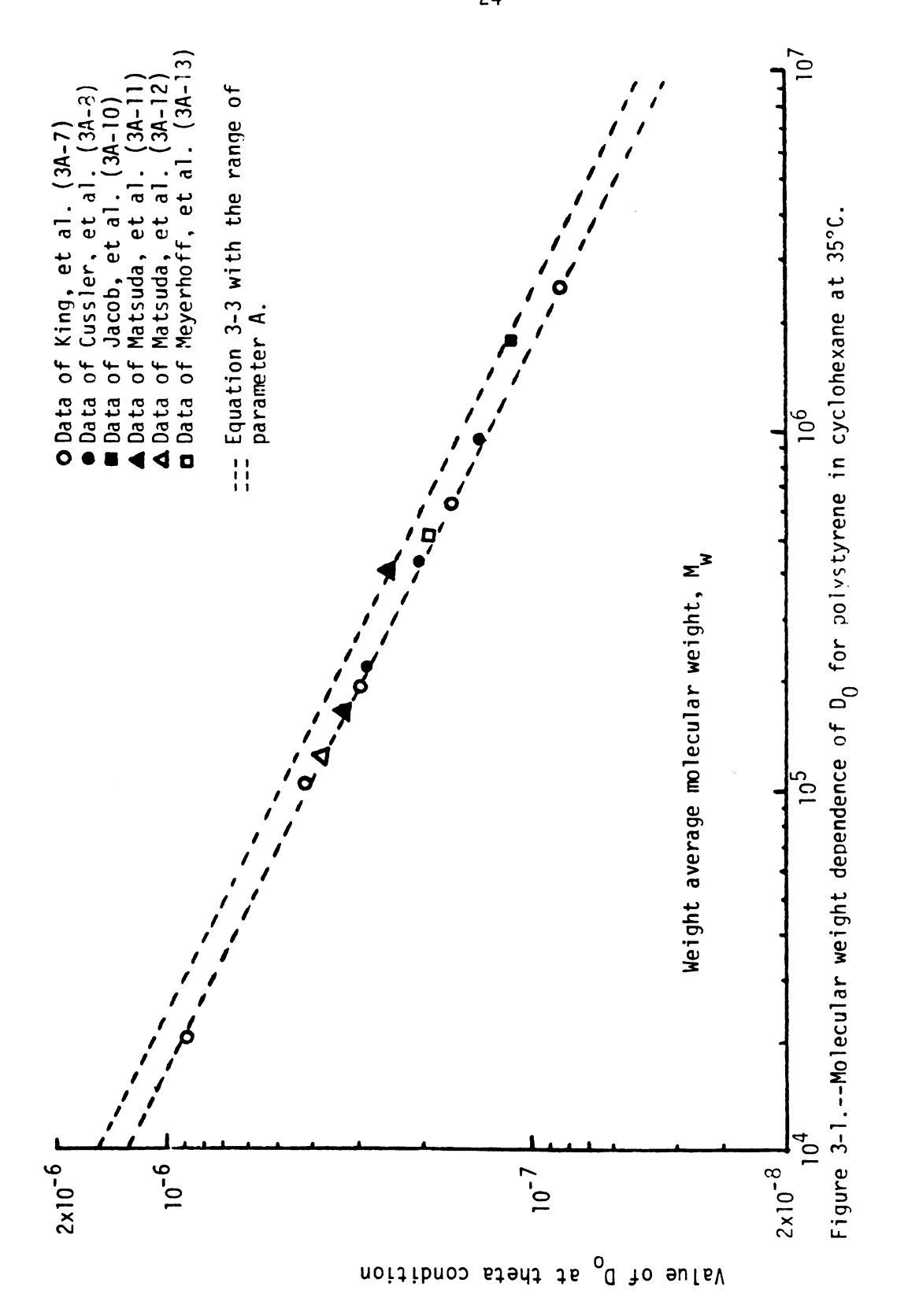
with that of the predictions from the theory with X = 0 and X >> 1. From the comparisons Yamakawa concluded that the case with X >> 1 describes the behavior of the experimental data well.

There is evidence that the case with X>>1 describes the polymer solution behavior at infinite dilution (3A-6). Consequently, for X>>1 equation 3-2 reduces to the following form

$$A = \left(\frac{\langle R_0^2 \rangle}{M}\right)^{\frac{1}{2}}$$

where $< R_0^2 >$ is the mean square end-to-end distance of the unperturbed chain, M is the polymer molecular weight, and $\left(D_0\right)_\theta$ is the value of D_0 under theta conditions.

In order to test the validity of equation 3-3, we have chosen data from the literature obtained on the polystyrenecyclohexane system at the theta temperature ($\approx 35^{\circ}$ C) and compared them with the predictions from equation 3-3. Figure 3-1 is a plot of $\left[D_{0}\right]_{\theta}$ versus M_W, the weight average molecular weight of the polymer, on a log-log paper. Since the molecular weight distribution of the polystyrene used in the various studies was not reported in the literature (except for the data of King, et al.) we have assumed that the characteristic molecular weight of the polymer is the weight average molecular weight. Values of the parameter A for this system vary from 645 x 10^{-11} to 775 x 10^{-11} cm, in the



literature (3A-9). The two dashed lines in Figure 3-1 correspond to the range of A values.

It is evident from Figure 3-1 that equation 3-3 predicts D_0 reasonably well within the range of A values, and there appear no systematic deviations. The experimental results serve as an effective verification of the Kirkwood-Riseman equation since the discrepancy between theory and experiment is quite small. Hence, the available data show that the Kirkwood-Riseman theory quite accurately describes polymer-solvent diffusion at infinite dilution of polymer under theta conditions.

Flory's Theory

Flory assumes that the frictional coefficient at infinite dilution, f_0 , of a polymer molecule in dilute solution varies directly as an average linear dimension of the coiled chain in solution. From this assumption equations are developed (3A-3), which are analogous to those used successfully in the interpretation of intrinsic viscosity measurements.

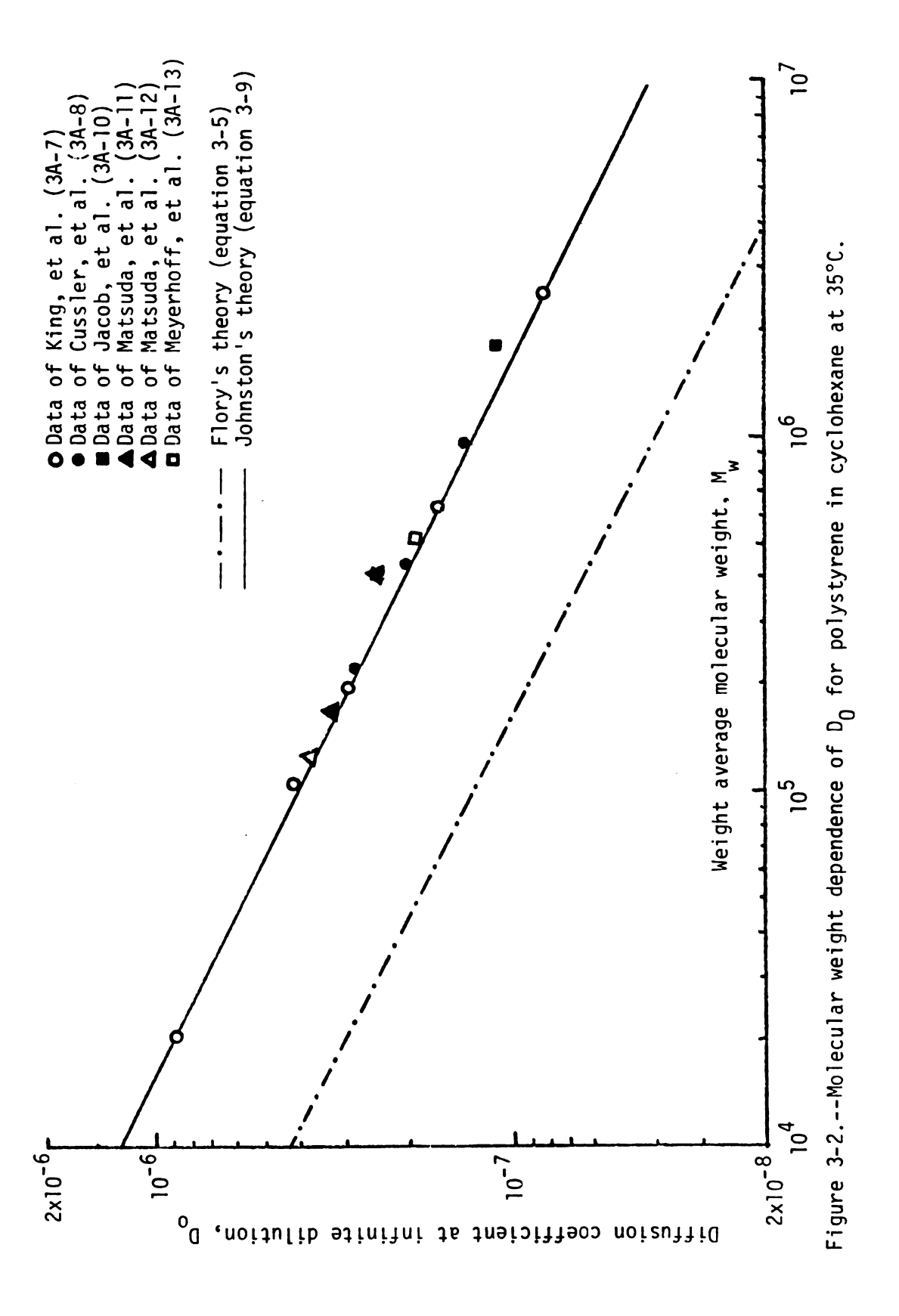
$$\frac{f_0}{\eta_0} = K_f M^{\frac{1}{2}} \alpha \tag{3-4}$$

where α represents the factor by which the actual mean square endto-end distance exceeds the unperturbed dimension and P is an universal constant as defined by Flory. Using the expression for f_{o} from equation 3-4 and equation 3-1, he obtained the following equation for D_{o} .

$$D_{o} = \frac{k T P^{-1} \phi^{1/3}}{\eta_{o} [M[n]]^{1/3}}$$
 (3-5)

where ϕ is also an universal constant, and [n] is the intrinsic viscosity of the solution. Equation 3-5 should predict D₀ both for theta and non-theta conditions because excluded volume effects were taken into account in deriving it. Flory in his paper showed that the theoretical value of P⁻¹ ϕ ^{1/3} is equal to 2.5 x 10⁶. Flory's theoretical prediction of the value of P⁻¹ ϕ ^{1/3} is in good agreement with some limited experimental data.

The validity of equation 3-5 was tested on various polymer-solvent pairs in both theta and non-theta conditions and is shown in Figures 3-2 through 3-5. The polymer-solvent pair used for comparisons under theta conditions is polystyrene in cyclohexane. Under non-theta conditions, the polymer-solvent pairs used are polystyrene in methyl ethyl ketone, toluene and benzene. For polystyrene, methyl ethyl ketone is an intermediate solvent, toluene is a good solvent, and benzene is a very good solvent. These pairs were chosen to see if Flory's theory could describe the diffusional behavior in various systems with different degrees of polymer-solvent interactions. All the experimental data used for comparison was obtained from literature. We have used the assumption that the characteristic molecular weight of the polymer is the weight average molecular weight



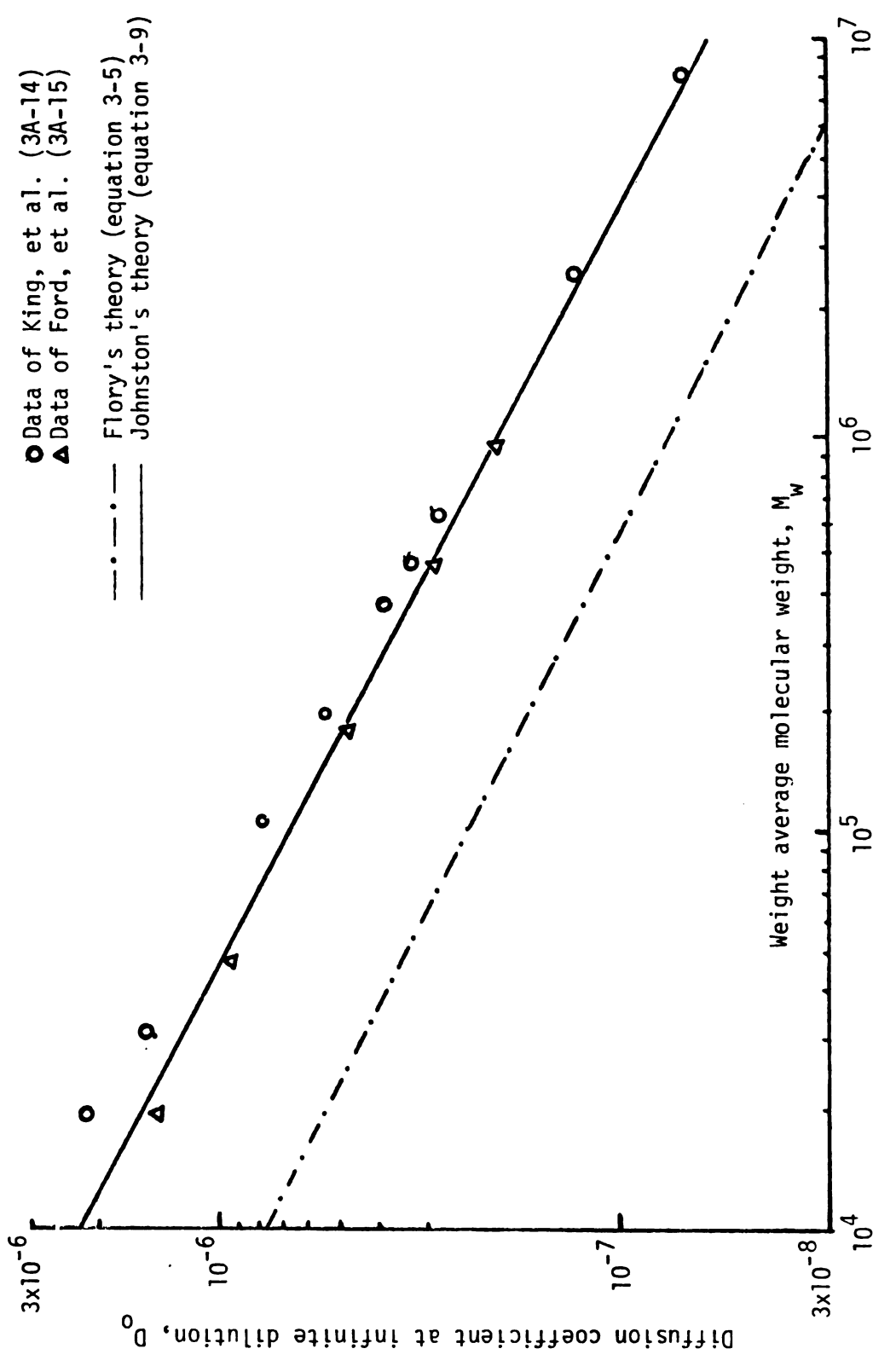


Figure 3-3.--Molecular weight dependence of ${
m D_o}$ for polystyrene in methyl ethyl ketone at 25°C.

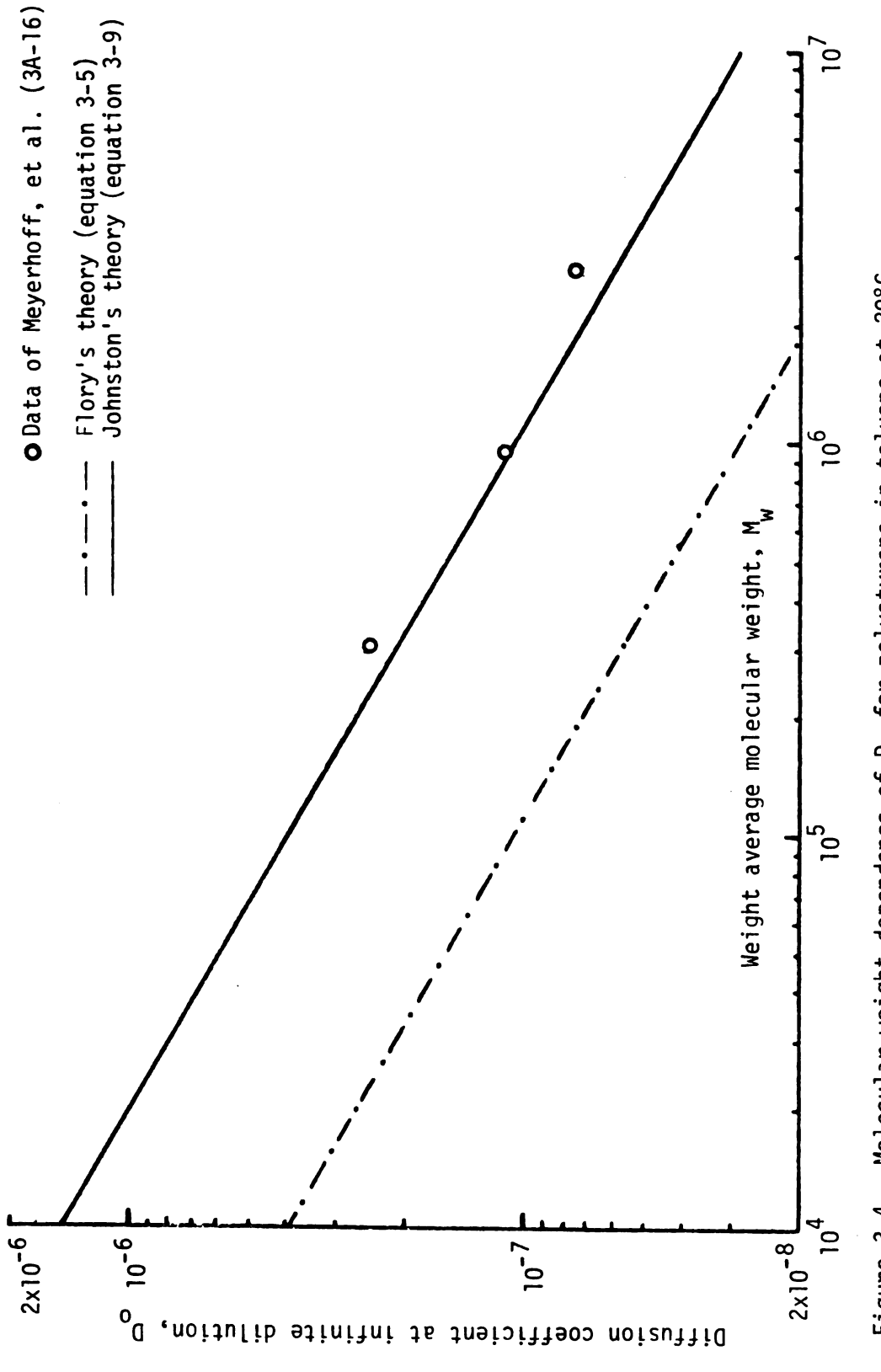


Figure 3-4.--Molecular weight dependence of ${\tt D_0}$ for polystyrene in toluene at $20^{\circ}{\tt C}$.

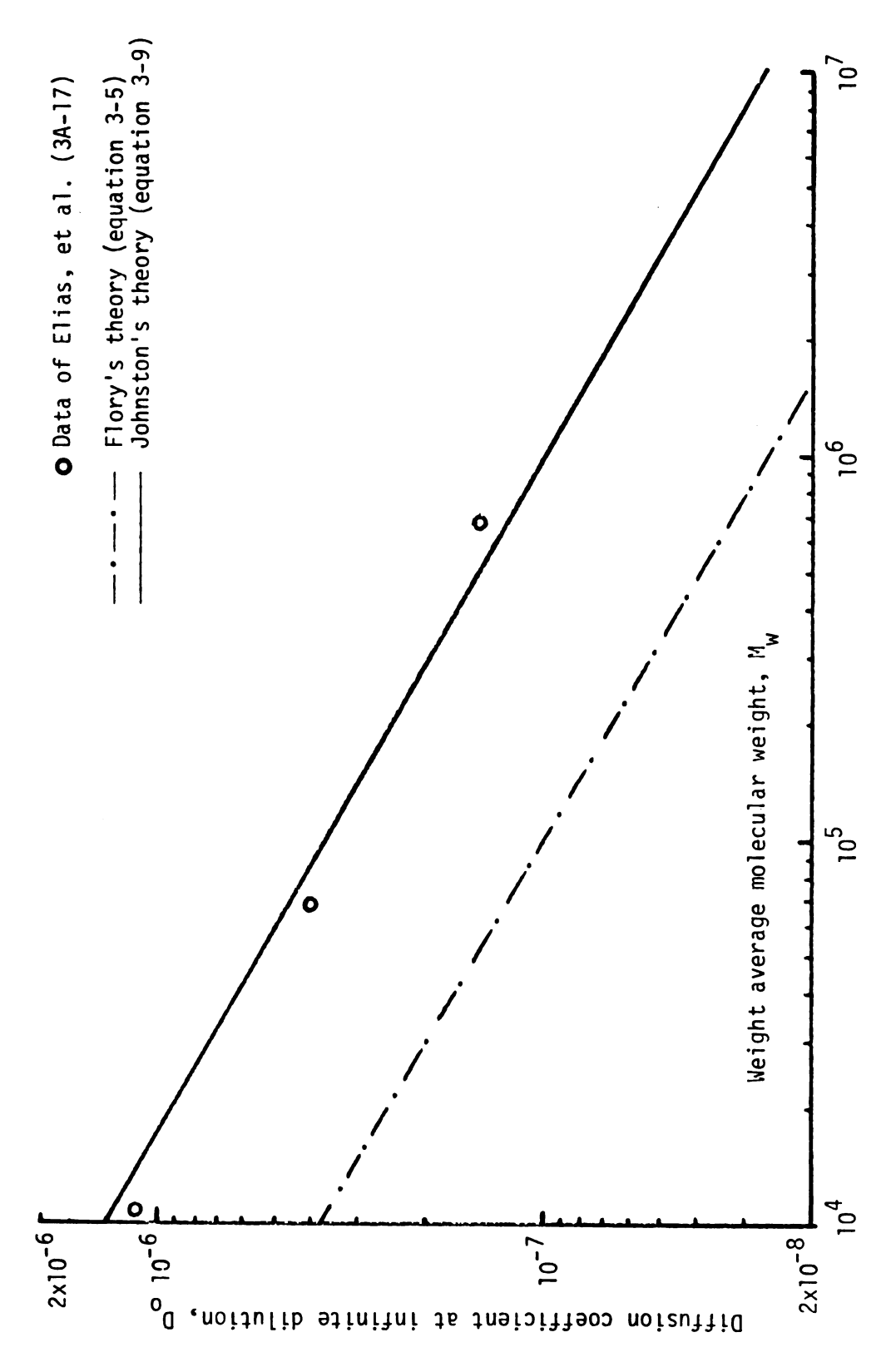


Figure 3-5.--Molecular weight dependence of \mathbb{D}_{O} for polystyrene in benzene at 25°C.

 $(M = M_W)$. Data were needed for [n], intrinsic viscosity, for all the systems. These were obtained from the Polymer Handbook (3A-9). Even though there were many relations for predicting the variation of [n] with molecular weight in the handbook, the relations for the molecular weight range of interest that were recommended by the editors of the book were used. These relations are shown in Appendix B.

From the Figures 3-2 through 3-5, it can be concluded that Flory's theory as given by equation 3-5 does not agree with experimental data for diffusion in infinitely dilute polymer solutions. Flory's theory predicts that ϕ should be a universal constant independent of the nature of the polymer and independent of the solvent medium. There exists still a controversy on the validity of ϕ being an universal constant (3A-18, 3A-19, 3A-20). The deviation of the experimental data from Flory's theory may be attributed to his assumption that all linear dimensions of a flexible coil change by the same factor when it is transferred from one solvent to another. Even though Flory's approach is theoretically sound, the value to be used for the universal constant ϕ was not exactly known.

Johnston's Theory

Recently Johnston (3A-4) combined some known expressions to offer a rather simple view of diffusion in infinitely dilute polymer solutions. Based on the concept of an equivalent hydrodynamic sphere, impenetrable to solvent, he obtained the expression for f_0

$$f_0 = 6 \pi \eta_0 R_a$$
 (3-6)

where R_a is the radius of the hydrodynamically equivalent sphere. He used an intrinsic viscosity expression for dilute polymer solutions based on Einstein's viscosity relation (3A-21)

$$[\eta] = \frac{2.5 \text{ N}_0 \text{ V}_e}{\text{M}_{II}}$$
 (3-7)

where N_0 is Avogadro's number, V_e is the volume of the equivalent hydrodynamic sphere and M_u is the viscosity average molecular weight. By eliminating the radius of the equivalent hydrodynamic sphere, R_a , between equations 3-6 and 3-7, and with the use of the Mark-Houwink expression,

$$[n] = K_{V} M^{a}$$
 (3-8)

Johnston derived an expression for $\mathbf{D}_{\mathbf{O}}$ as

$$D_{o} = \frac{k T}{6 \pi \eta_{o}} [(10 \pi N_{o})/3 K_{v} M_{u}^{a+1}]^{1/3}$$
 (3-9)

where K_{V} and a are called the Mark-Houwink constants and are constants for a particular polymer-solvent pair.

Once again the validity of equation 3-9 is put to test by comparing the calculated values for D_0 from equation 3-9, with the same experimental values that were used for comparing Flory's theory, both for theta and non-theta conditions. The comparisons are shown in Figures 3-2 through 3-5. To obtain D_0 values from

Johnston's theory we assumed that M_U is equal to M_W . This assumption is valid if the polymer molecular weight distributions are not broad. The values of K_V and a used in equation 3-9 are tabulated in Appendix B.

From the Figures 3-2 through 3-5, one can easily conclude that Johnston's theory agrees well with the available experimental data to within ten percent for all the cases where the Mark-Houwink parameters are well established. If we compare Flory's theory with that of Johnston's, it can be seen that both have the same molecular weight dependence. The difference is in the so-called universal constants of P^{-1} $\phi^{1/3}$. According to Johnston's theory P^{-1} $\phi^{1/3}$ is equivalent to $\frac{\left[10~\pi~N_{0}/3\right]^{1/3}}{6~\pi}$.

This does not imply that Johnston's theory is better than Flory's theory. For the few systems compared here Johnston's theory seems to be predicting diffusional behavior adequately. In this study, Johnston's theory was used for predicting D_0 for all the polymer-solvent pairs when the viscometric parameters were well established.

Semi-Empirical Relation

pa US ť ſ C

The semi-empirical relation, is a modified form of the Kirkwood-Riseman equation, obtained by multiplying equation 3-3 on the right hand side with 2(1-a), which gives

$$D_0 = \frac{0.196 \text{ k T}}{\eta_0 \text{ A M}^{1/2}} \qquad 2(1-a) \tag{3-10}$$

This relation should predict D_0 both in theta and non-theta conditions, because of the incorporation of the excluded volume effects through the parameter a. The factor 2 (1-a) was designed such that at theta condition (a = 0.5) it is equal to one. Thus at the theta condition the value of D_0 is still predicted by the Kirkwood-Riseman equation, however under non-theta conditions the value of D_0 is corrected by a factor less than one (since a lies between 0.5 and 0.75 for most of the commercial polymers). The correction for D_0 in non-theta conditions is in the appropriate direction since it is known that the polymer molecule expands under non-theta conditions compared to its size at the theta condition, and the diffusion coefficient should therefore decrease.

The validity of equation 3-10 is put to test by comparing the available data for polystyrene in different solvents. The experimental data used for comparison in the earlier theories are also used here. The theoretical predictions for the polystyrene-cyclohexane system by equation 3-10, under theta conditions would be exactly the same as those shown in Figure 3-1, because a = 0.5. Under non-theta conditions, for all the other solvents, the comparisons are shown in Figures 3-6 through 3-8. The two dotted lines in these figures correspond to the range of the parameter A available in the literature, as mentioned in the section on "Kirkwood-Riseman Theory" earlier in Chapter III. The values of the parameter a used are shown in Appendix B.

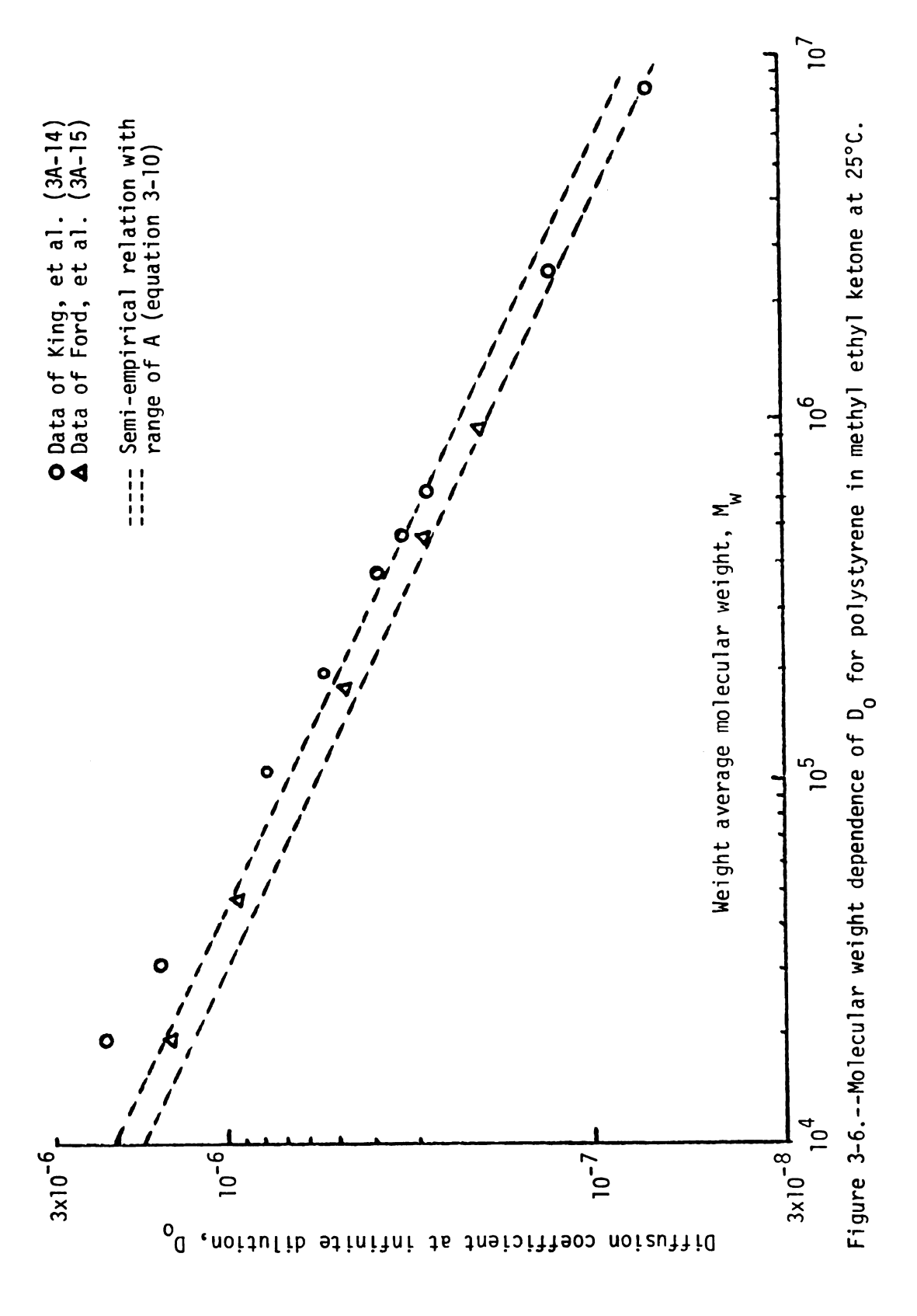
From the comparisons in Figures 3-1 and 3-6 through 3-8 it may be concluded that the relation for D_0 , given by equation 3-10, predicts the diffusion coefficient at infinite dilution under both theta and non-theta conditions surprisingly well. In this work whenever the viscometric parameters were not well established for the polymer-solvent pair, equation 3-10 was used to predict D_0 .

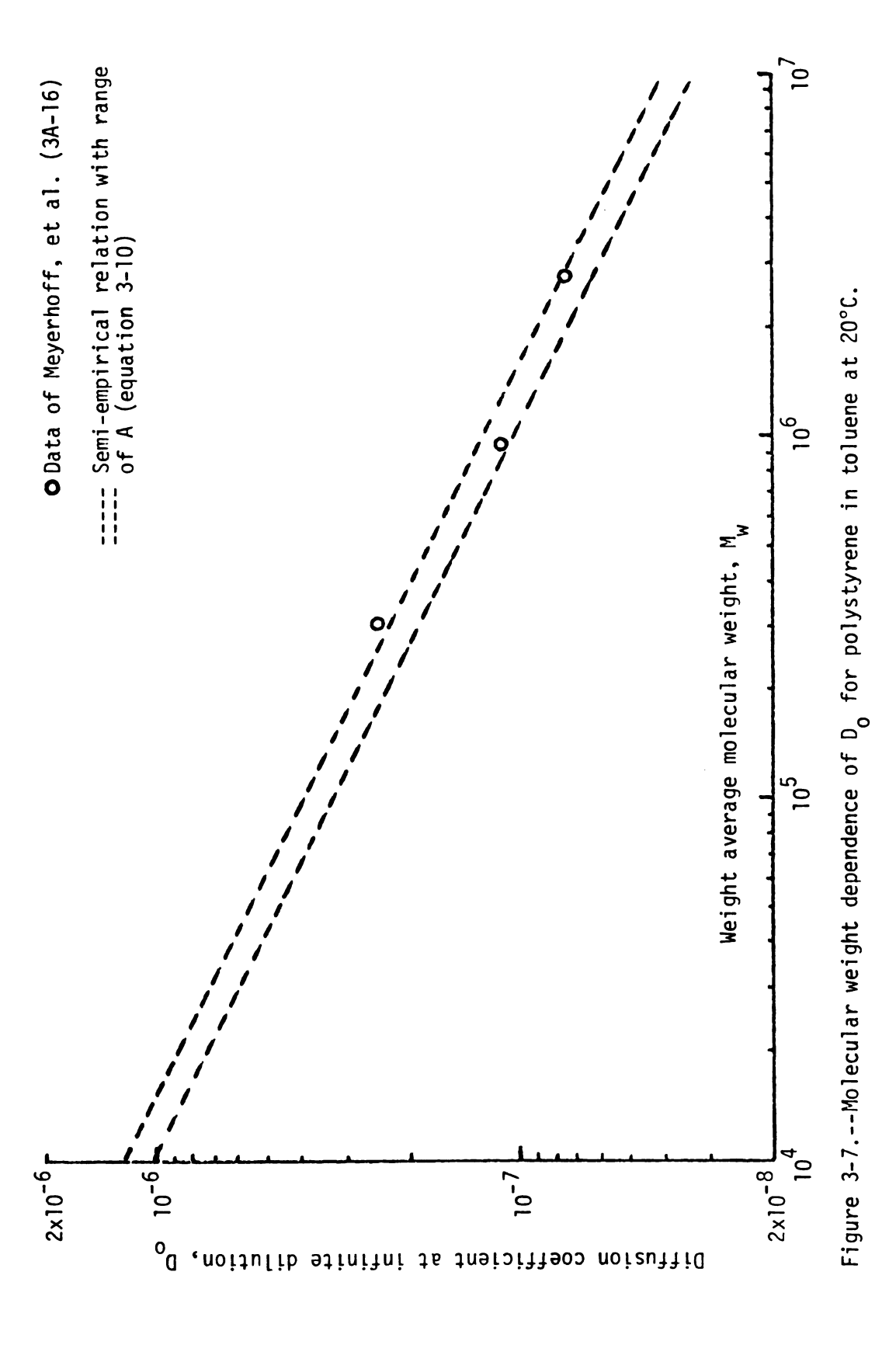
<u>Diffusion in Dilute and Moderately Concentrated</u> Polymer Solutions

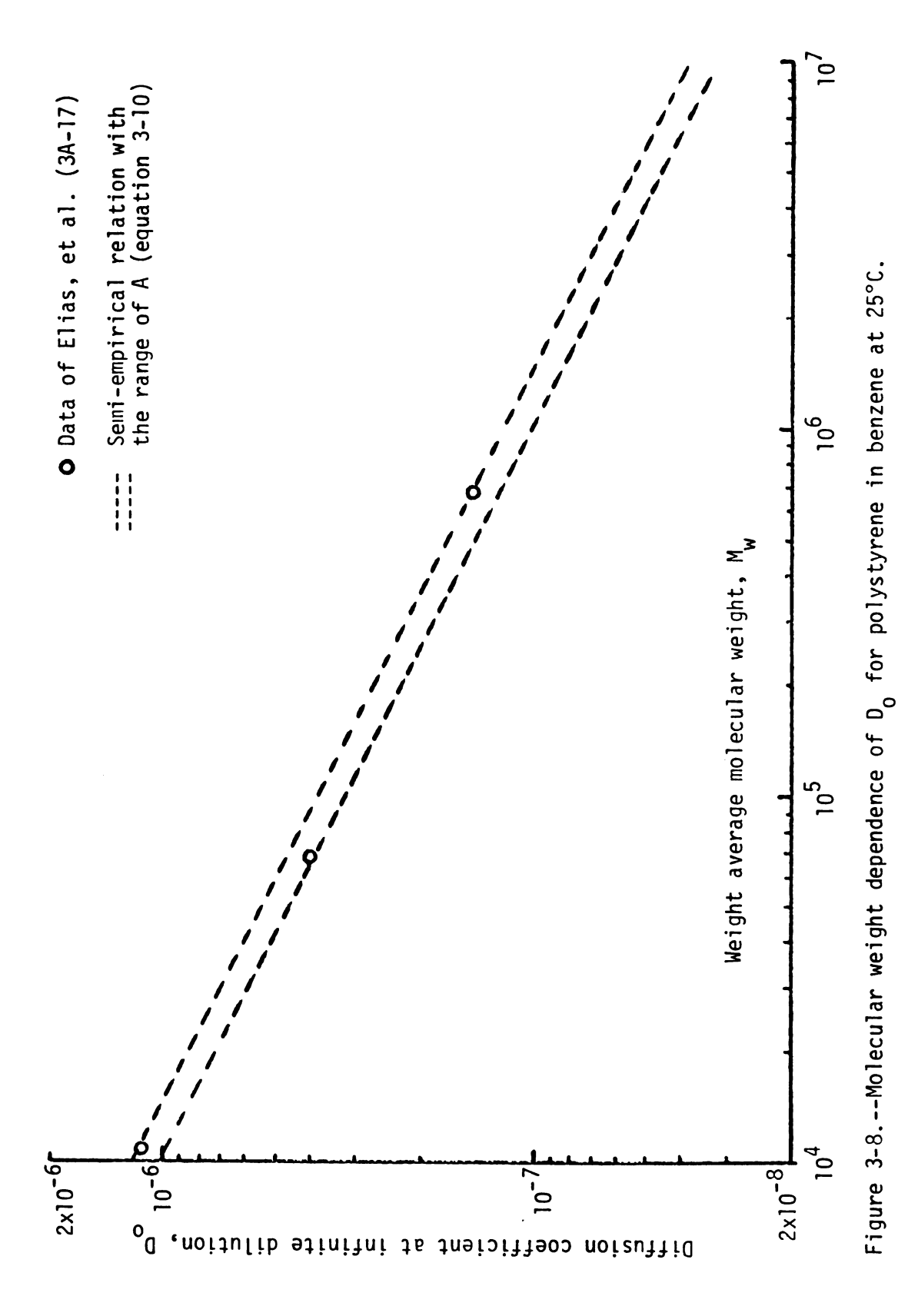
The concentration dependence of the translational diffusion coefficient in dilute polymer solutions is given by

$$D = D_0 [1 + k_d c + ...]$$
 (3-10A)

The concentration dependence of D has been the subject of a large







number of experimental and theoretical investigations. However, there still exist striking differences between the various results with regard to the concentration region within which equation 3-10A can be approximated by the first two terms (3B-1, 3A-15, 3A-7). Recently Duda, et al. (3B-2) showed that the coefficient k_d can be determined from the following equation

$$k_d = 2 A_2 M - k_s - b_1 - 2 V_{20}$$
 (3-11)

Here A_2 is the thermodynamic second virial coefficient, M is the molecular weight of the polymer and V_{20} is the partial specific volume of the polymer in the limit of zero polymer concentration. The quantity, b_1 , is defined by the series expansion

$$V_1 = V_{10} [1 + b_1 c + ---]$$

where V_1 is the partial specific volume of the solvent, and V_{10} is its value at infinite dilution. Similarly the quantity k_s is defined by the series expansion

$$f_{12} = (f_{12})_0 [1 + k_s c + ---]$$
 (3-11A)

where f_{12} is the friction coefficient defined by the following equation:

Force on a polymer molecule =
$$f_{12} (u_2 - u_1)$$

Here, u_1 and u_2 are the velocity of solvent and polymer respectively, with respect to a convenient reference frame. The parameter $(f_{12})_0$

is the value of the friction coefficient, f_{12} , in the limit of zero polymer concentration, which in theory is the same as f_0 defined in equation 3-1.

Prediction of diffusion coefficients for polymer-solvent systems in dilute solutions of polymer depend on both D_0 and k_d . In the previous section, theories for prediction of D_0 were given; the objective of this section is to devise a method for the prediction of k_d . The quantities b_1 and V_{20} in equation 3-11 can be determined experimentally. Predictions of A_2 are obtained utilizing the two parameter theory of dilute polymer solution thermodynamics. Duda, et al. (3B-3) modified the results of Pyun and Fixman (3B-4) to yield a method for predicting k_s . The rest of this section consists of a description of two parameter theory and a description of modifications to the Pyun and Fixman equations for predicting k_s . Finally the experimental values of k_d available in literature are compared with theoretical predictions.

Two Parameter Theory

A commonly accepted thermodynamic theory of polymer solutions actually consists of the results of a group of early theoretical papers which are now collectively referred to as the two parameter theory. Within the framework of the two parameter theory, the properties of dilute polymer solutions such as average molecular dimensions, second virial coefficients, etc., may be expressed in terms of two basic parameters. One is the mean square end-to-end distance $< R_0^2 >$ of a chain in the theta state, and the other is the

excluded volume parameter, which is usually designated by z. The excluded volume, and hence the parameter z, vanish at the theta condition. This is, indeed, the definition of the theta state. Therefore the heart of the two parameter theory are the interrelations between dilute solution properties and the two parameters $< R_0^2 >$ and z. A fundamental difficulty that arises in the two parameter theory is that z is not directly observable by experimental techniques. It is therefore impossible to make an explicit comparison of theory with experiment. This difficulty is circumvented by the technique discussed later in this section.

An approximate relationship for A_2 is described by Yamakawa (3B-5b), and can be expressed by the following equations:

$$A_2 = \frac{N_0 B h_0(\bar{z})}{2}$$
 (3-12)

$$\bar{z} = \frac{z}{\alpha} \tag{3-13}$$

$$z = (3/2\pi)^{3/2} \frac{M^{1/2}B}{A^3}$$
 (3-14)

The parameter B is a measure of the effective volume excluded to one segment by the presence of another and is related to the binary cluster integral β , for a pair of segments.

$$B = \beta/M_s^2$$

 $\boldsymbol{M}_{\boldsymbol{S}}$ is the molecular weight of a segment. $\boldsymbol{\beta}$ is defined by the

equation

$$\beta = \int [1 - g(R)] dr$$

where g(R) is the pair correlation function between segments with R the separation at infinite dilution. The parameter β represents the molecular interactions between segments, and can be obtained once the intermolecular potential is known. The function g(R) is a complicated function of R and is discussed in detail by Yamakawa (3B-5b).

The two parameter theory requires that α and h_0 be functions of z only. The function h_0 arises from intermolecular interactions. Duda, et al. (3B-3) suggest the use of Yamakawa-Tanaka (3B-6) expression for α and the Kurata-Yamakawa (3B-7, 3B-8) expression for h_0 :

$$\alpha = 0.541 + 0.459 (1 + 6.04 z)^{0.46}$$
 (3-16)

$$h_0(\bar{z}) = \frac{0.547 \left[1 - \left(1 + 3.903 \,\bar{z}\right)^{-0.4683}\right]}{\bar{z}}$$
 (3-17)

The above theoretical expressions are obtained by series expansion, and neglect higher order terms.

The theory does predict that $A_2=0$ and $\alpha=1$ at the theta condition, where B=0. The second virial coefficient, A_2 , increases with B, the greater the solvent power, the larger the second virial coefficient. The coefficient A_2 decreases with increasing molecular

weight. By knowing B, $\langle R_0^2 \rangle$ and M, the second virial coefficient A₂ can be predicted using equations 3-12 to 3-17.

Modified Pyun and Fixman Theory

Pyun and Fixman (3B-4) have calculated $\boldsymbol{k}_{\text{S}}$ in the expression for the frictional coefficient

$$f = f_0 (1 + k_s c + ----)$$

where f_0 is the frictional coefficient at infinite dilution, and c is the concentration of polymer in the solution. For the sake of clarity the same notation as used by Pyun and Fixman is also used here. They chose the following procedure for calculating the frictional coefficient: (1) They assumed in their model that any solvent inside the spherical polymer domain is trapped there and will be considered part of the sphere for the purpose of calculating the mean velocities, (2) They chose a particular reference point in the solution, (3) They computed the velocity of the sphere and the solvent at that point for a given configuration, (4) These quantities are then averaged over all possible configurations.

Pyun and Fixman define the friction coefficient ξ as

Force on the polymer molecule =
$$\xi$$
 (v_s - v_f)

 ${\bf v_s}$ is the average velocity of the spherical polymer cloud including the trapped solvent, and ${\bf v_f}$ is the average velocity of the untrapped solvent. The analysis of Pyun and Fixman yields the expressions

$$f = \xi (1 + \phi_v)$$
 (3-19)

$$\frac{f}{f_0} = 1 + [7.16 - k(A)] \phi_v + - -$$
 (3-20)

$$k(A) = 24 \int_{0}^{2} \left[\frac{2 \ln[1 + x + (2 + x^{2})^{1/2}]}{(2 + x^{2})^{1/2}} \right] x^{2} \exp$$
(3-21)

$$[-A_1(1 - x^2) (2 + x)] dx$$

$$A_1 = 3 n^2 X_s / 8 \pi a_s^3$$
 (3-22)

where ϕ_V is the volume fraction of spheres, n is the number of segments per molecule, X_S is the second virial coefficient for segment-segment interactions, and a_S is the radius of a sphere composed of solute and trapped solvent.

Duda, et al. (3B-3) modified the results of Pyun and Fixman based on the assumption that the radius a_s in equation 3-22 and hence the quantity A_1 , depend on polymer concentration. They first obtained a relation between ξ of Pyun and Fixman and f_{12} of equation 3-11A to facilitate the utilization of the Pyun and Fixman theory. Secondly they wrote series expansions for a_s , A_1 , and k(A) in terms of increasing powers of c, the polymer mass concentration, and substituted these expressions into 3-20, to arrive at

$$k_s = [7.16 - k(A^*)] 4\pi a_0^3 N_0/3M - V_{20} - b_1$$
 (3-23)

$$k(A^*) = 24 \int_{0}^{1} \left[\frac{2 \ln[1 + x + (2x + x^2)^{1/2}]}{(2x + x^2)^{1/2}} \right] x^2 \exp$$
(3-24)

$$[-A(1 - x^2) (2 + x)]dx$$

$$A^* = \frac{4096 \text{ z}}{72 \text{ m } \alpha} \tag{3-25}$$

$$a_0 = \frac{\sqrt{6\pi M} \quad A \quad \alpha}{16} \tag{3-26}$$

where A, z, and α are defined in equations 3-3, 3-14 and 3-16.

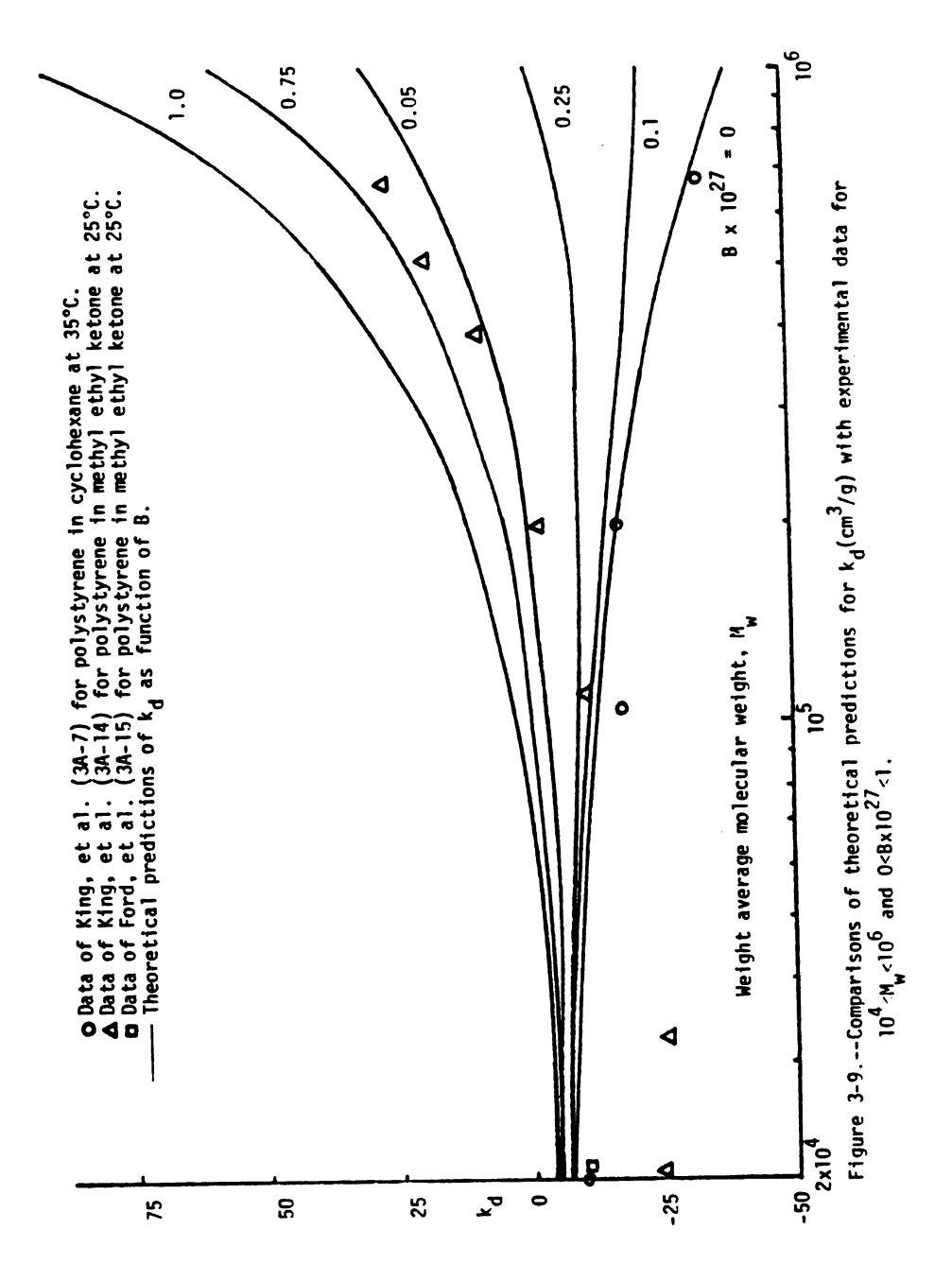
Therefore k_s can be predicted using equations 3-23 to 3-26. It is clear that if A, B, V_{20} and b_1 are known or can be estimated for a particular polymer-solvent pair, then equations 3-12 to 3-17 and 3-23 to 3-26 can be used to predict k_d as a function of molecular weight of the polymer for that particular polymer-solvent pair.

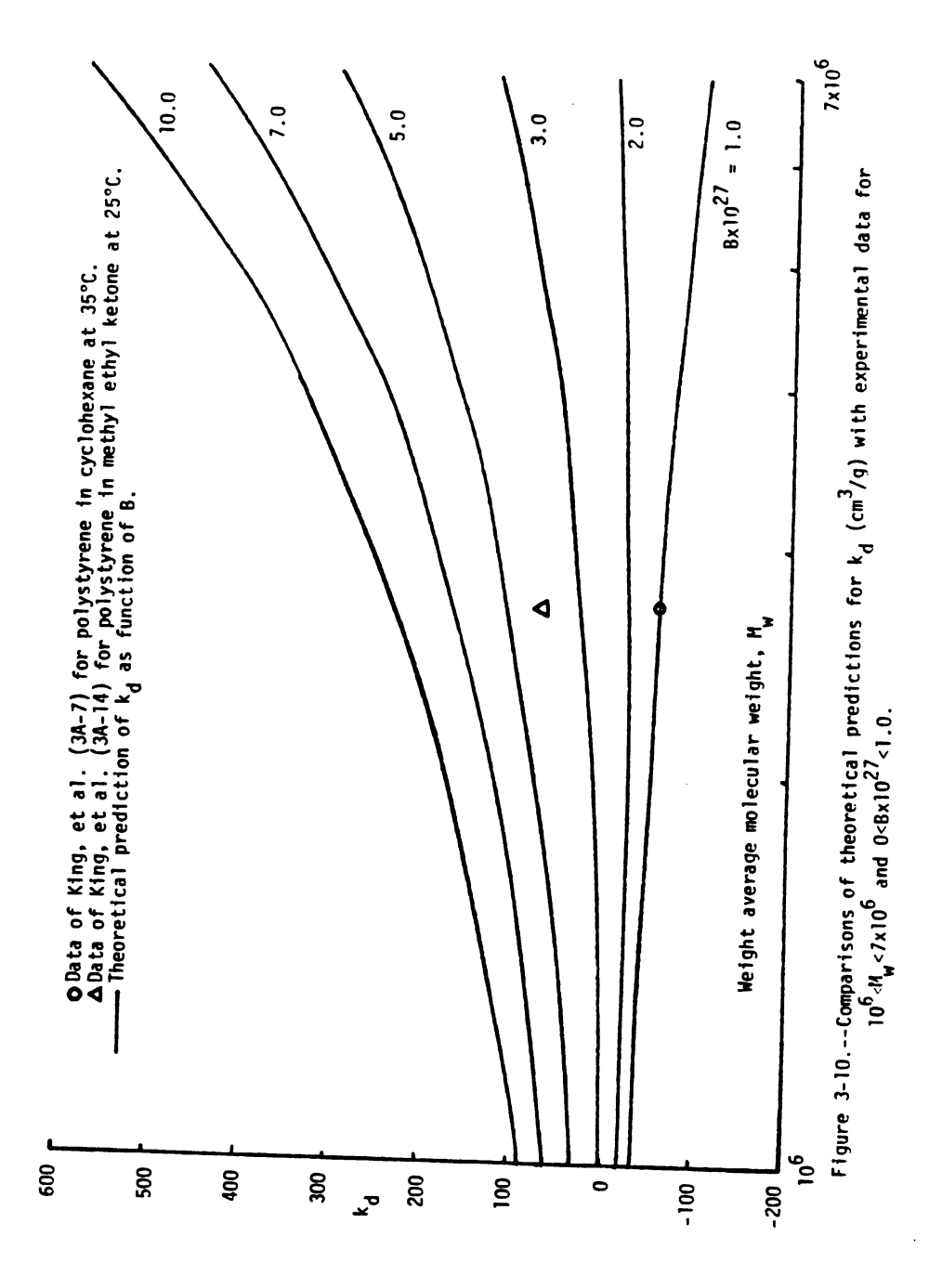
Comparison of Predicted Values of k_d with Experimental Data

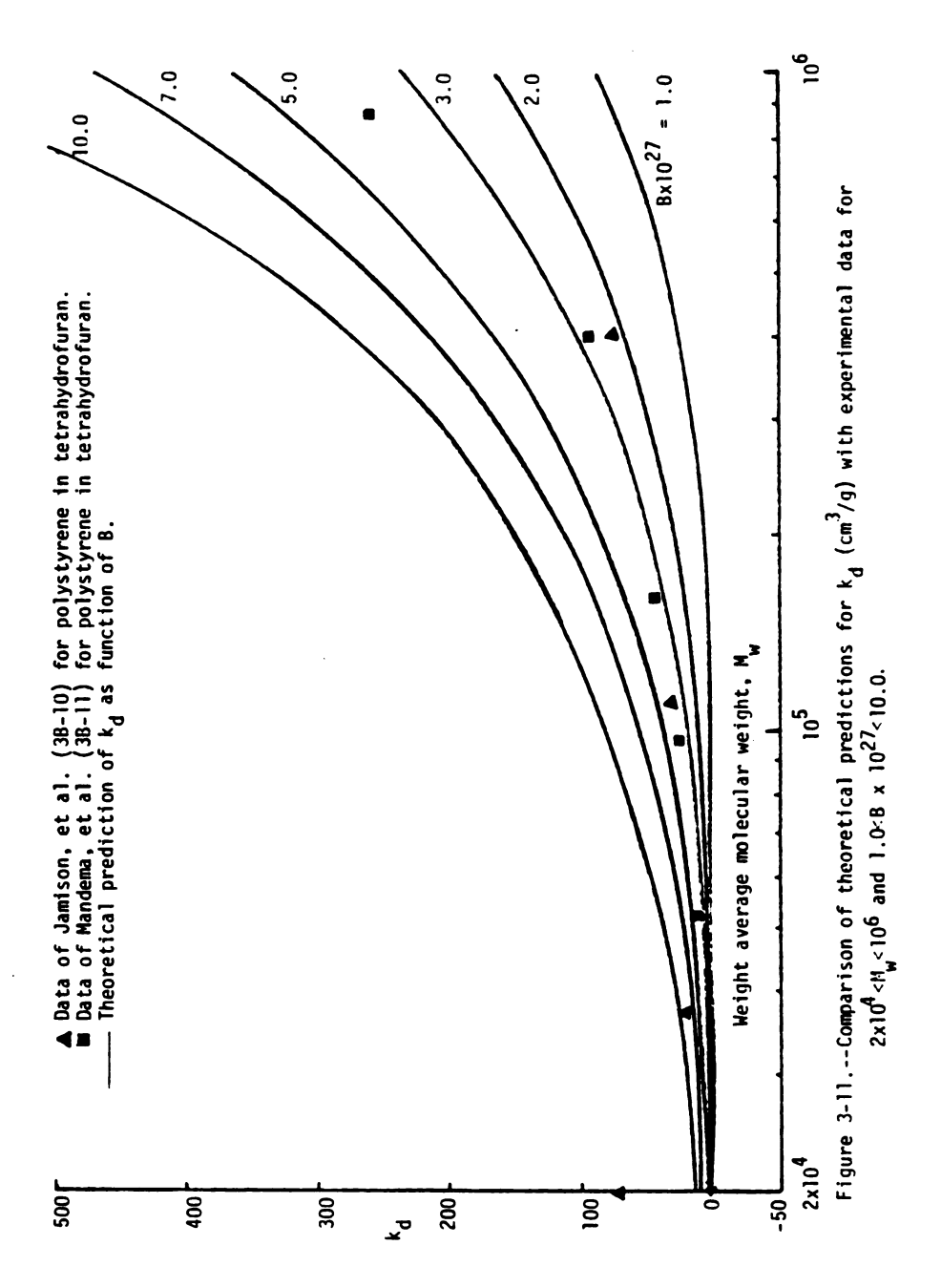
A FORTRAN program was written using equations 3-12 to 3-17 and 3-23 to 3-26. The inputs to the program were polymer molecule weight, M, the parameter A, and the excluded volume parameter B. Since B is not known precisely for any polymer solvent pair, a range of values of B were used. Using the program the values of k_d were generated as a function of molecular weight for polystyrene. The results of the computer program are displayed in Figures 3-9 through

3-11. All these figures contain theoretical predictions of k_d for polystyrene as function of polymer molecular weight and the excluded volume parameter, B. Figure 3-9 illustrates molecular weight dependence of \boldsymbol{k}_{d} for the values of B in the range of O to $1 \times 10^{-27} \text{cm}^3$, and polymer molecular weight in the range of 2 x 10^4 to 10^6 . Figure 3-10 is similar to Figure 3-9, except the molecular weight range is from 10^6 to 7×10^6 . Figure 3-11 is similar to Figure 3-9, with the values of B in the range of 1×10^{-27} to $10 \times 10^{-27} \text{cm}^3$. The value of A used was $700 \times 10^{-11} \text{cm}$. (3A-9), b = 0, and $V_{20} = 0.9 \text{cm}^3/\text{gram}$. The value of A in the literature varies from 645×10^{-11} to 755×10^{-11} cm, so the mid value in the range was chosen. The above value of V_{20} is for pure polystyrene. Since b_1 is not known for the polymer-solvent pairs used in this work, it was assumed to be zero. The choice of V_{20} and b_1 are not critical until the value of k_d is less than 10 cm^3/gram . Even at this low value of $\mathbf{k_d},~\mathbf{V_{20}}$ and $\mathbf{b_1}$ contribute only about 10% of the total value of k_d.

From Figures 3-9 to 3-11, it can be concluded that the value for k_d under theta conditions is always negative (the curve corresponding to B = 0), and decreases significantly as molecular weight is increased. As the polymer-solvent systems move away from the theta condition (increasing values of B), k_d has negative values for low molecular weights, but becomes positive as the molecular weight is increased. For diffusion in good solvents (large values of B), k_d is always positive for all molecular weights in the range of 10^4 to 10^7 . Therefore, for diffusion in dilute polymer solutions, D







should always decrease with concentration under theta condition, and D should always increase with concentration in good solvents. For solvents between these extremes, D should decrease with concentration for low molecular weight polymers, and should increase with concentration for high molecular weight polymers. This type of behavior was observed experimentally by Paul, et al. (3B-9) for diffusion of polystyrene in cyclohexanone.

As was pointed out earlier the excluded volume parameter, B, is not explicitly known for any polymer-solvent pair. Therefore, the very meager experimental data available for k_d in the literature were also shown on Figures 3-9 to 3-11. This was done in order to see if a single value of B is sufficient to predict the molecular weight dependence of k_d in the molecular weight range of interest. The experimental data of King, et al. (3A-7) for polystyrene in cyclohexane at the theta condition can be satisfactorily represented by the theoretical prediction with B = 0. This comparison of experiment with the theory does confirm the fact that at the theta condition the excluded volume parameter, B, is equal to zero. For polystyrene in a good solvent such as tetrahydrofuran, the theoretical curve with $B = 3 \times 10^{-27}$ and the data of Jamieson, et al. (3B-10) and Mandema, et al. (3B-11) agree quite well. It was shown by Duda, et al. (3B-3) that the data for polystyrene in toluene can be satisfactorily represented by the theoretical predictions with a value of $B = 2 \times 10^{-27}$. This value of B for the polystyrene-toluene system compares well with the value of B obtained from viscosity plots for the same system (3B-5e). Thus it can be concluded that the method for predicting $\mathbf{k}_{\mathbf{d}}$

under theta conditions and with good solvents appears to be satisfactory. However, it should be pointed out that the data of King, et al. (3A-14) and Ford, et al. (3A-15) are not in agreement with each other for the system polystyrene in methyl ethyl ketone. Compared with the theoretical curve it may be suggested that the data of King, et al. at low molecular weight is suspect. On the other hand at high molecular weight of 6.7 x 10^5 , the value of k_d reported by Ford, et al. is 190 cm 3 /gram. This point could not be shown on the Figure 3-9. Thus at high molecular weights, the value of k_d reported by Ford, et al. is suspect compared to theory. A detailed discussion concerning these discrepancies is presented in Chapter VII.

It is evident that the agreement between theory and experiment for polystyrene in methyl ethyl ketone is not very good. However, the data above a molecular weight of 2 x 10^5 can be approximately represented by a value of B = 0.5 x 10^{-27} , which compares well with a value of B = 0.75 x 10^{-27} reported by Berry and Casassa (3B-12) obtained from viscosity plots. This value of B also compares well with the value reported by Kurata (3B-5), B = 0.667 x 10^{-27} , obtained from viscosity plots for the same system. It appears reasonable to conclude that the method developed by Duda, et al. (3B-3) for predicting k_d by the combination of two parameter theory and modified Pyun and Fixman theory provides reasonable estimates for polymer-solvent systems with polymer molecular weight in the range of 2 x 10^5 to 10^7 . At low molecular weights, a critical analysis of the experimental data must be made.

CHAPTER IV

POLYMERIZATION AND FRACTIONATION

Styrene-acrylonitrile copolymers used in this work were synthesized by bulk, free radical polymerization. This was done in order to synthesize copolymers free of contamination from solvents used in polymerization, and to obtain a large quantity of each copolymer, with restricted conversion of monomers to copolymers. The latter condition is required to obtain uniform composition in the copolymer. This chapter contains a brief summary of the theory of copolymerization and a description of the synthesis of the copolymers. This is followed by the method adopted for fractionating the copolymers. Fractionations were performed to obtain polymers of low polydispersity.

Copolymerization Theory

The kinetic mechanisms of free radical polymerization of two monomers in solution have been well established (4A-1). The copolymerization of two monomers M_1 and M_2 leads to two types of propagating species, one with M_1 at the propagating end and the other with M_2 . Therefore, the four different chain growth steps are

$$M_1^* + M_1 \xrightarrow{k_{11}} M_1^*$$
 (4-1)

$$M_1^* + M_2 \xrightarrow{k_{12}} M_2^*$$
 (4-2)

$$M_2^* + M_1 \xrightarrow{k_{21}} M_1^*$$
 (4-3)

$$M_2^* + M_2 \xrightarrow{k_{22}} M_2^* \tag{4-4}$$

where superscript * denotes a radical at the end of a growing chain, subscripts 1 and 2 indicate the two types of monomers and k_{ij} 's are propagation rate constants.

If one assumes, as is commonly done in the development of free radical copolymerization theory, that the reactivity of the growing chain depends only on the terminal unit, and that any instant in the polymerization the total population of free radicals is at steady state, the following expression can be obtained (4A-1).

$$F_{1} = \frac{r_{1}f_{1}^{2} + f_{1}f_{2}}{r_{1}f_{1}^{2} + 2f_{1}f_{2} + r_{2}f_{2}^{2}}$$
(4-5)

where F_1 is the instantaneous mole fraction of monomer M_1 in the copolymer formed, f_1 and f_2 are the mole fractions of monomer M_1 and M_2 in the monomer mixture, and

$$r_1 = k_{11}/k_{12}$$

$$r_2 = k_{22}/k_{21}$$

for styrene and acrylonitrile at 60° C, r_1 is 0.41 and r_2 is 0.04 (4A-1).

Since the values of r_1 and r_2 are both less than unity, the F_1 versus f_1 curve crosses the line representing $F_1 = f_1$. At this intersection, the copolymer and monomer mixture compositions are the same and copolymerization occurs without a change in the overall composition. Such copolymerizations are termed azeotropic copolymerizations. The condition under which azeotropic copolymerization occurs is given by

$$F_1 = f_1 = \frac{(1 - r_2)}{(2 - r_1 - r_2)}$$
 (4-6)

For all copolymerizations other than azeotropic, the comonomer and copolymer compositions could be different from each other at any time during the polymerization. For styrene-acrylonitrile copolymer, the azeotropic composition, from equation (4-6), occurs at $F_1 = f_1 = 0.6194$ mole fraction or at 0.7615 weight fraction of styrene.

Rate of Copolymerization

The rate of copolymerization, unlike the copolymer composition, depends on the initiation and termination steps as well as on the propagation steps. In the usual case both monomers combine efficiently with the initiator radicals and the initiation rate is independent of the feed composition. Two different approaches have been used to derive expressions for the rate of copolymerization.

Chemical-controlled termination.--This approach assumes the termination reaction to be chemically controlled. Copolymerization consists of four propagating reactions (4-1 to 4-4) and the three termination steps

$$M_1^* + M_1^* \xrightarrow{k_{t11}}$$
 (4-7)

$$M_1^* + M_1^* \xrightarrow{k_{t11}}$$
 (4-7)
 $M_2^* + M_2^* \xrightarrow{k_{t22}}$ dead polymer (4-8)
 $M_2^* + M_1^* \xrightarrow{k_{t12}}$ (4-9)

$$M_2^* + M_1^* \xrightarrow{k_{t12}}$$
 (4-9)

corresponding to termination between like radicals, equations 4-7 and 4-8, and cross termination between unlike radicals, equation 4-9. The rate of copolymerization is then given as (4A-1)

$$R_{p} = \frac{(r_{1} [M_{1}]^{2} + 2[M_{1}] [M_{2}] + r_{2} [M_{2}]^{2}) R_{i}^{1/2}}{(r_{1}^{2} \lambda_{1}^{2} [M_{1}]^{2} + 2 \phi_{k} r_{1} r_{2} [M_{1}] [M_{2}] + r_{2}^{2} \lambda_{2}^{2} [M_{2}]^{2})^{1/2}}$$
(4-10)

where R_i is the rate of initiation of chain radicals of both types, and

$$R_i = 2 f k_{de}[I]$$
 ; $\lambda_1 = (2 k_{t11}/k_{11}^2)^{1/2}$

$$\lambda_2 = (2 k_{t22}/k_{22}^2)^{1/2}$$
; $\phi_k = k_{t12}/2(k_{t11} k_{t22})^{1/2}$

[I] represents initiator concentration, moles/liter; k_{tii} and k_{ii} are termination and propagation reaction rate constants for monomer i;

 fk_{de} is the effective initiator decomposition rate constant, and k_{t12} contained in ϕ_k , is a cross termination rate constant. Values of ϕ_k <1 indicate that cross-termination is not favored, while ϕ_k >1 favors cross-termination.

<u>Diffusion-controlled termination</u>. A kinetic expression for the rate of diffusion-controlled copolymerization was obtained by North and Atherton (4A-2) by considering the termination reaction as

$$M_1^* + M_1^*$$
 $M_1^* + M_2^*$
 $M_2^* + M_2^*$

dead polymer (4-11)

where the termination rate constant $k_{t(12)}$ is a function of copolymer composition. Then the rate of copolymerization was found to be

$$R_{p} = \frac{(r_{1} [M_{1}]^{2} + 2 [M_{1}] [M_{2}] + r_{2} [M_{2}]^{2}) R_{i}^{1/2}}{k_{t(12)}^{1/2} (r_{1} [M_{1}]/k_{11} + r_{2} [M_{2}]/k_{22})}$$
(4-12)

where $[M_1]$ and $[M_2]$ are the concentrations of the two monomers.

Synthesis of Copolymers

Styrene-acrylonitrile copolymers used in the diffusion measurements in this work were synthesized by free radical polymerization in bulk. To do the synthesis it was necessary to analyze which of the two kinetic mechanisms, equations 4-10 or 4-12, is useful for

predicting the rates of styrene-acrylonitrile copolymerizations. Blanks and Shah (4A-3) showed that neither the kinetic φ_k factor alone, nor the diffusion parameter $k_{t(12)}$ alone, satisfactorily describe the data for copolymerization of styrene and acrylonitrile. Since the theoretical rate expressions could not be relied upon to determine the time of reaction for required conversion, it was decided to use the kinetic data of Shah (4A-4), which he obtained from small scale experiments. The three copolymers that were synthesized were all of azeotropic composition. This was done in order to ensure copolymers of uniform chemical composition, so that chemical hetrogenity corrections may be neglected in the diffusion measurements.

Initiator

The initiator used in this work for the synthesis of styrene-acrylonitrile copolymers is α - α '-Azo-Bis-Isobutyronitrile (AIBN). The reasons for using AIBN are: (1) The rate of initiation is independent of monomer composition, because AIBN releases primary radicals that combine efficiently with both monomers; (2) the spontaneous decomposition rate of AIBN is substantially independent of the reaction medium; and (3) unlike benzoyl peroxide, AIBN is not susceptible to induced decomposition. The AIBN, obtained from Eastman Kodak Company, was purified by recrystallization from acetone. A large quantity was dissolved in acetone at room temperature till saturation. The solution was filtered, and cooled in an ice water bath until a crop of crystals were obtained. The procedure was

repeated twice and the crystals were dried under vacuum at room temperature. The purified AIBN crystals were stored in a refrigerator.

Monomers

Both the monomers used in this work, styrene (ST) and acrylonitrile (ACN) were of high purity when they were obtained from the manufacturers. Styrene was obtained from Dow Chemical Company and acrylonitrile from Eastman Kodak Company. The containers were stored in a refrigerator and only the approximate amounts needed for each run were withdrawn at one time. The required monomers for an experiment were withdrawn and passed through columns of activated alumina to remove the dissolved inhibitor. The inhibitor-free monomers were used in the polymerization reactions.

Polymerizations

Each polymerization reaction was carried out in a two-liter, round-bottomed flask at 60°C under nitrogen atmosphere. Cold monomer mixture was heated up to 60°C in the reactor as quickly as possible, and then the initiator AIBN was added. After completion of the reaction, the contents of the flask were poured into chilled methanol in a waring blender to precipitate the polymer. The volume of methanol used for each precipitation was four times the volume of the reaction mixture. The polymers were then redissolved in methyl ethyl ketone, filtered, and reprecipitated in methanol. The polymers were dried to constant weight in a vacuum oven at 30°C, for

approximately ten hours. Table 4-1 gives the details of bulk polymerization at 60°C using AIBN.

Molecular Weights and Molecular Weight Distribution

Samples of all the polymers that were synthesized were sent to the analytical laboratories of Dow Chemical Company for determination of molecular weight and molecular weight distribution by Gel Permeation Chromatography (GPC). Table 4-2 contains the GPC results. The GPC results were cross checked against results from viscometry.

Fractionation of Copolymers

Polymer fractionation experiments were performed for preparing copolymers of narrow molecular weight distribution. The
method used was fractional precipitation. Fractional precipitation
offers the best opportunity for a close approach to equilibrium and,
thereby, the greatest efficiency in each step. One of the practical
difficulties with the method is the long time required for the
settling of the precipitate with the result that about one day is
required for the separation of each fraction. The large volumes of
solution that must be handled in this method also pose a problem.
For efficient fractionation, precipitation must be carried out at
low concentration, about one percent for low molecular weight
polymer and one tenth of a percent for polymer of one million
molecular weight. This means that in fractionation of a 25 gram

TABLE 4-1.--Details of bulk polymerization at 60°C using AIBN.

ייייייייייייייייייייייייייייייייייייייי	ואטרר אין.יייטפנמון?		polymer 12ac 10.	of buth polymerization at 60 c using Albin.	. IDIN .		
Polymer	Monomer Composi Styl	Monomer Mixture Composition for Styrene	Amount of Monomer Mixture	Initiator Concentration	Amount of Initiator	Reaction Time	Amount of Copolymer Obtained
	Mole%	Weight%	Grams	MOles/Liter	urams	Minutes	Grams
SAN-1	62.0	76.2	1000	0.03216	5.9989	50	125
SAN-2	62.0	76.2	1000	0.00477	0.8908	130	107
SAN-3	62.0	76.2	1000	0.0008	0.1492	151	40

TABLE 4-2.--Molecular weight and molecular weight distribution of copolymers by GPC.

Polymer	M _w	^M n	M _z	M _w /M _n
SAN-1	211,700	135,500	321,100	1.6
SAN-2	398,400	239,700	553,500	1.7
SAN-3	749,300	550,900	921,800	1.4

sample one is dealing with initial solution volumes of 2.5 liters to 25 liters.

Shimura, et al. (4C-1) investigated the fractionation of styrene-acrylonitrile (SAN) copolymers of azeotropic composition by precipitation from chloroform using methanol as a non-solvent at 30°C. Mino (4C-2) fractionated SAN copolymer containing 26% of acrylonitrile by dissolving it in chloroform and separating it with benzene, then redissolving the precipitate in chloroform and precipitating with methanol. Ljerka (4C-3) used the following solvent-non solvent systems for SAN copolymers: benzene-triethylene glycol at 60°C and dichloromethane-triethylene glycol at 25°C. Since there was no agreement in the literature, on the solvent-non solvent pair for fraction of SAN copolymer, we decided to run some small scale fractionations for finding the better solvent-non solvent pair.

Small-Scale Fractionations

Small-scale fractionations were performed on six solvent-non solvent pairs. The results of the fractionations are presented in Table 4-3. Only one non solvent was used; this was methanol. Six solvents were used; they were: chloroform, benzene, acetone, tolune, methyl ethyl ketone, dimethyl formamide. All the fractionations were performed at room temperature. From the results presented in Table 4-3, it was decided to use chloroform and methanol as the solvent-non solvent pair. One of the reasons for deciding on this particular system was the small amounts of solvent and non solvent

TABLE 4-3.--Results of small-scale fractionations.

Solvent	Non solvent	Grams of polymer	Amount of solvent used, cm ³	Amount of non solvent added till the appear- ance of first precipitate	Comments on the appearance of first precipitate	Comments on the clarity of solution and the precipitate after it was allowed to settle for 24 hours
Chloroform	Methanol	1.6058	31.26	27.33	Appearance of cloudiness was precise and very clear	The precipitate has settled to the bottom of the container
Benzene	Methanol	1.6007	52.74	36.00	Appearance of cloudiness not clear	The precipitate has settled but the solution was still cloudy
Acetone	Methanol	1.6387	60.31	34.00	Appearance of cloudiness not clear	The precipitate has settled and the solution was not cloudy
Toluene	Methanol	1.6119	54.00	•	The system was discarded because the solution was cloudy initially	The undissolved polymer settled to the bottom of the container
Methyl ethyl ketone	Methanol	1.6067	57.83	42.50	Appearance of cloudiness not clear	Precipitate has set- tled and the solu- tion was not cloudy
Dimethyl formamide	Methanol	1.6295	50.23	81.50	Appearance of cloudiness was clear	Precipitate has settled and the solution was not cloudy

needed compared to other systems. The amount of solvent used was calculated from the following equation (4C-4)

Volume fraction of copolymer in solution =
$$1/X_n^{1/2}$$
 (4-13)

Large-Scale Fractionations

The aim of the fractionation was to obtain copolymer of low polydispersity. It was decided to obtain only the low molecular weight fraction of SAN-1, the middle fraction of SAN-2, and the high molecular weight fraction of SAN-3. All the large-scale fractionations were performed at 25°C in a 4.5 liter flask. The volume fraction of polymer dissolved in chloroform was calculated using equation 4-13. This clear solution was filtered and methanol added until a cloudiness appeared. The solution was then warmed to 35°C and allowed to cool to 25°C. The precipiate was removed and redissolved in chloroform and reprecipitated in chilled methanol in a waring blender. The fraction obtained was dried to constant weight in a vacuum oven at 30°C. Table 4-4 contains the results of the final three fractions for the three copolymers that were fractionated. Small amounts of these fractionations were sent to the analytical laboratory of Dow Chemical Company for determination of molecular weights and molecular weight distributions by Gel Permiation Chromatography. Table 4-4 also contains the Gel Permiation Chromatography results.

Comparison of the polydispersity ratios (ratio of $\rm M_W/M_{\rm n}$) of the copolymers in Table 4-2, with those of the fractions in

TABLE 4-4.--Results of large-scale fractionations.

Fraction	Weight of copolymer used in fractionation, grams	Amount of fraction obtained, grams	Σ3	Σ	ν Σ	E _R
Low molecular weight fraction of SAN-1	35.4	6.21	147,600	100,600	212,000	1.5
Middle molecular weight fraction of SAN-2	64.2	8.41	572,100	379,700	741,500	1.5
High molecular weight fraction of SAN-3	38.8	7.04	833,600	594,000	1,025,800	1.4

Table 4-4, shows that the fractionation was not very successful. No additional work was carried out with these fractions in this investigation. Instead the copolymers were used as they were, with polydispersity ratios of 1.4 to 1.6. It should be noted, however, that the Gel Permeation Chromatography apparatus used by the Dow Chemical Company to obtain the polydispersity ratios for the copolymers had been calibrated with polystyrene samples. Thus the ratios may not reflect the true molecular weight distributions in these copolymer samples. However, because of the time and expense required to obtain polydispersity measurements by other techniques, the copolymers were used for the diffusion studies without further analysis.

CHAPTER V

EXPERIMENTAL METHODS FOR MEASURING DIFFUSION COEFFICIENTS

<u>Light Beating Spectroscopy</u>

Recent developments in the technique of laser light beating spectroscopy make it possible to measure polymer diffusion coefficients in solution with accuracies on the order of 3 to 4%, in as little as a few minutes. In principle this makes light beating spectroscopy an attractive tool for measuring diffusion coefficients of macromolecules in solution. Although diffusion measurements for homopolymers have been reported by this method (3A-7, 3A-14, 3A-15 for example), relatively few applications of the method to solutions of copolymers have been reported (5A-3, 5A-4).

Background

The interaction of light with matter has provided, for a long time, information on molecular structure and behavior of molecules in solution. When light is allowed to pass through a perfectly homogeneous transparent solution, it will not be scattered. If, however, the solution contains inhomogeneities, as most solutions do, the inhomogeneities or local fluctuations in the dielectric constant cause the incident light to be scattered. Most investigators are familiar with the classical use of light scattering for

polymer solutions. The scattered light intensity is measured as a function of scattering angle, which provides information about the weight average molecular weight, shape and size of polymer in solution and also information pertaining to the thermodynamic interaction between the polymer and solvent (virial coefficients). In addition, however, information about the Brownian motion of molecules in solution can be obtained by studying the spectral distribution of the scattered light (5A-19).

The frequency of the scattered light is not exactly the same as the frequency of the incident light. This was first observed experimentally by Gross (5A-5). He observed a spectrum consisting of three peaks (refer to Figure 5-1). One peak was below and one peak was above the incident light frequency, and they were positioned symmetrically about the incident light frequency. The third (central) peak was unshifted in frequency. The two shifted peaks are due to the Doppler shift of the frequency of the light caused by thermally excited sound waves of extremely high frequency. The wave lengths of the sound waves are of the same order as the wave length of the incident light, although the frequencies are widely different, because of the difference in propagation rate of sound and light. The velocity of the sound waves can be calculated from the frequency shift of the Brillouin peaks (refer to Figure 5-1), and the lifetimes of the sound waves can be found from the width of the Brillouin peaks. This implies that a study of the Brillouin peaks can give information about the thermal and transport properties of the solution at frequencies around 10¹⁰Hz. Adequate resolution for

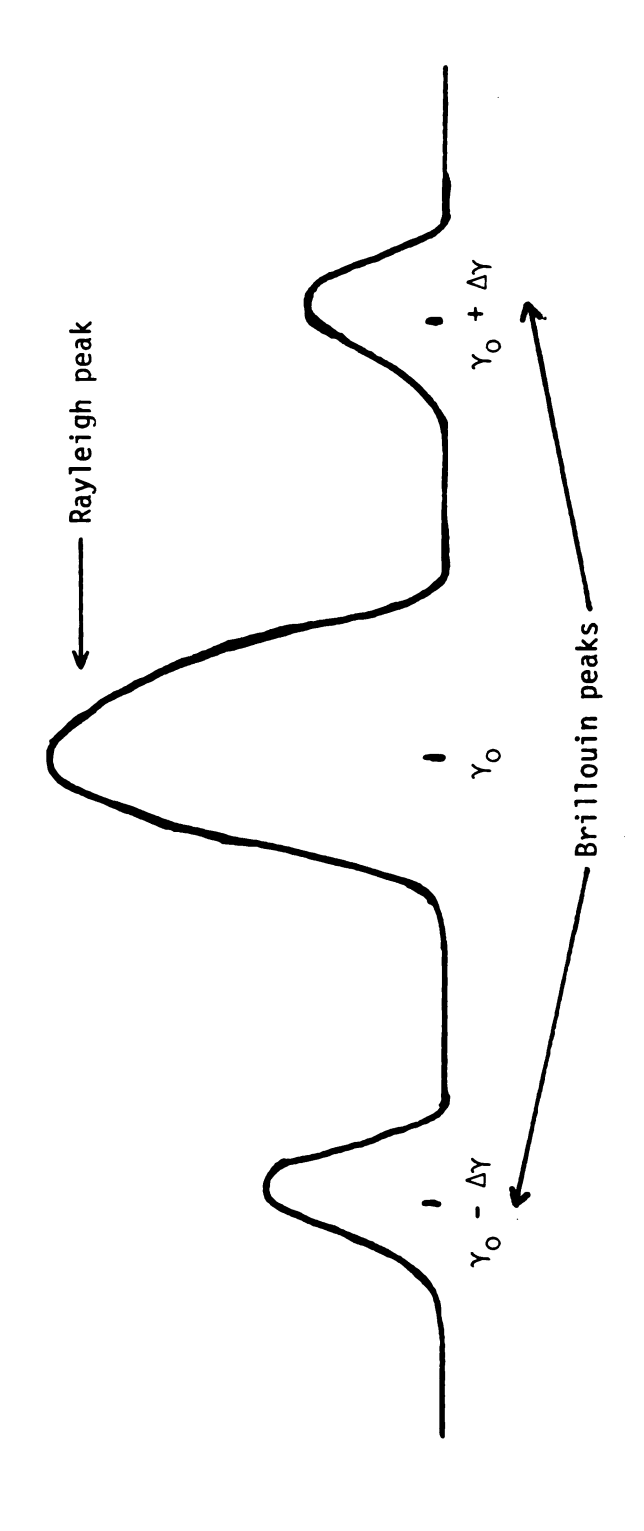


Figure 5-1.--Spectrum of scattered light for polymer solutions.

 $\gamma_{\rm O}$ - frequency of incident light

the Brillouin peaks can be obtained with a pressure scanning Fabry-Perot interferometer, which is used to study viscoelastic relaxation process in polymers. The center peak, called the Rayleigh peak (refer to Figure 5-1), is often of a Lorentzian functional form with half width proportional to the diffusion coefficient (5A-6). For solutions of polymers the Rayleigh peak contains information about the rates of motions as well as the types of motions of the polymer molecules. Pecora has derived theoretical equations which relate the shape of the spectra to translational diffusion of rods, spheres and gaussian coils; rotational diffusion of rods; and intermolecular motions of flexible coil polymers (5A-7 to 5A-12), to molecular parameters.

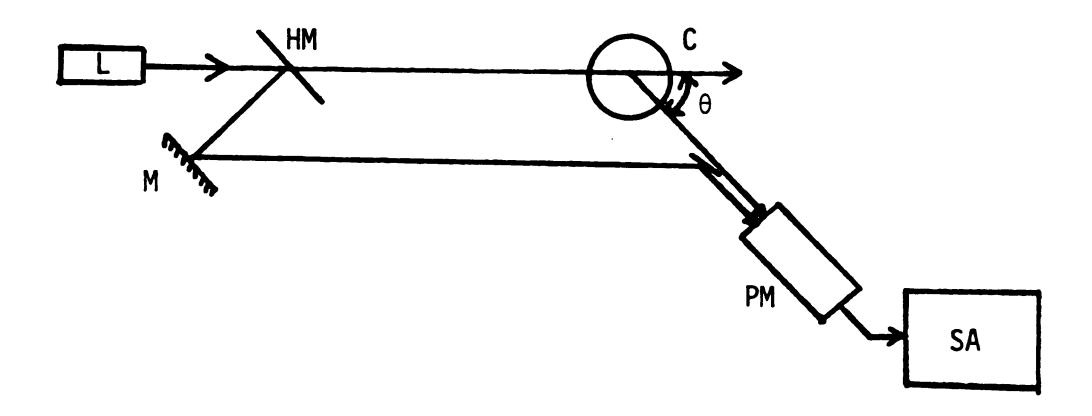
Experimental techniques have been developed apace with the theoretical work of Pecora. As a result, during the past decade, light beating spectroscopy has developed into a major new method for analyzing optical fields with an effective resolution orders of magnitude greater than was available with traditional spectroscopic techniques. Forrester, et al. (5A-13) proposed that two beams of light with slightly differing frequencies could be mixed (heterodyned) resulting in a beat note which could be detected in a nonlinear detector. This concept was accomplished experimentally with the aid of lasers. Since lasers have an extremely narrow line width of a few Hz or less, it is possible to detect frequency shift as small as 10 Hz. This high level of sensitivity makes possible the study of thermodynamic properties and transport coefficients that constantly fluctuate about mean values.

The first experimental application of the principle of light beating spectroscopy to study polymer solutions was made by Cummins, et al. (5A-14). They developed an optical heterodyne technique shown in Figure 5-2. The scattered beam from the solution and the reflected beam from the laser follow parallel paths to the surface of a photomultiplier tube. The photomultiplier tube observes the beating of the scattered light with the reflected laser light.

Later the optical self beat method, shown in Figure 5-2, was developed (5A-15). The scattered light at the photodetector has a frequency distribution. The components of this spectrum beat with each other causing fluctuations in the output current of the photomultiplier tube which are analyzed by a spectrum analyzer. The optical self beat spectrometer is superior to the heterodyne system, in that it is much simpler from the experimental point of view, the half width is twice as large as that of the optical heterodyne method resulting in improved accuracy, and it does not detect any uniform motion of the solution (i.e. convection does not affect the measurement). The optical self beat method was used in this work.

A survey of the literature shows that the technique of light beating spectroscopy has been used to obtain the spectrum of scattered light from many types of polymer solutions and solutions containing biologically interesting molecules, with components whose molecular weight ranges from 10⁴ to 10⁸. The theory and experimental aspects of light beating spectroscopy are thoroughly discussed in the literature; for example, reference may be made to recent review articles (5A-16, 5A-17, 5A-18, 5A-19, 5A-20), several of which

A. Optical heterodyne method:



B. Optical homodyne method:

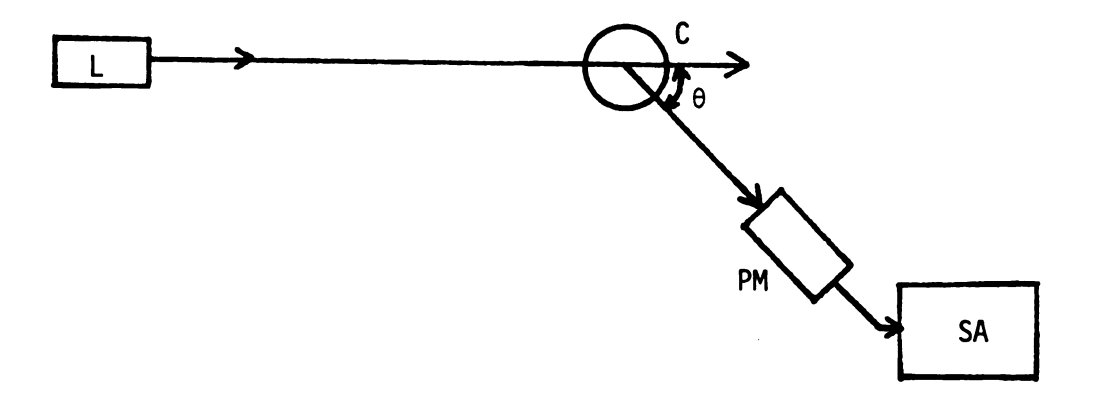


Figure 5-2.--Differences in heterodyne and homodyne methods.

L - laser light source HM - half silvered mirror M - full reflection mirror C - sample cell

PM - photomultiplier tube

SA - spectrum analyzer θ - scattering angle

contain extensive bibliographies. Other recent work of interest in polymer solutions are studies of polystyrene in the following solvents: cyclohexane (3A-7, 5A-21, 5A-22), methyl ethyl ketone (3A-14, 3A-15, 5A-25), tetrahydrofuran (3B-10, 3B-11) and benzene (5A-27).

Theory

Since the technique of light beating spectroscopy has been thoroughly discussed in the literature, only the relevant portion of the theory will be discussed here. In order to measure the spectrum of scattered light centered at the incident laser frequency of about 5.83×10^{14} Hz ($5145 \, ^{\circ}$ A), and to obtain a measurement of the half width of the spectrum, in the order of 50 to 10,000 Hz, a resolution of about 10^{10} to 10^{11} Hz is required. This very high resolution is achieved by optical beating leading to the name "Light Beating Spectroscopy."

Beat frequency.--For the sake of clear understanding of what a beat frequency is, let us consider a simple example that illustrates the self beating technique. Suppose that the light incident on the photocathode surface of a photomultiplier tube contains only two component waves with only two discrete frequencies, w_1 and w_2 . The electric field of this light spectrum is represented by

$$E(t) = A \cos w_1 t + B \cos w_2 t \qquad (5-1)$$

where A and B are constants and t is time. The light beating

technique employs a unique property of the photomultiplier tube, namely that the current output of the tube is proportional to the square of the incident electric field (or power) of the light striking the photocathode. Therefore

$$i(t) = C E^{2}(t)$$
 (5-2)

where C is a constant. Substitution of equation 5-1 into equation 5-2 gives

$$i(t) = C \left[A^{2}(1 + \cos 2w_{1}t)/2 + B^{2}(1 + \cos 2w_{2}t)/\right]$$

$$(5-3)$$

$$2 + AB \cos(w_{1} + w_{2})t + AB \cos(w_{1} - w_{2})t$$

The photomultiplier tube does not have an unlimited frequency response and the highest frequency that it can follow is limited to approximately one kilomegahertz. Therefore the first three terms in equation 5-3 result in a D.C. electrical component. The fourth term, however, is a low frequency component and the frequency difference is referred to as the "beat frequency." It is this component which is measured and resolved by light beating spectroscopy.

Polymer solutions contain many molecules in the scattering volume, and the spectrum of the scattered light is a continuous spectrum, E(w), and more complicated than the discrete two component example discussed above. If the scattered field incident on the photomultiplier tube is not a discrete frequency but a spectrum, then the beat signal from the tube will not be a single discrete

frequency, but it too will exhibit a spectrum. The relation between the beat signal spectrum in the photomultiplier tube current, i(w), and the incident field E(w) is given by the convolution integral

$$i(w) = C \int_{-\infty}^{\infty} E(\lambda) E(\lambda - w) d\lambda$$

where C is a constant. It was shown (5A-28) that if the power spectrum of the light scattered from a source is Lorentzian, centered at $w = w_0$, and with a half width Γ , the self-beat power spectrum of the photocurrent from a photomultiplier tube detector is also Lorentzian, but with its center frequency at w = 0, and with a half width of 2Γ .

Theory of Brownian motion.--It has been well established that the spectral distribution of scattered light yields information about the Brownian motion of the molecules in a solution responsible for scattering (5A-6). The motion of a Brownian particle in solution will appear to be irregular and random. The force exerted on such a Brownian particle consists of two parts. The first is the frictional force due to the drag exerted on the particle by the fluid. In this case, if u is the velocity of the particle, then this force is given by γu , where γ is the friction constant. The second part of the force is the fluctuating force, A'(t), representing the constant molecular bombardment exerted on a particle by the surrounding fluid. It is assumed that A'(t) varies extremely

rapidly compared to the variations in u. The equation of motion for such a Brownian particle is

$$\frac{du}{dt} = - \zeta u + A(t)$$
 (5-30)

where $\zeta = \gamma/m$ and A(t) = A'(t)/m. The differential equation 5-30 is called a stochastic differential equation because A(t) is a randomly varying function. The solution to the above differential equation can be obtained by finding the probability that the particle has velocity u at time t, given that $u = u_0$ at t = 0. This is given by the probability density function $W(u, t; u_0)$. The probability density function $W(r, t; r_0, u_0)$ written in terms of the displacement of the particle, r, instead of the velocity u has some important properties. For such a Brownian particle it has been shown (5A-35) that the mean-square displacement of the particle, for large times, is

$$<|r-r_0|^2> = \frac{6 k T}{m \zeta} t = 6Dt$$
 (5-31)

where $\frac{kT}{m\zeta}$ = D, the translational diffusion coefficient. Using the above expression for the mean square displacement of the particle, it was shown, (5A-35) for large times, that

W (r, t;
$$r_0$$
, u_0) $\approx \frac{1}{(4\pi Dt)^{3/2}} Exp { - \frac{|r - r_0|^2}{4Dt} }$ (5-32)

This is the well known solution to the diffusion equation

$$\frac{\partial C}{\partial t} = D\nabla^2 C \tag{5-33}$$

which becomes $\delta(r-r_0)$ as $t \to 0$. The solution to equation 5-33 with the initial condition that $C(r, 0) = C_0 \delta(r)$ is

$$C(r, t) = \frac{C_0}{8(\pi Dt)^{3/2}} \exp \left\{-\frac{r^2}{4Dt}\right\}$$
 (5-34)

Therefore, the probability density function $W(r, t; r_0, u_0)$, which is a solution to the equation of motion for a Brownian particle, is also the solution to the diffusion equation.

In a dilute polymer solution, the macromolecule is constantly bombarded by the solvent molecules, which leads to the translation of the macromolecule. The probability P(r, t) of finding a molecule at position r at time t, if it is at the origin at time zero is given by the diffusion equation

$$\frac{\partial P(r, t)}{\partial t} = D\nabla^2 P(r, t)$$

where D is the translational diffusion coefficient of the macro-molecule. The light wave monitors the translation of the molecule in the solution through the molecular polarizability which translates with the molecule.

<u>Application to polymer solutions</u>.--Consider a polymer solution composed of identical, isotropic, polymer segments in a solvent.

The density of the segments in a particular volume under observation fluctuates with time and hence scatters light. Fluctuations in the density of the solvent itself will be ignored. Let ϵ be the excess dielectric constant of polymer solution, the dielectric constant of the solution minus that of the pure solvent. The excess dielectric constant fluctuations $\delta \epsilon$, in turn, correspond to a high degree of approximation to local segment density fluctuation, or to concentration fluctuations of polymer segments, $\delta \epsilon$. Local concentration is a function of time t, and of position within the scattering medium, r. Therefore we may write

$$\delta \varepsilon (r, t) = \frac{\delta \varepsilon}{\delta c} \delta c(r, t)$$
 (5-4)

Based on the theory of Brownian motion, we assume that the microscopic concentration fluctuations obey, on the average, the macroscopic translational diffusion equation, Fick's Law (5A-36, 5A-37, 5A-38)

$$\frac{d\delta c(r, t)}{dt} = D\nabla^2 \delta c(r, t)$$
 (5-5)

where D is the translational diffusion coefficient.

Since the concentration fluctuations cannot be observed with the naked eye, the fluctuations are observed by observing the scattered light. The scattered light from the polymer solutions contains two major components. One component arises from the incident light on the polymer solution, represented by $[\exp(-iw_0t)]$, where w_0 is the frequency of incident light. The second component

arises from the concentration fluctuations represented as $\delta c(r,t)$. Therefore the scattered light field E(t) can be represented as

E(t) is proportional to
$$\delta c(r,t) [exp(-iw_0t)]$$
 (5-6)

The detailed expression for E(t) may be found in other works (5A-18, 5A-19).

The scattered electric field is analyzed using a photomultiplier tube. The spectral composition of the photoelectric current from the photomultiplier is obtained after substituting the value of E(t) from equation 5-6 into equation 5-2 and then taking the Fourier transform of the equation 5-2. Since E(t) is a function of both r and t, the Fourier transformation is done in two steps. The first step would be transforming the r dependence to the Fourier spatial form, and the second step would be transforming the time domain into the frequency domain.

In E(t) only $\delta c(r,t)$ is dependent on r. Let us transform this into the Fourier space domain. Since in Fourier space domain, all the positions are treated as vectors, let us define a scattering vector K as

$$K = k_0 - k_s$$

where k_0 is the wave vector for the incident light and k_s represents the vector for the scattered light. The next step is to relate K to the scattering angle, θ , and the wavelength of incident light λ_0 . The wavelength of the scattered field is related to the wavelength

of the incident field by the Bragg Law (5A-19)

$$\frac{\lambda_{0}}{n} = 2 \lambda_{f} \sin(\theta/2) \tag{5-7}$$

where n is the refractive index of the scattering medium. The relation between the scattering vector K and the wavelength of the scattered light $\lambda_{\mathbf{f}}$, is given by

$$K = \frac{2\pi}{\lambda_f}$$

from equation (5-7)

$$K = \frac{4\pi}{(\lambda_0/n)} \sin(\theta/2)$$
 (5-7A)

Now equation 5-5 in Fourier space domain is written as

$$\frac{d\delta c(K,t)}{dt} = D\nabla^2 \delta c(K,t)$$
 (5-8)

From equation 5-7 we know that, by fixing the scattering angle θ , and the wavelength of the incident light λ_0 , we fix the spatial Fourier component from which scattering is being observed. By solving equation 5-8, at t=0, it can be shown that (5A-28)

$$c(K,t) = c(K,0) \exp(-K^2Dt)$$
 (5-9)

combining equations 5-6 and 5-9 we find that

E(t) is proportional to
$$exp(-K^2Dt) exp(-iw_0t)$$
 (5-10)

Now, to transform equation 5-10 into the frequency domain, principles of autocorrelation functions are utilized. The spectrum of the scattered light may be related to the autocorrelation function, $C(\tau)$, of the electric field of light. The autocorrelation function is the time average of the product of the signal, at any time t, with the signal at any time t + τ .

$$C(\tau) = \langle E(t) E(t + \tau) \rangle \tag{5-11}$$

The power spectrum of the scattered light can be obtained from the autocorrelation function of the scattered light by using the Wiener-Khintchine theorem (tA-18)

$$P(w) = \frac{1}{2\pi} \int_{-\infty}^{\infty} C(\tau) e^{iwt} d\tau \qquad (5-12)$$

P(w) is the power spectrum of the scattered light. The autocorrelation function of the scattered field is generally expressed in terms of the correlation function as

$$C(\tau) = \langle I \rangle q^{(1)}(\tau)$$
 (5-13)

where $\langle I \rangle$ = total intensity of the scattered light, and $g^{(1)}(\tau)$ is the correlation function of the scattered field.

The correlation function of the scattered field is simply an expression that characterizes the optical field incident upon the photomultiplier tube surface. For dilute polymer solutions it has

been shown that $g^{(1)}$ (τ) is of the form (5A-18)

$$g^{(1)}(\tau) = \exp(-iw_0\tau) \exp(-DK^2\tau)$$
 (5-14)

This form for $g^{(1)}$ (τ) is obtained from the proportionality shown in equation 5-10. The photocurrent correlation function, $g^{(2)}$ (τ), corresponds to the photocurrent power spectrum which results from the response of the photomultiplier tube to the incident scattered light field. The correlation function of the photocurrent $g^{(2)}$ (τ), is related to the correlation function of the scattered field by (5A-18)

$$g^{(2)}(\tau) = 1 + |g^{(1)}(\tau)|^2$$
 (5-15)

Using equations 5-11 to 5-15, and performing the integration, the photocurrent power spectrum associated with the scattered field is given as (5A-18)

$$P(w) = \frac{e < i>}{2\pi} + < i> i > 2 \delta(w) + < i> 2 \frac{2DK^2/\pi}{w^2 + (2DK^2)^2}$$
 (5-16)

The photocurrent consists of three components. The first term in the above equation $\frac{e < i>>}{2\pi}$ is the shot noise term. Shot noise is the outcome of the random time behavior of the anode pulses as a result of incident radiation on the photomultiplier tube. The shot noise level can be determined by examining the spectrum at high frequencies, beyond the range in which the beat signal is significant. The second term in equation 5-16 is the D.C. component. The third term is a

Lorentzian of half width $\Delta w_{1/2}$, and centered at w=0. Thus, measurement of the photocurrent spectrum from w=0 to $10 \times \Delta w_{1/2}$ permits accurate determination of the half width of the optical spectrum. If half width is measured in Hertz (cycles per second)

$$\Delta w_{1/2} = 2 K^2 D$$
 (5-17)

Using 5-17 and 5-7A one obtains

$$D = \frac{\Delta w_{1/2} (\lambda_o/n)^2}{16 \sin^2(\theta/2)}$$
 (5-18)

The spectral half width is proportional to the square of sin $(\theta/2)$.

The analysis developed till now in this section holds only for noninteracting systems of monodisperse macromolecules, which are small compared to λ_0 , the incident light wavelength. For polydisperse polymers $g^{\left(1\right)}\left(\tau\right)$ of equation 5-14 consists of a sum or distribution of single exponentials

$$\left| g^{(1)}(\tau) \right| = \int_{0}^{\infty} G(\Gamma) e^{-\Gamma \tau} d\Gamma \qquad (5-19)$$

where $\Gamma = 2 D K^2$.

The distribution function of decay rates, G (Γ) may be a broad continuous distribution. G (Γ) d Γ is the fraction of the total intensity scattered, on the average by molecules for which Γ = DK², within d Γ . In studying polydisperse systems, one must

adopt a procedure of data analysis that recognizes this aspect. The procedure used for data analysis in this work is covered in detail in the data analysis section.

Experimental Apparatus

In this work diffusion coefficients in the dilute solution range were obtained using a laser homodyne spectrometer. A diagram of this spectrometer is shown in Figure 5-3. It consists of a laser light source, the scattering cell, light collecting optics, photomultiplier tube, spectrum analyzer and averager, an X - Y recorder, oscilloscope, and a computer along with its peripherals.

The laser was a Spectra Physics model 165 argon ion, operating on a single mode at 5145°A. It had also a polarizer which permitted only plane polarized light to pass through. The light beam from the laser was reflected from its path by a mirror and directed through the center of a cylindrical sample cell. The light beam was focused into the cell by using an appropriate lens. The sample cell was situated on a rotating table which was used to select the desired scattering angle. The incident laser light beam could be redirected through the center of the sample cell at any scattering angle by rotation and translation of the reflecting mirror on its moveable mount. Scattering angles from 0 to 180° were possible with this arrangement.

A Spectra Physics model 132 He-Ne laser was used for aligning the optics and the light collecting system. The light collection optics are shown in Figure 5-4. The light scattered from the sample

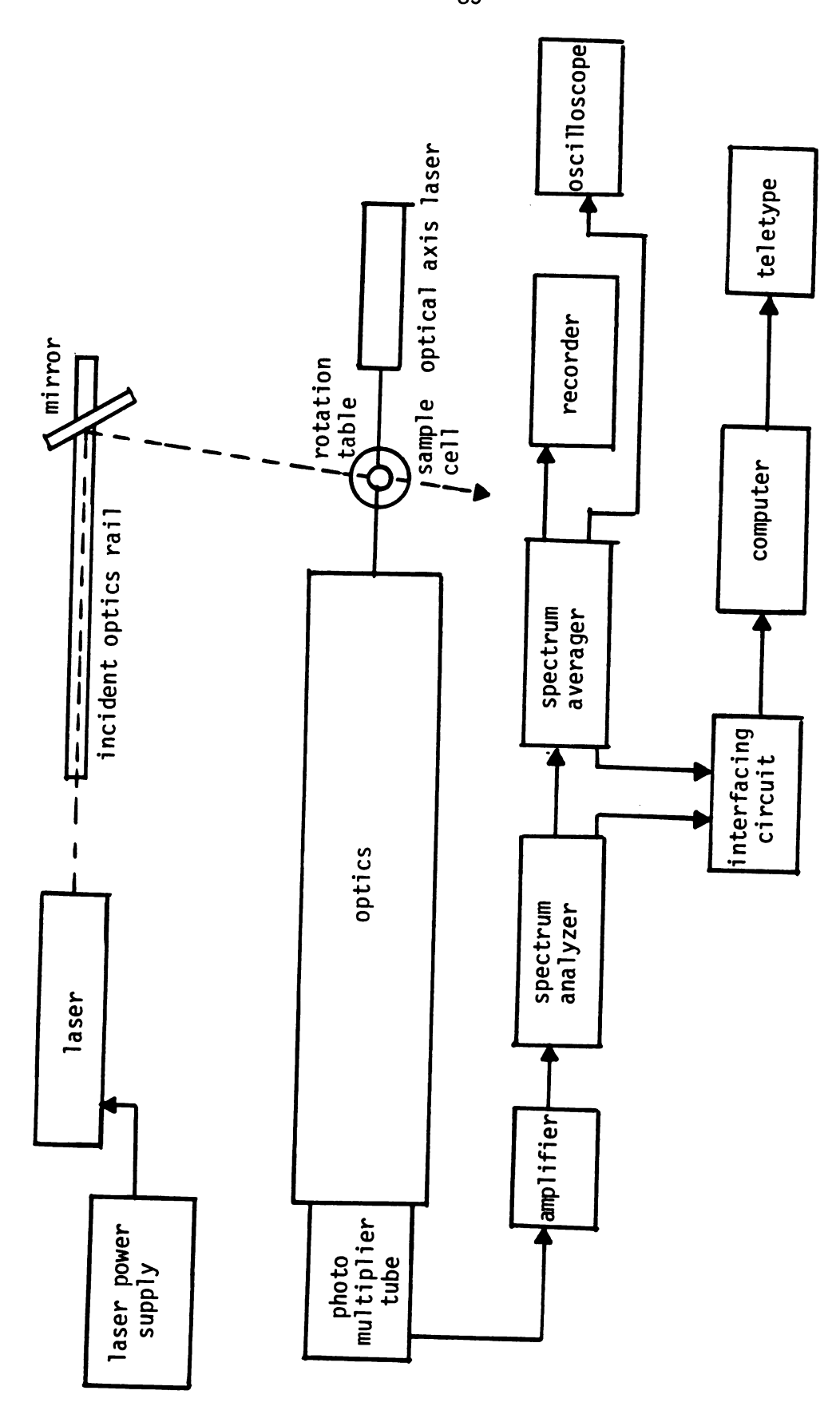


Figure 5-3.--Lightbeating spectrometer.

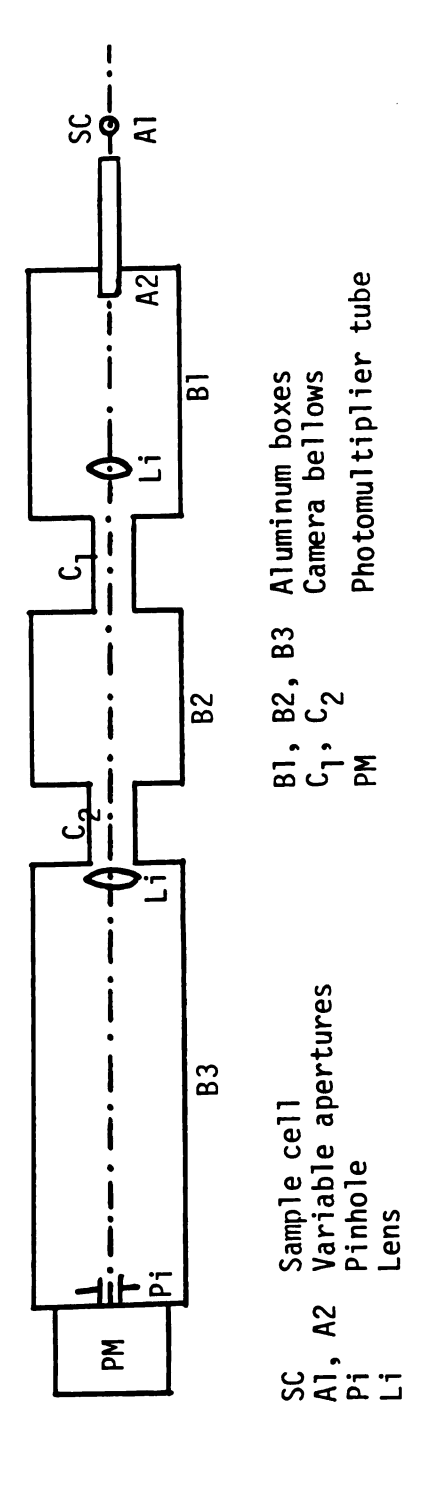


Figure 5-4.--Light collection optics.

cell at the desired angle was collected by a series of apertures, lenses and pinholes and focused upon the surface of the photomultiplier tube. For more details about the collection system and alignment refer to the work of Gyeszly (5A-4) and Stutesman (5A-29). The photomultiplier tube was an EMI model 9558 B. It was placed in a refrigeration chamber to reduce the level of dark current.

The output of the photomultiplier tube was connected to the spectrum analyzer-averager system. The spectrum analyzer was a Federal Scientific model UA - 14A, and the averager was also Federal Scientific Model 1014. This combination provided "real time" analysis of the scattered light spectrum.

The spectrum analyzer is capable of measuring spectra on 12 frequency ranges from 0 - 10 Hz to 0 - 50,000 Hz. It also provides 400 line resolution and a variety of output options. The averager decreases the random noise in the signal by averaging the instantaneous spectra as many times as desired. In this work all spectra were averaged 1024 times. The output of the averager was a voltage versus frequency spectrum, which was connected to the oscilloscope for instantaneous display of the full spectrum at all times. The spectrum could also be plotted on a Varian Associates $F-80\ X-Y$ recorder. To make data handling easier, quicker and more accurate, the spectrum averager was interfaced to a PDP 8/E mini computer. The details of the interfacing will be described in the next section.

Computer Interfacing of the Averager

When a device or instrument is electrically connected to a computer so that it provides data to the computer or receives data from it, it is said to be interfaced to the computer. The device or instrument thus interfaced becomes a computer peripheral. Interfacing an instrument to a computer is accomplished by connection of the data source to the computer input bus. Frequently the form and level of data must be adjusted to suit the output and input requirements of the computer and peripheral, also data transfer timing information must be provided. These functions are performed by the interfacing circuit. As was mentioned earlier, the spectrum averager was interfaced to a PDP 8/E mini computer. The main purposes of interfacing the averager are to obtain accurate data and to make data handling and analysis fast and simple.

The spectrum averager is used in conjunction with the spectrum analyzer and receives three timing signals from the analyzer in addition to the output spectrum. These timing signals are: the averager sweep gate, the circulation pulses, and the averager start trigger. The function of these signals are important for a clear understanding of the operation of the interfacing circuit.

The averager sweep gate is high during every spectrum readout from the analyzer. Each of the 400 frequency elements is timed to the circulation pulses. Within the high interval of the sweep gate, 400 circulation pulses are emitted. The first corresponds to frequency element 1, the last corresponds to frequency element 400 as shown in Figure 5-5. The pulses which occur during the interval that the sweep gate is low correspond to no frequency elements stored in the averager; they are ignored. The circulation pulses generated during every sweep gate are used in the averager to read out the contents of each memory cell location and to write this information back into memory. The data written back may be modified, such as during an averaging cycle, when new data are added to the contents of the memory, or an erase cycle, when the data re-entered is forced to zero. However, the operation of reading every cell location and writing data back into the same location is unconditional. The averager start trigger is used to permit loading of spectrum data into the memory. It is used only during an averaging cycle. Thereafter, it has no further function. After the averaging has been completed all the averager is doing is reading out the contents of each memory cell location and writing them back when ever the sweep gate is high. The two timing signals, the averager sweep gate and the circulation pulses, are used for generating the data transfer timing information between the computer and the averager. The form and level of data was the same both in the computer and the averager (both of them had TTL logic).

During the read out cycle the amplitude corresponding to each of the 400 frequency locations was available at the averager outputs in digital form (10 binary bits), when the circulation pulse went high. Since 400 circulation pulses occur in 100 msec., the time between two pulses is around 250 μ sec. The circulation pulses and one bit of the digital data were observed on a dual beam dual

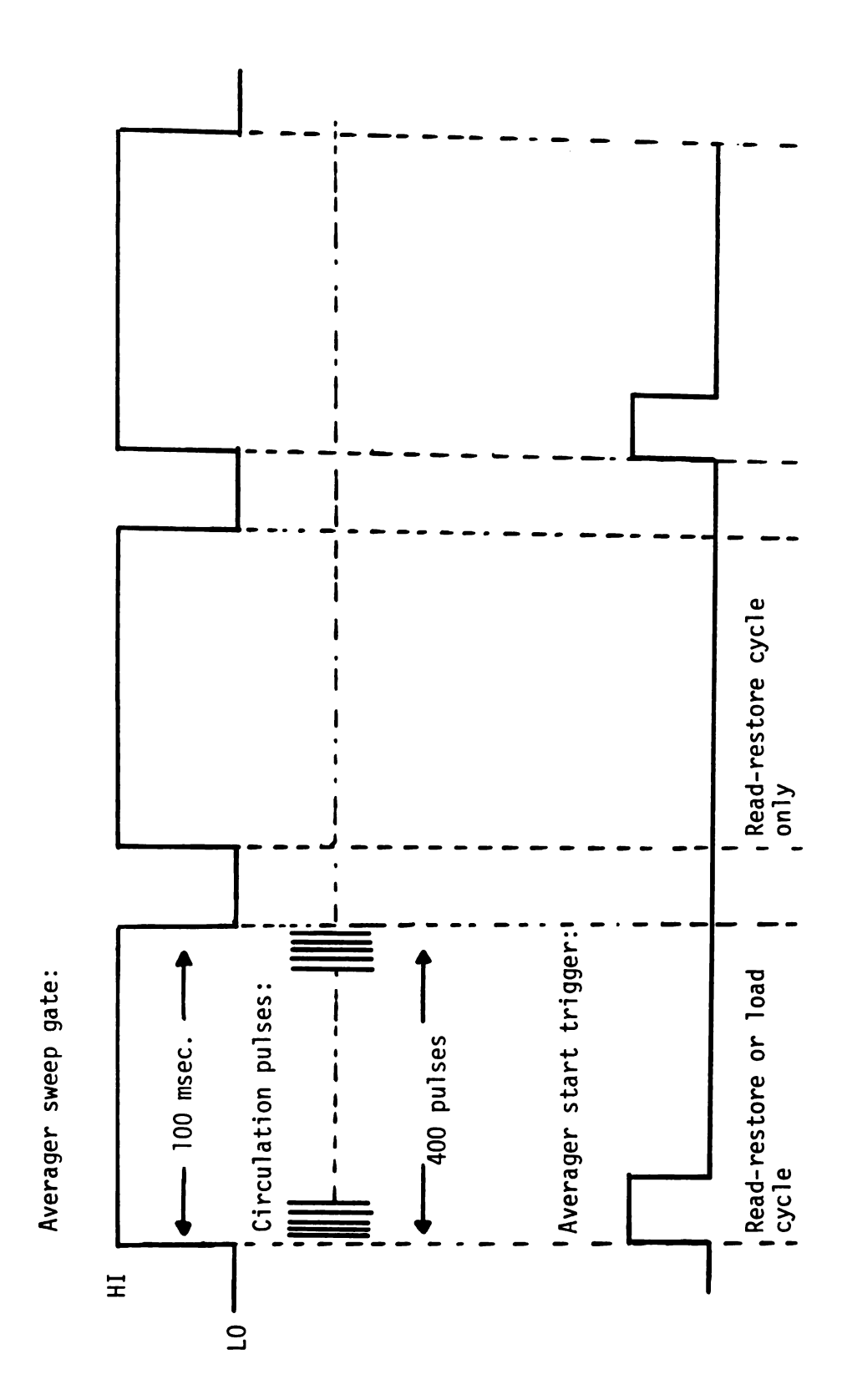


Figure 5-5.--Basic timing diagram.

trace oscilloscope, to find out the exact time of the availability of digital data at the output of the averager. The results of this observation are shown in Figure 5-6. The circulation pulse was high for 12 μ sec. and the digital data was available around 24 μ sec. before the circulation pulse went high and around 64 μ sec. after the circulation pulse went low. Thus, we had around 60 μ sec. to transfer the data once the circulation pulse was high.

The connections to the computer which are used for programmed data transfer are shown in Figure 5-7. All data are transferred into or out of the accumulator as 12-bit words during an input/output (here after written as I/O) instruction. The bit assignments of an I/O instruction word are shown in Figure 5-8. Bits 0-2 must be octal 6, the operation code for an I/O transfer. The operation decoder, upon detecting a 6 enables the IOP generator, which generates pulses, to be used to synchronize the input or output data with the computer cycle. Three IOP pulses can be generated, designated IOP 1, IOP 2, and IOP 4 in that sequence. Bits 9-11 of the instruction word control which of the IOP pulses will be generated. The middle six bits of the instruction word are used to identify the external device which is to provide or accept the data. During an IOP cycle, the accumulator input connections AC 0-11 are active so that the data connected to them at that time will appear in the accumulator. A few connections to the operation controller of the computer are also available and are very useful. These are: the skip line (SKP) which is active during an IOP and which can be used to cause the computer to skip the next instruction in the

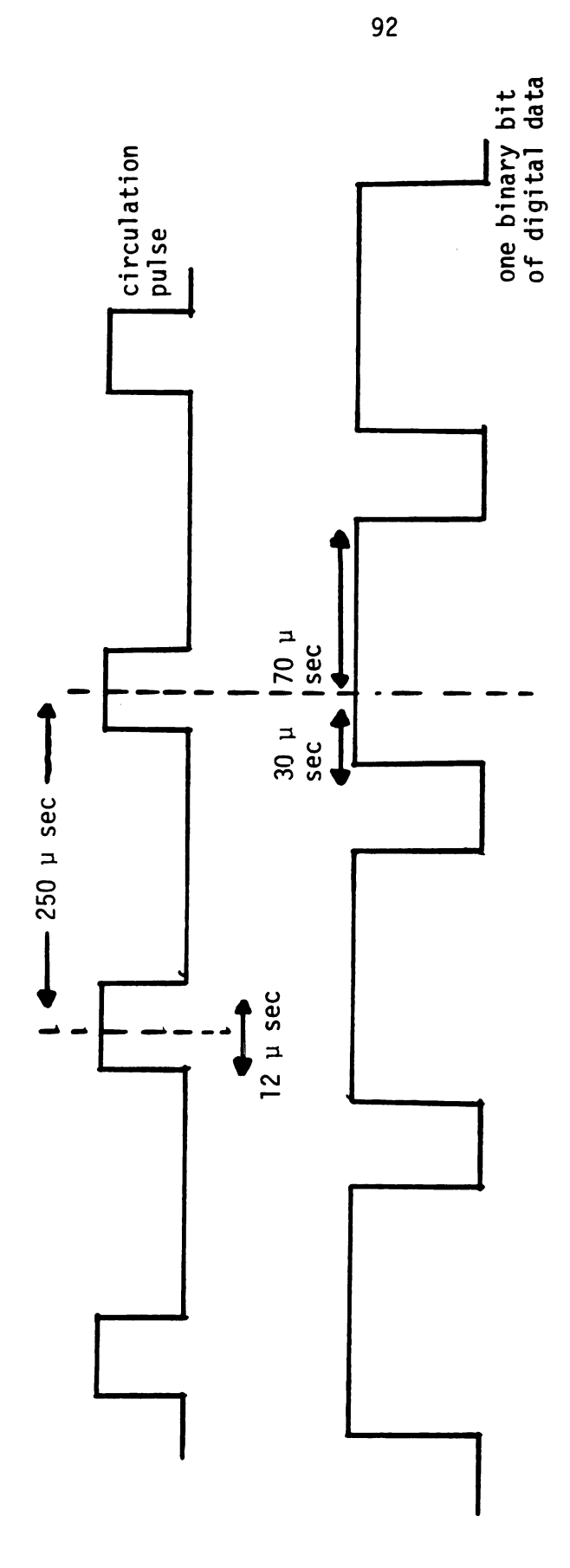


Figure 5-6.--Timing diagram for circulation pulse and one binary bit of digital data.

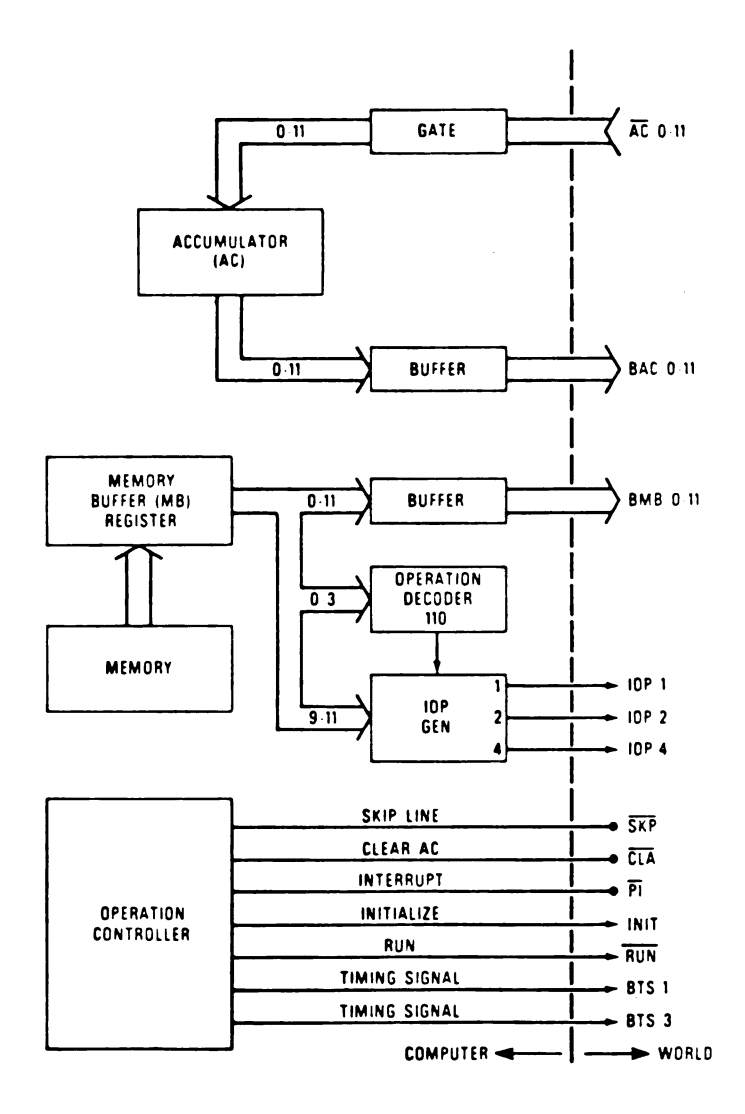


Figure 5-7.--Computer connections for programmed data transfer.

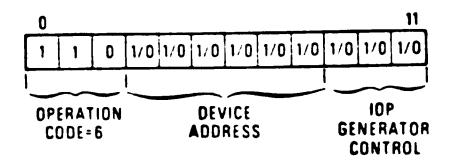


Figure 5-8.--I/O instruction word.

program; the clear accumulator line (CLA) which is convenient for clearing the accumulator before new information is read into it.

In order to facilitate the connections of devices with TTL logic level inputs and outputs to the computer I/O lines, an interface buffer box is used. This unit protects the computer I/O lines from damage from erroneous connections, and provides I/O line drivers and buffers so that ordinary TTL circuits can be used for data inputs and outputs. An I/O patch card is used to bring the I/O connections from the buffer box into the Analog Digital Designer (ADD) for convenience in building the interface circuit (see Figure 5-9).

The interface circuit was built using the following cards: I/O patch card, gated driver card, dual flag card, octal decoder card and a NAND gate card. All these cards consist of 32 pins, and they sit in the sockets provided in the ADD. For details of these cards refer to Appendix G. The arrows pointing towards the pins on the cards indicate the signal is an input to the card. The arrows pointing out of the pin indicate that the signals may be obtained out of the card. All of the input and output connections of the cards are brought to the top of the card for patch wiring.

All the connections between the cards in the interfacing circuit are shown in Figure 5-10. For the sake of clarity the patch wiring connections are not shown completely, but only the connections on each card are shown. The 10 bit digital data from the averager is connected to data inputs (pins 3-12) on the gated driver card. The pins 1 and 2 are grounded, because they are not being

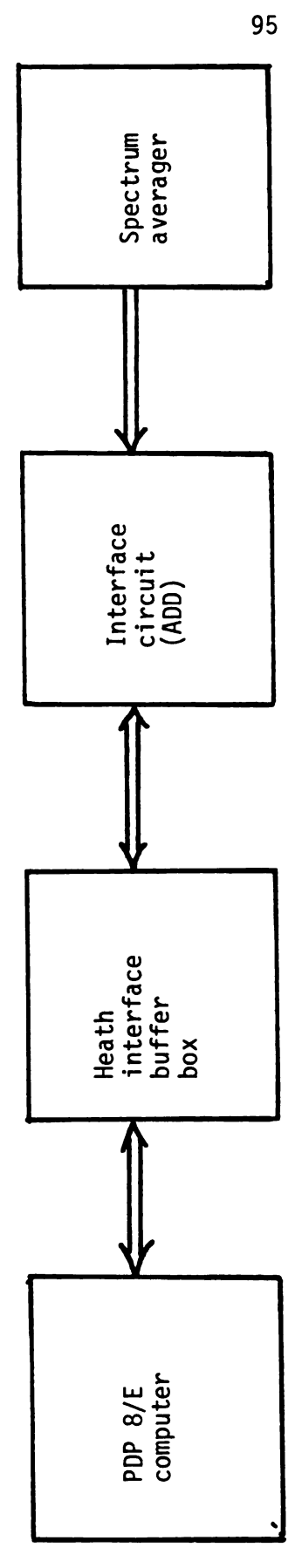
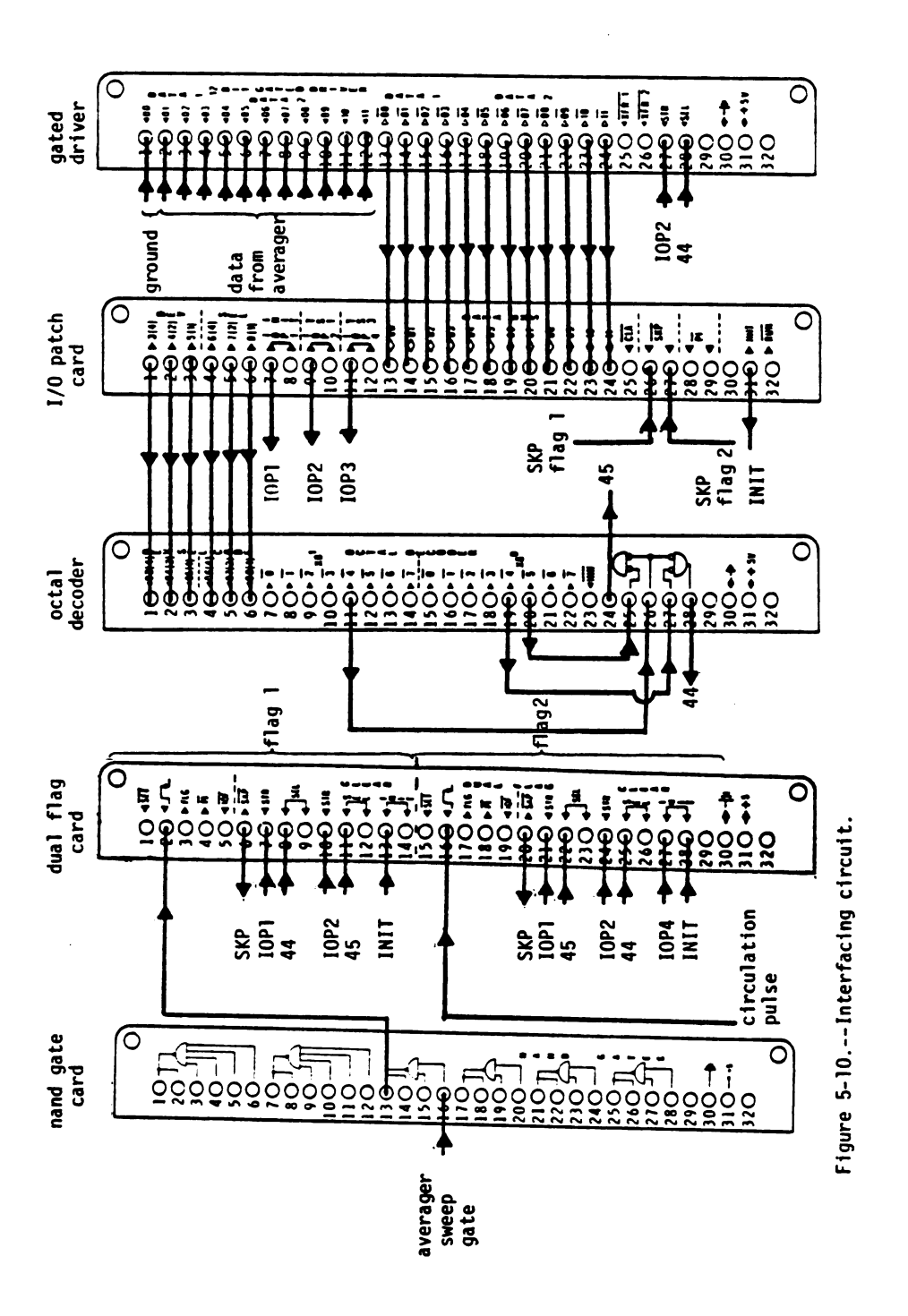


Figure 5-9.--Flow of data from the averager to the computer.



used. The data outputs of the gated driver card (pins 13-24) are connected to accumulator inputs (pins 13-24) on the I/O patch card. Device addresses of 44 and 45 are used in this work. The octal decoder card was wired to give device addresses 44 and 45. These addresses along with the IOP pulses were used as the timing information for the computer. In order for the computer to know that the averager is ready to transmit data, a dual flag card is used. Flag 1 is used for averager sweep gate and flag 2 for circulation pulses. Since the flag is set only on the falling edge of the signal, the averager sweep gate was inverted using a NAND gate, and this signal was connected to pin 2 on the dual flag card. Device address 44 and IOP 1 were used to check when the sweep gate went HI. To clear flag 1 device address 45 and IOP 2 were used. Since the digital data from the averager was available till 60 μ sec after the circulation pulse went LO, the circulation pulse signal was directly connected to pin 16 on the dual flag card. Device address of 44 and IOP 2 and IOP 4 were used to clear the flag 2 after it was set.

The operation of the interface circuit is easily understood by following the computer program used for data transfer which is attached in Appendix H. The program is a combination of FORTRAN and SABER languages. The letter S in column one indicates it is a SABER statement. The software of the PDP 8/E is set up such that if a variable is defined in the common statement, the storage locations for that variable are in ascending order in field 1 beginning at location 200. The first 7 steps in the program are

directed towards achieving this object of writing this data at field 1 and location 200, so that it can be retrieved very easily later. After the averaging function was completed in an experimental run, the program was executed. The program first clears the sweep gate flag (flag 1) by using the instruction 6452. After clearing flag 1 it enters a DO loop where it waits until the sweep gate goes HI. This is done in order that the sweep gate is at the beginning of its cycle. So when the sweep gate goes HI, the SKP line from flag 1 that is connected to the SKP on I/O patch card goes LO or is grounded momentarily. This LO on the SKP on I/O patch card produces a jump to the next instruction in the program. The next instruction 6452 clears the flag 1. In any of the above instructions there is no data transfer because the signals that control data transfer to the computer are device address 44 and IOP 2. This combination has not been used till now, in either clearing or checking flag 1. Once the sweep gate goes HI, the program next clears the circulation pulse flag (flag 2) with the instruction 6444. Then it checks if the circulation pulse 1 is HI, by instruction 6451 in a DO loop. Once the circulation pulse 1 goes HI, it produces a momentary ground on SKP line connected to the I/O card at pin 27. This produces a jump to the next instruction in the program which is 6442; this produces HI logic levels at pins 27 and 28 on the gated driver card, which controls data transfer. The instruction 6442 is used both to transfer data into the computer and also to clear the flag of the circulation pulses. The program next transfers data from the accumulator to the prescribed storage

location. Then it enters the DO loop to check for the second circulation pulse. This process is repeated until all 400 circulation pulses are found. After reading all 400 locations the program asks for information on shot noise, the scattering angle, and the experimental number. Then it writes all this information on to the Floppy disk, under file name read in, which is used later for data analysis.

After successful interfacing, several experiments were run whereby half widths obtained from the recorder graphs and the computer were compared. The results are shown in Table 5-1. From the table it can be seen that the half widths are very close to each other. After the interfacing the time required for running the experiment and to obtain the half width was reduced from around two hours to around two minutes.

Procedure for Experimental Run

- 1. A careful alignment of the optics in the homodyne spectrometer is necessary in order to achieve accurate results. The beam from the sighting laser is used to align pin holes and lenses so that they define a straight optical path.
- 2. The refrigeration chamber for the photomultiplier tube should be turned on at least twelve hours before the start of the experimental run. This is done to insure that a stable temperature of -10° C is attained in the chamber.
- 3. The laser power supply is turned on, and the laser is allowed to lase at the lowest output power, for at least 30 minutes.

TABLE 5-1.--Comparison of half widths obtained from the recorder and computer.

	Half Widths of Spectrum	E	
Angle	Analysis Range H _z	From Digital Data H _z	From Graph H _Z
06	(5000 10000	324.67 296.71	325.01 295.19
09	10000	209.03	206.64
45	10000	153.5 144.7	157.44
30	10000	80.67	88.1

- 4. The path of the main ion laser beam is adjusted so that the desired scattering angle is achieved.
- 5. After the whole system is aligned and ready, the computer is started up, and all the required programs are loaded into the memory.
- 6. The sample cell is carefully placed in the particular slot on the bench so that the incident laser beam passes directly through the center of the sample cell.
- 7. The light scattering measurements are made with the room lights turned off, to prevent stray light from entering the system. The power of the laser is adjusted to give a good signal to noise ratio for that particular sample.
- 8. After the averaging of the spectrum is completed, the computer is instructed to read the data and store it on floppy disks, for further processing.

Data Analysis

The power spectrum, P(w), of light scattered from a solution of monodisperse, non-interacting polymer molecules (equation 5-16) was shown to consist of three terms. The first was the shot noise. This term was determined by obtaining spectra for each sample in the 50,000 Hz analysis range and determining the amplitude at the highest frequency. The frequency of 50,000 Hz is in the range at which the beat signal level is insignificant. The amplitude at this frequency arises from noise in the photomultiplier tube. The second term is the D.C. component. This was blocked off in the

spectrum analyzer by using a capacitor. The third term defines a spectrum which is Lorentzian for a monodisperse sample and with a half width at half height proportional to the diffusion coefficient (equation 5-18).

The data obtained from the spectrum averager consist of amplitudes (voltage) corresponding to 400 frequency locations. If these amplitudes are squared and shot noise subtracted from them, the results obtained correspond to the third term in equation 5-16.

$$P(w)' = \frac{A_c^{\Delta w} 1/2}{[w^2 + \Delta w^2]/2}$$
 (5-20)

where P(w)' is the power spectrum without the shot noise or the D.C. components, and A_{C} is a constant. Equation 5-20 is of Lorentzian functional form, with half width at half height

$$\Delta w_{1/2} = 2 D K^2$$
 (5-21)

If the polymer solution is not monodisperse, but contains instead polydisperse polymer with a distribution of macromolecular sizes, the spectrum of scattered light will no longer be described by a single Lorentzian (equation 5-20), but instead will be a sum of Lorentzians, all centered at the same frequency but with different half widths and intensities. The analysis of this situation has been carried out by several groups (5A-10, 5A-22, 5A-25, 5A-30, 5A-31, 5A-32). Frederick, et al. (5A-25) have made detailed numerical calculations of the spectrum of light scattered from

polydisperse polymer solutions, with a polymer molecular weight distribution described by the Schulz-Zimm equation (5B-13). They showed that the spectra of solutions of samples with moderate molecular weight and broad distributions are difficult to distinguish from single Lorentzians, and also that the halfwidths remain nearly proportional to K^2 .

Benbast and Bloomfield (5A-33) extended the treatments of Frederick, et al. by indicating additional ways for graphically analyzing light beating data for polydisperse macromolecular solutions, and showed how the average diffusion coefficients obtained from this analysis are related to averages obtained from other types of physical measurements. They obtained explicit expressions relating the average diffusion coefficient determined by their graphical procedures for a polydisperse sample to the diffusion coefficient corresponding to a monodisperse sample whose molecular weight equaled the weight average molecular weight of the sample, in terms of parameters of the molecular weight distribution. In this work the method of analysis of Benbast and Bloomfield was used.

It can be seen from equation 5-20 that a plot of $\frac{1}{P(w)}$, versus w^2 should be linear,

$$\frac{1}{P(w)'} = \frac{w^2}{A_c \Delta w_{1/2}} + \frac{\Delta w_{1/2}}{A_c}$$
 (5-22)

enabling extrapolation of the term $\frac{1}{P(w)}$ to zero frequency and permitting the half width to be determined from the slope and intercept.

Since for polydisperse polymers, equation 5-20 is not a single Lorentzian, a plot of equation 5-22 will not be strictly linear. However, one can work with the limiting slopes and intercepts at large and small values of w. These limiting values will emphasize different regions of the molecular size distribution.

Benbast and Bloomfield showed that if the data are fit to a linear equation of the form of 5-22, the average diffusion coefficient obtained from the limiting slope and intercept at low frequencies, D_{av} , is related to the diffusion coefficient of the weight average species, $D(M_w)$, by the relation

$$\frac{D_{av}}{D(M_{w})} = \left(\frac{I(4+h,1)}{I(6+h,3)}\right)^{1/2} \frac{1}{2} \left(\frac{\Gamma(4+h)}{\Gamma(2+h)}\right)^{1/2}$$
 (5-23)

where

$$I(m,n) = \frac{\Gamma(m+1) \Gamma(m+1) \Gamma(2m-n+2)}{\Gamma(2m+2)}$$
 (5-24)

and $\Gamma(x)$ is the Gamma function of x, h is the Schulz distribution parameter related to weight average and number average molecular weights by the relation

$$\frac{M_{W}}{M_{n}} = \frac{h+1}{h} \tag{5-25}$$

 M_W is the weight average molecular weight and M_n is the number average molecular weight. Equation 5-24 for I(m,n) is not the same

as reported by Benbast and Bloomfield. The error in their derivation was corrected, and the details concerning the derivation are given in Appendix J.

All the data analyses in this work were performed using equation 5-22, finding the limiting slope and intercept at the low frequencies. From these the half width of the spectrum $\Delta w_{1/2}(\theta)$ at that particular scattering angle, θ , was determined. Then the average diffusion coefficient, D_{av} , was determined from the straight line fit of $\Delta w_{1/2}(\theta)$ versus $\sin^2(\theta/2)$. The value of D_{av} was converted to $D(M_W)$ by using the equation 5-23. The values of $D_{av}/D(M_W)$ for all the polymers used in this work are shown in Table 5-2.

Calibration

Although the technique of light beating spectroscopy is widely used, there are sometimes technical difficulties with the optics or electronics such that a final check of the overall performance of the entire system by using aqueous solutions of polystyrene latex spheres is a very useful safeguard against experimental errors. The polystyrene spheres can be prepared with a precise spherical shape and small dispersion about the diameter. Such material has been frequently used as a standard in light beating experiments (5A-19).

Polystyrene spheres were obtained from the Dow Chemical Company. The diameter of the spheres used in our experiment were 1090°A, with a standard deviation of 59°A. The dense solution as supplied by the Dow Chemical Company was diluted with water which

 $D_{av}/D(M_{w})$ 0.642 0.614 0.697 0.682 0.893 0.534 1.786 1.515 2.778 117,800 239,700 37,900 135,500 550,900 TABLE 5-2.--Ratios of $D_{av}/D(M_{w})$. 338,500 398,400 80,400 211,700 Polymer SAN-2 SAN-1 PS-1 PS-2

was deionized, distilled and filtered through a millipore filter of 5000°A pore size. The values of the diffusion coefficient and the half widths obtained for these polystyrene latex spheres using the light beating technique are compared with those calculated from the Stokes-Einstein formula

$$D = \frac{k T}{6\pi \eta_{O} R}$$
 (5-26)

where k is the Boltzman constant, T is the absolute temperature, $\eta_{\rm O}$ the viscosity of the solvent, and R the radius of the latex spheres. The results of this comparison are shown in Table 5-3. From the results in Table 5-3 it may be concluded that the experimental values are in good accord with theoretical values, which means that the light beating spectrometer is a reliable tool for obtaining diffusion coefficients in dilute solutions. The data also show consistency from day-to-day measurements.

Sample Preparation

The presence in the solution of even a very small amount of particles other than polymer and solvent may cause a major change in the experimental results, and lead to erroneous interpretations of the results of the light beating experiments. This problem becomes especially acute for weak scatters, and the results depend heavily on the unpredictable and distorting effect of scattering by foreign particles. Sample cleanliness may be one of the single most important factors in sample preparation. Unless all dirt

TABLE 5-3.--Results of calibration runs for polystyrene spheres in water.

Angle	Half Width Theory (using eq. 5-26)	Half Width Exptl. (3/24/76)	Half Width Exptl. (4/26/76)
30	100	101	105
35	135	135	144
40	174	175	174
45	218	205	194
Avg. Diffusion Coeff.	4.444×10^{-8}	4.317×10^{-8}	4.338 x 10 ⁻⁸
% Error		2.7	2.4

particles are removed, the scattering spectrum will be dominated by the impurities.

The most commonly used methods of dust removal in polymer solutions are millipore filtration and ultracentrifugation.

Recently Nelson (5A-34) in his work on polystyrene samples concluded that there was general agreement between the values of diffusion coefficients obtained from samples prepared using the two different dust removal techniques. In this work it was decided to use millipore filtration for dust removal.

Stock solutions of polystyrene and styrene-acrylonitrile copolymers were made in all the desired solvents. The concentrations of the stock solutions prepared were determined by the maximum concentration of each polymer in a particular solvent desired for that particular polymer-solvent pair. After the solutions were prepared, they were mixed on an automatic shaker until complete dissolution of the polymer had occurred. These stock solutions were then filtered through a millipore filter of 5000°A pore size. The required quantities of the stock solutions were withdrawn and diluted with appropriate quantities of solvent in order to obtain the desired concentrations for the final samples. These final samples were again filtered through a millipore filter of 5000°A pore size before being transferred to the sample cells. The sample cells used in this work were circular with two centimeter internal diameter and were ten centimeters long. The cylindrical type cells were chosen because they require virtually no angular corrections for refraction since

the entering and emerging beams are always at right angles to the faces of the scattering cell.

Error Analysis

The major source of errors in this work can be attributed to the following factors:

- 1. Although all the samples were filtered through millipore filters, inevitably some small amounts of dust may be present in the samples.
- 2. Uncertainty in determining the level of shot noise from the photomultiplier tube in the light beating apparatus.
- 3. Lining up the incident laser light so that the scattering angle was precisely known.
- 4. Centering the sample cell directly in the laser beam.
- 5. Inhomogeneties in the cell walls which will scatter some light.

The minor source of errors may arise from the uncertainties in determining actual concentrations of the polymer solutions, from inherent inaccuracy of the photomultiplier tube, and from the electronics, which is the combination of the spectrum analyzer, averager and the computer. Some of these errors can be adequately estimated, and others are not quantitatively known. All of the errors in measurement and data analysis would be reflected in the differing values obtained for the diffusion coefficients of a sample at different scattering angles. The data in this work show good agreement with the linearity condition imposed for the plot of half width versus sin $^2(\theta/2)$, where θ is the scattering angle. Therefore the standard deviation obtained from this linear plot is a reasonable indication of the error in that particular sample.

From the calculated standard deviations, the diffusion coefficients obtained by light beating spectroscopy in this work are accurate to within 3.5%.

<u>Interferometry</u>

In the past few years little interest has centered around the use of the technique of interferometry, which offers in principle an attractive method for measuring diffusion coefficients for moderately concentrated and dilute polymer solutions. Very viscous fluids may be handled by this technique although there is a practical upper limit for convenient handling of the fluids.

Background

Several types of optical interference methods have been used for the measurement of refractive index distributions that are associated with free diffusion experiments (5B-1). The conventional interferometers such as Rayleigh and Gouy differ from each other in their optical configurations. The actual free diffusion takes place in a cell, whose design generally does not depend on the particular method used. In recent years an interference technique based on the formation of interference patterns by a thin wedge has been described in the literature for measuring diffusion in polymer solutions (5B-2 to 5B-6). In this apparatus the diffusion cell is an integral part of the interferometer because the light interference is produced by partially metallized cell walls which are arranged to form a thin wedge in which free diffusion takes place. The most difficult step in any free diffusion experiment, including the use of

wedge interferometer, is the initiation of the diffusion process with a sharp interface between two adjacent phases. In the wedge interferometer the diffusion is initiated by simply allowing two drops of different compositions to come together at an interface. This technique is not satisfactory when dealing with very volatile solvents, such as those used in this study. There have also been reported in the literature several problems concerning initial mixing effects in the wedge interferometer (5B-3).

This work made use of the Mach-Zehnder (5B-7) interferometer, which was modified by Babb and associates (5B-8) to study binary diffusion in nonelectrolyte solutions. Many of the difficulties encountered in the wedge interferometer are eliminated with this method. The optical system produces integral fringes proportional to the refractive index distribution in the cell and each point in the cell is focused as a point on a photographic plate. This system provides exactly the same information as does the Rayleigh interferometer. Caldwell, Hall and Babb (5B-8) claim a precision of 0.2% when measuring diffusion coefficients in aqueous solutions and approximately 1% for binary systems composed of organic liquids.

Experimental Apparatus

Diffusion coefficients in the intermediate concentration range were obtained with a Mach-Zehnder interferometric method. This technique involves bringing a more concentrated polymer solution into contact with a less concentrated solution in an optical cell where diffusion occurs. The cell was immersed in a constant temperature

bath and the diffusion was followed by measuring the rate of change of refractive index of the solution (5B-7). Two solutions of slightly different concentrations were carefully flowed one on top of the other into the cell and free diffusion allowed to take place. The concentration of the measurement was taken as the arithmetic average of the two solutions. The experimental set-up was similar to the diffusiometer described by Caldwell, Hall and Babb (5B-8) and also described in detail by Bidlack (5B-9).

A diagram and photograph of the interferometer are shown in Figures 5-11 and 5-12. The various components of the interferometer were supported by ordinary laboratory bench carriages stationed along a continuous rail composed of three optical benches. These in turn were bolted to an I-Beam mounted on a concrete block on inverted rubber cup-like cushions to dampen outside disturbances and vibrations.

Monochromatic light from a Cenco quartz mercury arc lamp source, filtered to isolate the 5461 °A green mercury line, was collimated and then split in amplitude by a half-silvered mirror (mirror 1). Half of the beam was reflected to a full reflecting mirror (mirror 2) and the other half passed through to a full reflecting mirror (mirror 3). The two beams were then combined at a half-silvered mirror (mirror 4). Constructive interference of the two beams occurred when the path lengths 1-2-4 and 1-3-4 were equal or differed by a whole multiple of the wavelength of the incident light. The mirrors were adjusted to give straight, vertical, parallel fringes.

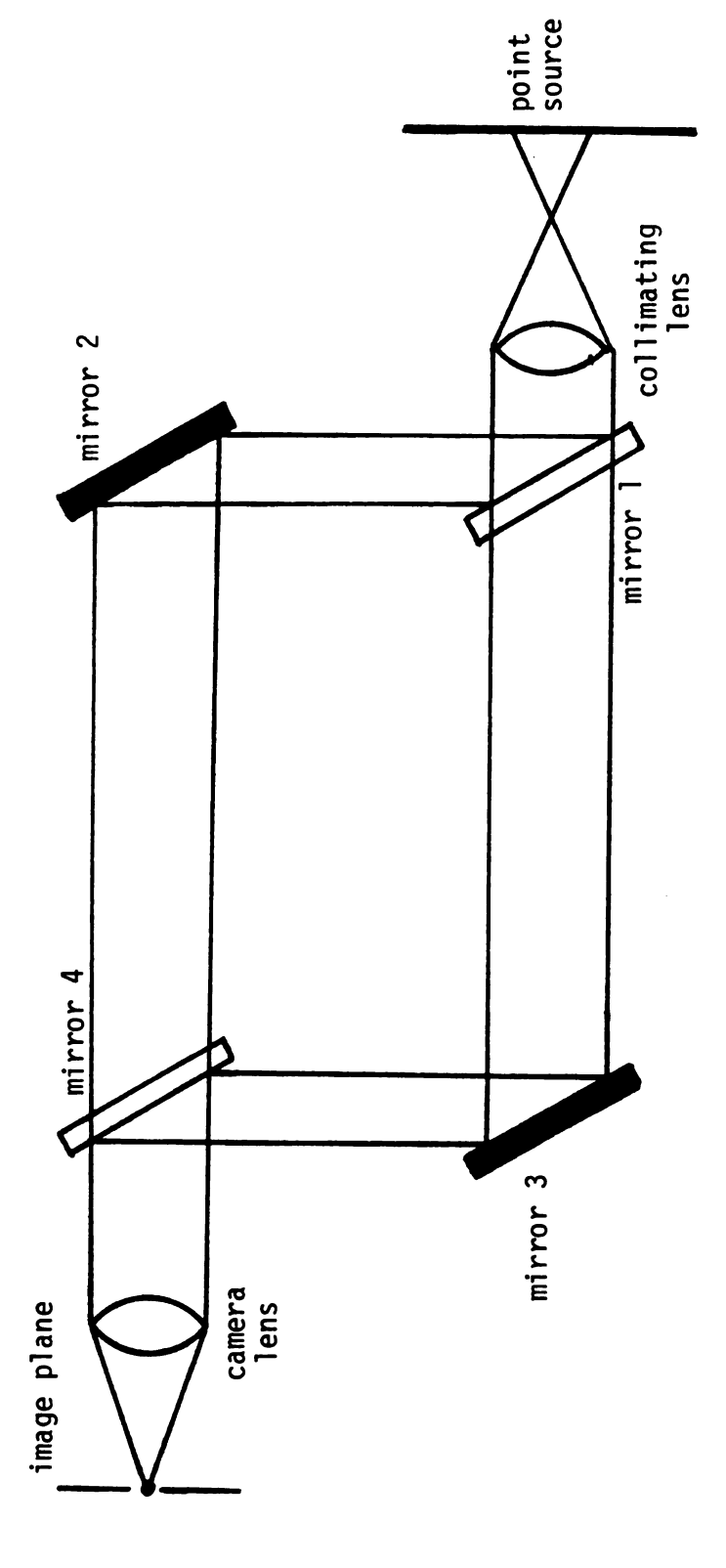


Figure 5-11.--Schematic diagram of interferometer showing position of mirrors.

Figure 5-12. Photograph of Mach-Zehnder interferometer showing components.

The interference beam was arranged so that it could be photographed directly by a camera. The camera consisted of a 3 foot long aluminum tube of 3 1/2 inch diameter containing a lens with a 343 mm. focal length set in the end towards the interferometer. The lens was focused on a type M, 3 1/4 x 4 1/4 inch Kodak plate located at the opposite end. A lever mechanism on the plate holder enabled fourteen successive exposures to be taken per plate. The magnification factor of the camera was found to be 1.929.

The diffusion cell was fixed in a water bath maintained at 25 ± 0.2 °C by a proportional controller. The water bath consisted of an $18 \times 18 \times 18$ inch stainless steel tank covered with 3/4 inch plywood and rested on the cement block without touching the interferometer. Two 3 inch diameter optical flat windows were clamped and sealed into the water bath and aligned to allow passage of the light beams through the bath and the cell windows. Distilled water was preferred over tap water since it did not cloud up as fast.

In Figures 5-13 and 5-14 a photograph and a diagram of the diffusion cell are shown. The main body of the cell consisted of a 1/4 by 3 1/4 inch slot cut into a stainless steel plate with optically flat windows clamped over the slot to form a sealed channel. The channel was situated to allow both light beams to pass through it; thus, a vertical concentration gradient in the solution across one of the beams resulted in a fringe displacement pattern that was a direct measurement of refractive index versus distance. All parts of the cell which would be in contact with the liquid solutions were stainless steel or glass.

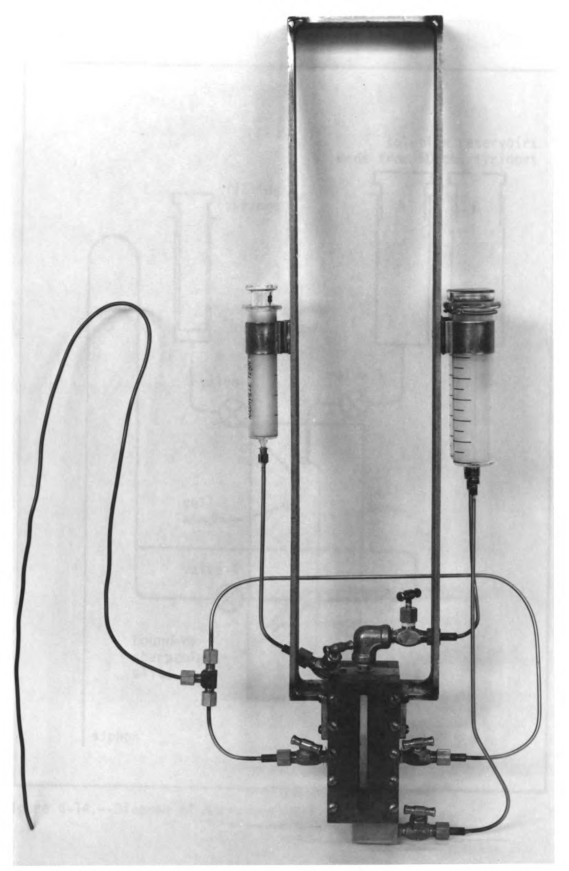


Figure 5-13.--Photograph of diffusion cell for measurement of diffusion coefficients.

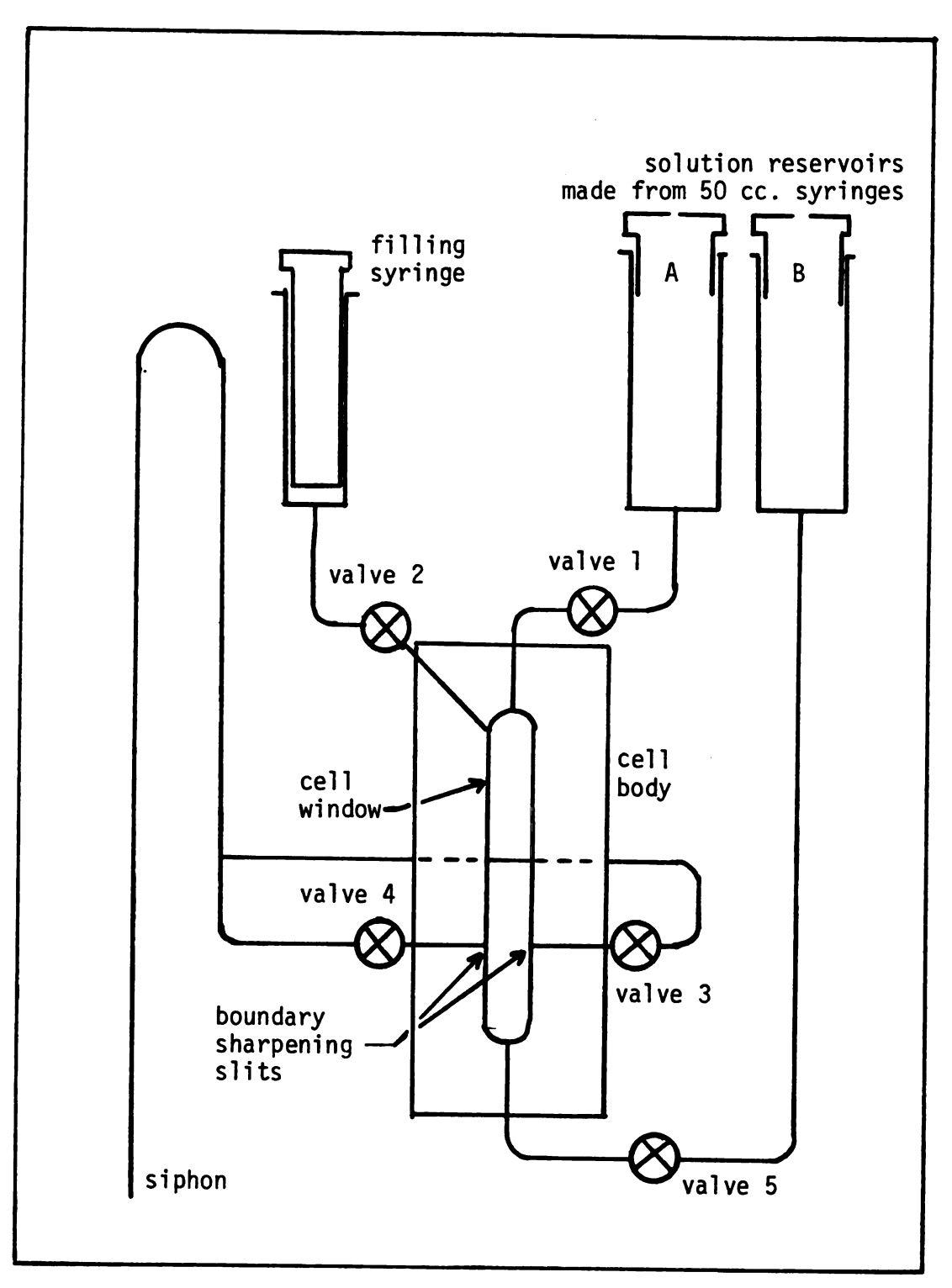


Figure 5-14.--Diagram of diffusion cell.

A framework was bolted to the cement block and positioned above the bath so that the cell could be hung from the top and immersed in the bath. Two small position pins were placed on the framework to insure that the cell was always placed in the same position.

The cell was provided with two inlets, one in the top and one in the bottom, and two outlets directly across from each other about one third the way up the channel sides. Two solutions of slightly different concentration were then slowly flowed simultaneously into the cell, the denser solution through the bottom inlet and the other through the top, and then out the two outlets. A sharp boundary was thus formed between the two layered solutions. This boundary was located in the center of the lower beam. All the valves were then closed and the solution allowed to diffuse freely.

Procedure for Experimental Run

- 1. The light source and water bath heater were first turned on.
- 2. The cell was then placed in a rack away from the rest of the apparatus for convenience in filling.
- 3. All the cell valves except valve 2 were then closed and approximately 30 cc. of less dense solution were placed in reservoir A. Some of this solution was then allowed to flow into the cell through valve 1 until the liquid level was one inch above the outlets. Valve 1 was then closed.

- 4. Valve 4 was next opened slightly and liquid was forced into the exit line by means of the filling syringe plunger until the liquid level in the cell was just above the outlets. Valve 4 was then closed and more solution from the reservoir A was passed through valve 1 into the cell as in step 3. More liquid was forced into the exit line through valve 4 and the whole procedure repeated until liquid dripped from the outlet line. This was done to ensure that liquid had filled the exit line as far as the end of the line without any air bubbles. Valve 4 was then closed.
- 5. The same procedure of adding liquid to the cell through valve I was repeated and exit valve 3 opened. The filling syringe was then used to force liquid into the exit line until the cell liquid level was just above the outlet. At this point, valve 3 was closed.
- 6. Step 5 was repeated until the liquid flowed freely from the exit line by means of a siphon.
- 7. Valve 1 was next opened until the cell was completely filled with solution from reservoir A. Then valve 2 was closed. Then valve 5 was opened very slowly and the solution allowed to flow into the line that connects valve 5 to reservoir B. Valve 5 was closed when the solution filled the line but did not enter reservoir B. So at this point all the exit and entrance lines including the cell were filled with the less dense solution.
- 8. Reservoir B was then filled approximately to the same level as A with the more dense solution. Throughout care was taken to see that there were no air bubbles.

- 9. At this point the cell was placed in position in the water bath. The reservoir valves, valves 1 and 5, were then opened one full turn followed slowly by valve 3 until the rate of flow from the exit line was one drop every 8 seconds. The opposite outlet valve, valve 4, was then opened until the combined exit flow rate was one drop every 4 seconds. It was important to maintain balanced flow rates into both halves of the cell as well as through both outlets.
- 10. Since the cell was full of less dense solution, it generally took on the order of three to four hours for the more dense solution to come up to the level of the exit slits. The formation of a sharp boundary was watched through the telescope. The boundary formation was aided by the boundary sharpening slits in the two outlets. These slits allowed the liquid to flow evenly out the entire width of the cell.
- and 4 were closed followed by valves 1 and 5. The solutions were allowed to diffuse for a few minutes until the fringes could be seen distinctly across the diffusion zone. Then the mirror reflecting the image into the telescope was swung away from the beam so that the beam was in view of the camera. The interference fringe patterns caused by the diffusion were photographed at predetermined time intervals. The series of exposures taken for one run is shown in Figure 5-15.
- 12. After the run was completed, the cell was again clamped in a rack away from the rest of the apparatus and allowed

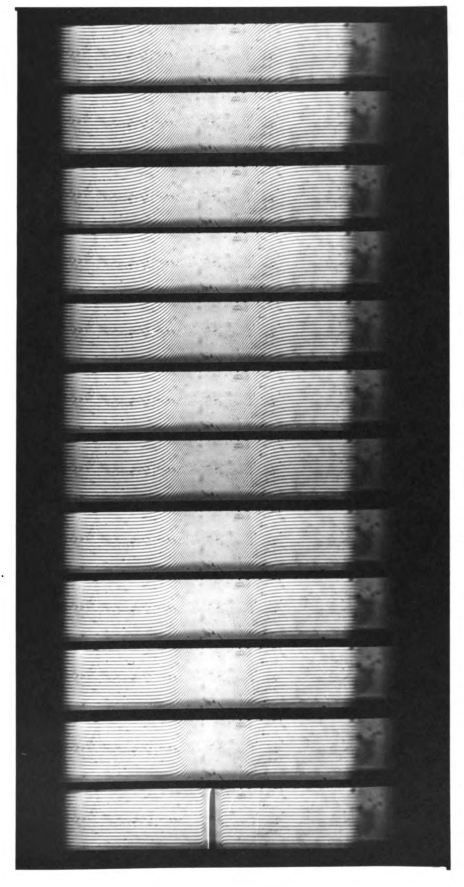


Figure 5-15.--Typical set of photographs taken during diffusion run (experimental run no. R18).

to drain. It was then rinsed twice with the solvent used for the solutions and then once with acetone. Finally, the cell was thoroughly dried with air.

Theory and Calculations

Consider a differential volume element in the section of the cell where diffusion occurs, as shown in Figure 5-16. By writing a material balance on the differential volume element, which describes the mass transfer in and out of the element, we obtain equation 5-27 which is known as Fick's Second Law

$$\frac{\partial^2 c}{\partial x^2} = \frac{1}{D} \frac{\partial c}{\partial t}$$
 (5-27)

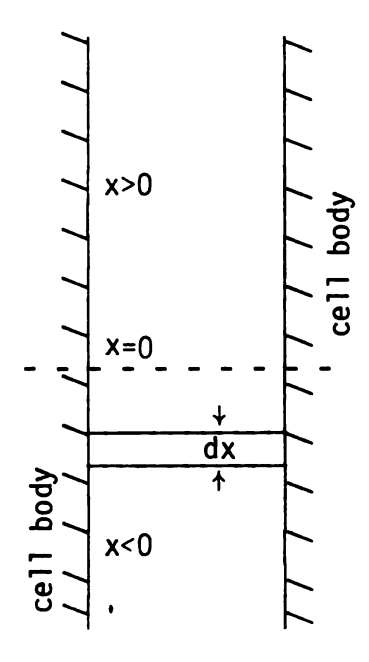


Figure 5-16.--Diffusion cell coordinates.

Case I
$$(x \ge 0)$$
 (i) $x \to \infty$ $t \ge 0$ $c = c_1$ (ii) $t = 0$ $c = c_1$ $\infty > x > 0$ (iii) $x = 0$ $c = (c_1 + c_2)/2$ $t \ge 0$

Case II
$$(x \le 0)$$
 (i) $x \to -\infty$ $t \ge 0$ $c = c_2$ (ii) $t = 0$ $c = c_2$ $0 > x > -\infty$ (iii) $x = 0$ $c = (c_1 + c_2)/2$ $t \ge 0$

where x is defined in Figure 5-16.

In order to solve equation 5-27 with the above boundry conditions it is necessary to assume that (1) the concentration dependence of the diffusion coefficient D is neglibible over the small concentration range involved, and (2) the diffusion gradient has the properties of normal distribution curves. These assumptions are valid if c_1 and c_2 are nearly equal.

The solution of equation 5-27 may be obtained with Laplace transforms to give the following identical solution for both Case I and Case II.

$$\frac{c-c_0}{c_2-c_1} = \frac{1}{2} \text{ erf. } \left(\frac{x}{\sqrt{4Dt}}\right)$$
 (5-28)

where c_0 is the concentration at the zero position in the cell and as a result of assumption (2) above is equal to $(c_1 + c_2)/2$, and erf. (z) is the error function of variable z. The refractive index, n, in the small concentration range used may be assumed to be proportional to the concentration, so that

$$\frac{n - n_0}{n_2 - n_1} = \frac{1}{2} \text{ erf. } \left(\frac{x}{\sqrt{4Dt}} \right)$$
 (5-29)

The fringe pattern obtained from the interferometer is equivalent to a plot of the refractive index versus distance in the diffusion cell. The distances on the photographic plate are not equal to the distances in the cell because the camera magnifies the image by the factor M, which is the magnification factor of the camera. A representation of the fringe pattern is shown in Figure 5-17. Because the fringe pattern is a representation of refractive index versus distance in the cell the refractive index difference may be represented by the number of fringes displaced. In traversing from point A to point B on Figure 5-17, the total number of fringes crossed will be the number of fringes displaced because of the difference in refractice index between solutions at point A and B. Each fringe will correspond to a change in refractive index by an amount Δn .

Let J be the total number of fringes from top to bottom; k is the local fringe number in the top half of the cell and j is the local fringe number in the bottom half of the cell. Let x_j be the measured distance corresponding to fringes j and k respectively. Therefore, where x>0

$$\frac{n - n_0}{n_2 - n_1} = \frac{k - \frac{1}{2}J}{J} = \frac{2k - J}{2J}$$

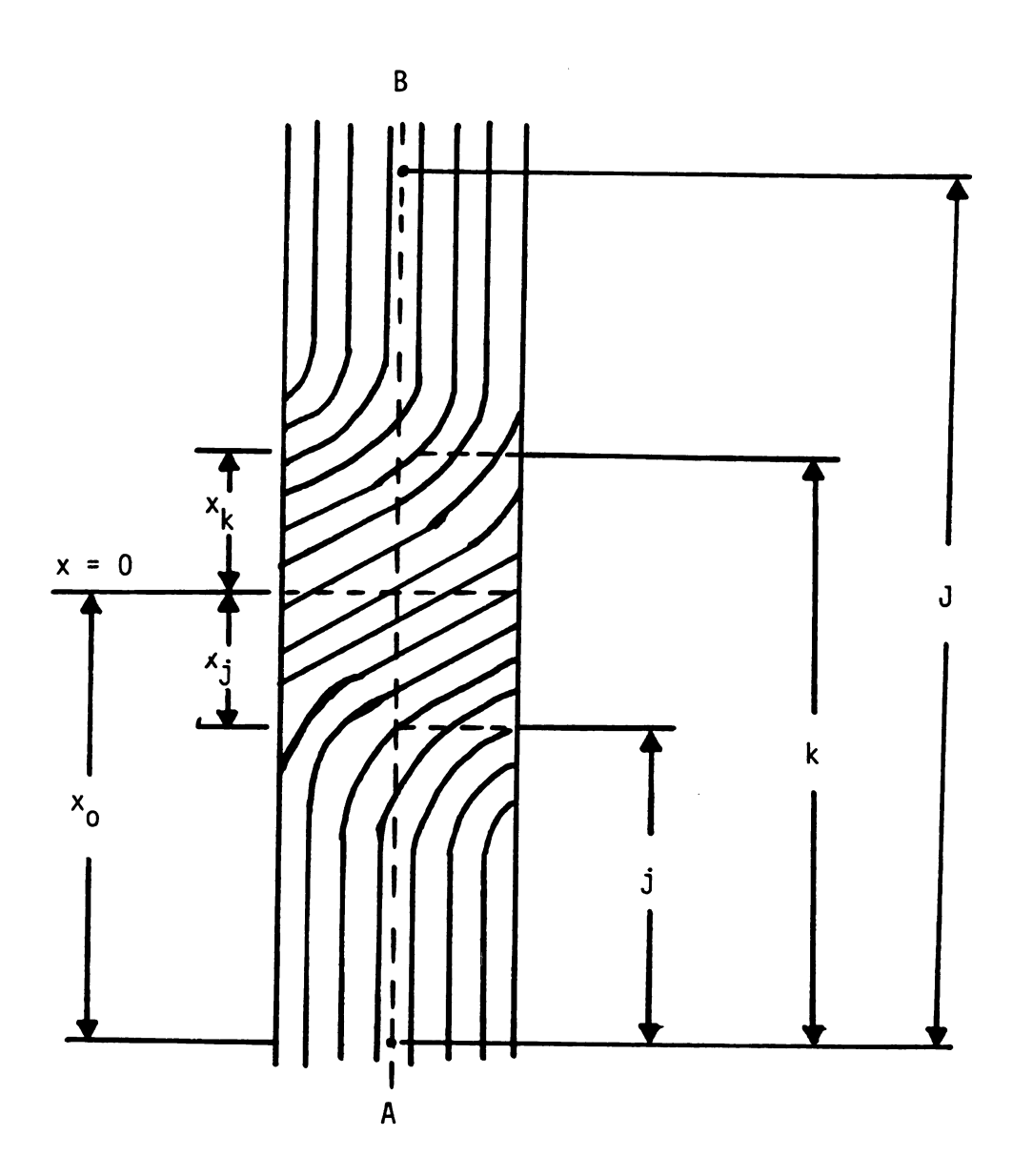


Figure 5-17.--Fringe pattern.

and equation 5-29 becomes

$$\frac{x_k}{\sqrt{4Dt}} = erf^{-1} \left(\frac{2k - J}{J} \right)$$
 (5-30)

Similarly, where x < 0

$$\frac{n - n_0}{n_2 - n_1} = \frac{J - 2j}{2J}$$

and

$$\frac{x_{j}}{\sqrt{4Dt}} = erf^{-1} \left(\frac{J - 2j}{J} \right)$$
 (5-31)

It is very difficult to determine the exact midpoint of the diffusion zone; however, the distance, $x_k + x_j$, is very easily determined by difference measurements. Therefore

$$\frac{x_{j}}{\sqrt{4Dt}} + \frac{x_{k}}{\sqrt{4Dt}} = erf^{-1} \left(\frac{J - 2j}{J} \right) + erf^{-1} \left(\frac{2k - J}{J} \right)$$
 (5-32)

The measurements taken from the photographic plate are different from the cell distances because of the magnification by the camera. The image is magnified by a factor M. Therefore

$$\frac{x_j + x_k}{\sqrt{4Dt}} = \frac{x_j' + x_k'}{M\sqrt{4Dt}}$$
 (5-33)

where x_{j} and x_{k} are distances on the photographic plate. Hence,

$$Dt = \frac{1}{4M^2} \left[\frac{x_j' + x_k'}{erf^{-1} \left(\frac{J - 2j}{J} \right) + erf^{-1} \left(\frac{2k - J}{J} \right)} \right]$$
 (5-34)

The value

$$\left[\frac{x_{j}^{\prime} + x_{k}^{\prime}}{\operatorname{erf}^{-1}\left(\frac{J-2j}{J}\right) + \operatorname{erf}^{-1}\left(\frac{2k-J}{J}\right)}\right]$$

is obtained for several j's and k's for each exposure and averaged.

The averages for several exposures are plotted versus exposure time.

The slope of the resulting line is determined and thus,

$$D = \frac{\text{slope}}{4M^2} \tag{5-35}$$

This diffusion coefficient is assumed equal to the mutual diffusivity at the average concentration c_0 . As mentioned previously, M = 1.929, so that the factor $4M^2$ equals 14.884.

The distances on the photographic plate were measured with an optical comparator made from Gaertner microscope fitted with a traveling eyepiece. The traveling eyepiece could scan a total distance of five centimeters by turning a crank and the distance traveled was indicated on a vernier scale accurate to 0.0001 centimeters. See Appendix A for details of a sample experimental run, and data analysis.

Extension to polymer solutions.--If there is more than one solute, as in polydisperse polymer solutions, the theory developed in the last section is still valid, however the measured diffusion coefficient is an average value representing the average D for all the individual species in the solution. In this section a relation between the average diffusion coefficient measured D_{avg} , and the diffusion coefficient of the individual species, D_i , is determined. Before deriving relations for a multicomponent system, let us take a closer look at the two-component system.

If the refractive index, n, of a two-component system is a linear function of the solute concentration over the concentration range encountered in the cell, we may write

$$n = n(c_0) + R(c-c_0)$$
 (5-36)

where $n(c_0)$ is the refractive index at concentration c_0 and the constant R, which is the differential refractive index increment, is the change in refractive index corresponding to unit change of solute concentration. Substitution of equation 5-36 into 5-28 yields the refractive index distribution for free diffusion for the case of D independent of c,

$$n = n(c_0) + \frac{\Delta n}{2} \left(\frac{2}{\sqrt{\pi}}\right) \int_{0}^{e^{-\lambda^2}} e^{-\lambda^2} d\lambda \qquad (5-37)$$

Here Δ n denotes R Δ c, the total difference in refractive index across the initial boundry. Equation 5-37 is another representation of equation 5-29. An expression for the refractive index gradients is obtained by differentiating equation 5-37

$$\frac{\partial n}{\partial x} = \frac{\Delta n}{2\sqrt{\pi D t}} \exp(-x^2/4Dt)$$
 (5-38)

One of the methods of obtaining diffusion coefficients from refractive index gradients is called the Reduced Height-Area ratio, where

$$D_{avg} = \frac{(\Delta n)^2}{4 t (\partial n/\partial x)^2}$$
 (5-39)

For the case of a two-component system in which D is independent of c and n is linear in c, it may be shown by substitution of equation 5-38 into equation 5-39, that

$$D_{avg} = D ag{5-40}$$

When two or more solutes are present in the cell, the situation is sufficiently complicated so that we consider here only the case of a linear dependence of n on the concentration of the N solutes. It has been shown in the literature that for solutions of polymer of sufficiently high molecular weight, the refractive index of the solution is independent of the molecular weight of polymer (5B-11). This makes the analysis less complicated, therefore we can write

$$n = n(c_{10}, c_{20}, ---, c_{N0}) + \sum_{i=1}^{N} R_i(c_i - c_{i0})$$
 (5-41)

where $n(c_{10}, c_{20}, ----, c_{No})$ denotes the refractive index of a solution in which the concentration of the N solutes are c_{10} ----- c_{No} . We also assume that there is no interaction of solute flows and that each c_i is sufficiently small that the concentration dependence of the several diffusion coefficients may be neglected. It has been shown (5B-12) that equation 5-28 can be used for multicomponent systems by replacing c by c_i and d by d0, where d1 and d2 correspond to d3 and d4 of the d4 species. Substitution of equation 5-41 into equation 5-28, gives

$$n = n(c_{10}, ----, c_{n0}) + \frac{\Delta n}{2} \sum_{i=1}^{N} w_i (2/\sqrt{\pi}) \int_{0}^{x/\sqrt{4D_i t}} e^{-\lambda^2} d\lambda$$
 (5-42)

where Δ n is the total difference of refractive index across the starting boundry and

$$w_{i} = \frac{R_{i} \Delta c_{i}}{\Delta n}$$
 (5-43)

are solute fractions on the basis of refractive index. Since the value of R_i is the same for every solute, w_i is the weight fraction of solute i. The refractive index gradient is obtained by differentiating equation 5-42.

$$\frac{\partial n}{\partial x} = \sum_{i=1}^{N} \frac{w_i \Delta n}{\sqrt{4 D_i t}} \exp(-x^2/4D_i t)$$
 (5-44)

Therefore for systems containing N solutes without interacting flows, and with each D_i independent of every concentration and n a linear function of concentration, substitution of equation 5-44 into 5-39 leads to the relation

$$\frac{1}{\sqrt{D_{avq}}} = \sum_{i=1}^{N} \frac{w_i}{\sqrt{D_i}}$$
 (5-45)

Equation 5-45 gives a relation between individual diffusion coefficients of the N solutes and the average diffusion coefficient measured by the interferometer. It is frequently convenient to introduce distributions for \mathbf{w}_i in equation 5-45 and change the sum into an integral. Most of the commercial polymers are generally represented by a Schulz (5B-13) distribution. The Schulz distribution for weight fraction of polymer of length y is given by

$$w_y = \frac{h}{x_n \Gamma(h+1)} (hy/x_n)^h \exp(-hy/x_n)$$
 (5-46)

where

$$\frac{M_{W}}{M_{D}} \approx \frac{X_{W}}{X_{D}} = \frac{h+1}{h}$$

To solve equation 5-45 with the distribution of 5-46, we need a relation between D_y and M_y , where M_y is the molecular weight of polymer chain of length y. The only simple relation available is

$$D_{y} = K \left(M_{y}\right)^{-\alpha} \tag{5-47}$$

where K and α are constants. This relation is strictly valid for D of polymers only at infinite dilution. However, due to the lack of any relations, it was decided to use 5-47. If equation 5-47 and 5-46 are substituted into equation 5-45, and the integration performed we obtain

$$D_{avg} = \frac{A}{M_n}$$
 (5-48)

where
$$A = [\Gamma(h + 1)/\Gamma(h + \alpha/2 + 1)]^2 K h$$

A is a constant for a particular distribution. The result of equation 5-48 is very important because it leads to the conclusion that the average diffusion coefficient measured using interferometry depends on M_n , the number average molecular weight. Since M_n is biased towards the small chains in the polydisperse polymer, the D_{avg} measured by interferometry would also be biased towards the small chains.

Calibration

In this study, the accuracy of the interferometric technique was established by measurement of the concentration-dependent diffusion coefficient for the binary system sucrose-water at 25°C.

This particular system was chosen because accurate, widely accepted diffusion data over a concentration range are available for comparison. The accuracy of the method used in this work was tested by comparing diffusion coefficients at 25°C for five aqueous solutions of sucrose with those reported by Gosting and Morris (5B-14). The data of Gosting and Morris have been carefully checked by several investigators (5B-15 to 5B-17) and are thought to be accuarate to \pm 0.2%. Gosting and Morris fit their data to the following empirical relationship using the method of least squares.

$$D_s = 5.226(1 - 0.0148 c_0) \times 10^{-6} \pm 0.002$$
 (5-49)

where $\rm D_{\rm S}$ is the binary diffusion coefficient for sucrose-water system at 25°C and $\rm c_{\rm O}$ is the concentration of sucrose in 100 cm 3 of solution.

The results of comparison are summarized in Table 5-4. The results deviated by only 1% or less from equation 5-49. From Table 5-4 it can be concluded that the precision of the interferometer is no worse than about $\pm 1\%$.

Error Analysis

The source of errors in interferometry can be attributed to the following factors:

- 1. The accuracy in determining the fraction of a fringe when measuring the total fringes on a particular exposure.
- The assumption that the concentration dependence of D
 is negligible over the small concentration difference
 involved in the experimental run.

TABLE 5-4.--Results of the calibration runs on the interferometer.

Percentage Deviation	+ 0.755	- 0.330	+ 0.290	- 0.020	- 0.140
$D_{\rm S} \times 10^6 { m cm}^2/{ m sec}$ This Laboratory	5.124	5.195	5.133	5.119	5.171
Diffusion Coefficient, Reference (58-14)	5.164	5.178	5.148	5.118	5.178
Conc. of Sucrose 3 Gms of Sucrose/100 cm	0.8	0.4	1.0	1.4	0.4
Experimental Run No.	_	2	က	4	ĸ

- 3. The magnification factor of the camera.
- 4. Errors in measurement of distances on the photographic plate.

The average diffusion coefficient is calculated by using equation 5-34, and requires that the average of the right-hand side of the equation 5-34 for several exposures when plotted versus exposure time must be linear. From the slope of this line the average diffusion coefficient is obtained. The estimated standard error in determining the slope is a quantity that contains some of the above mentioned errors, although perhaps not all of them. Given the unavailability of any other direct method for determining the error, the estimated standard error in the slope is used. From this, the diffusion coefficients obtained here by the interferometric technique are accurate to within 2.5%.

CHAPTER VI

PRESENTATION OF EXPERIMENTAL DATA

Light Beating Spectroscopy

The value of the diffusion coefficients measured for all the polymer-solvent systems studied in this work are presented in Appendix D. The concentration dependence of the diffusion coefficients for all the polymers in various solvents is illustrated in Figures 6-1 through 6-5. As previously described the diffusion coefficients are accurate to within 3.5%. For each of the polymer-solvent systems, linear least squares extrapolations were performed to obtain the value of the diffusion coefficient at infinite dilution, $D_{\rm O}$, and also the slope of the diffusion coefficient-concentration line at low concentration. In performing the linear extrapolations each experimental diffusion coefficient is attributed equal weight. From the slope of the calculated line the value of $k_{\rm d}$ as represented by equation 3-10 is obtained.

The resulting values of k_d and D_0 are displayed in Table 6-1. It is evident from the experimental results in Figures 6-1 through 6-5, that the concentration dependence of D may be approximated by a linear relationship over a relatively large concentration range, at least up to about 20 grams per liter, for all the molecular weights used in this work. These results confirm the recent findings on polymer systems, such as polystyrene in butanone (3A-14) and polystyrene in tetrahydrofuran (3B-10, 3B-11) where the linear dependency

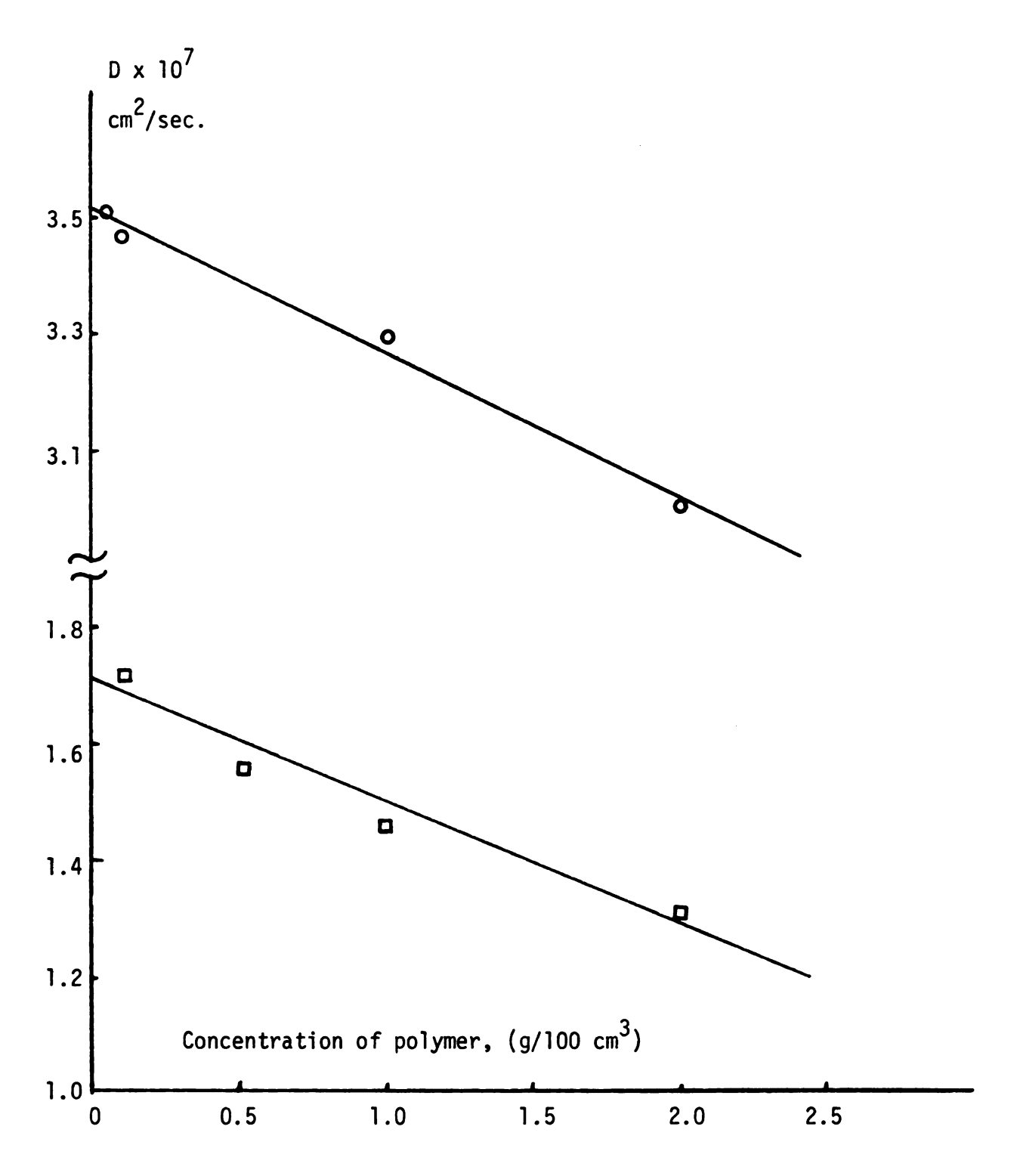


Figure 6-1.--Concentration dependence of diffusion coefficients obtained from light beating for PS-1 in benzene (O) and decalin (C) at 25°C.

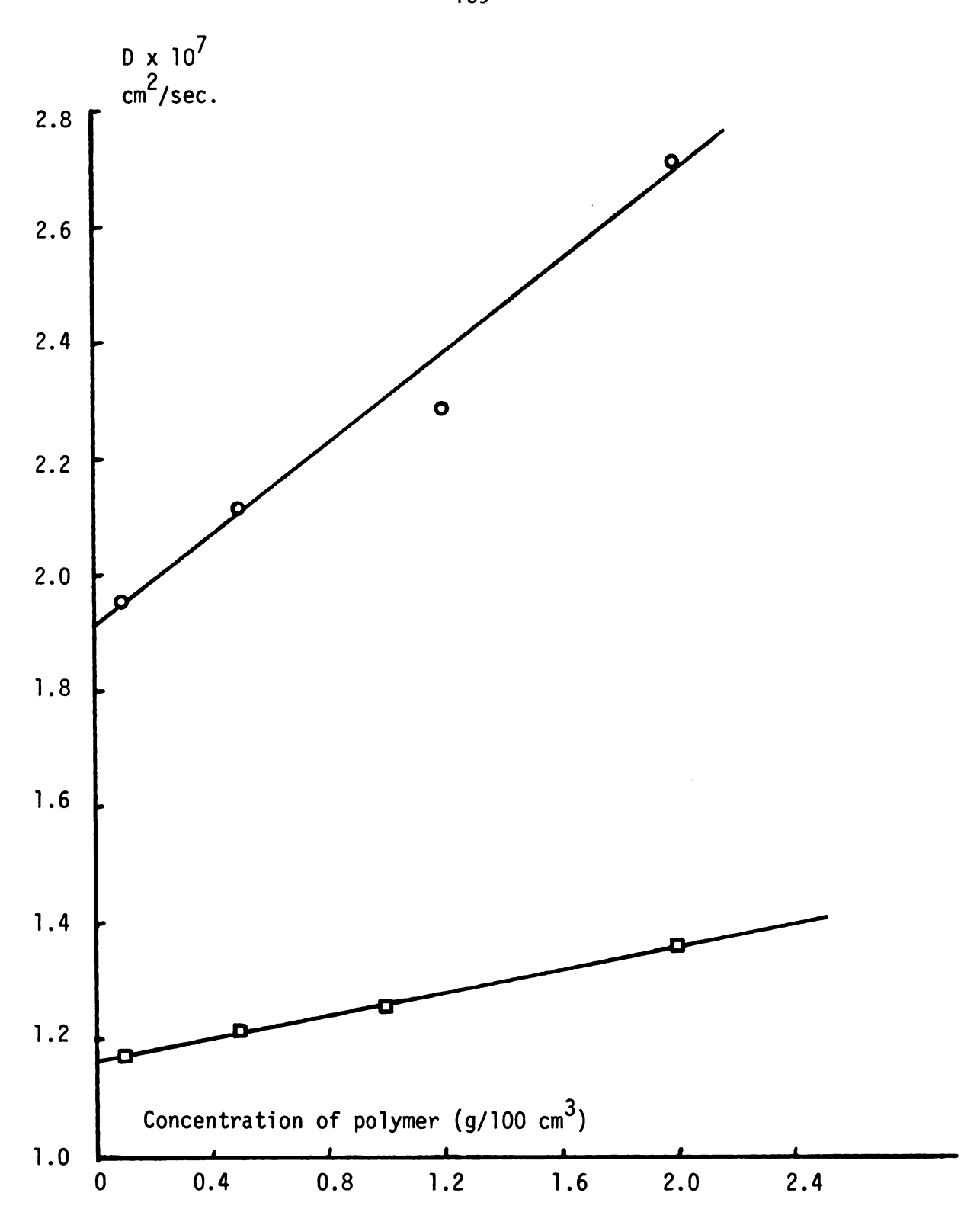


Figure 6-2.--Concentration dependence of diffusion coefficients obtained from light beating for PS-2 in benzene (◆) and decalin (□) at 25°C.

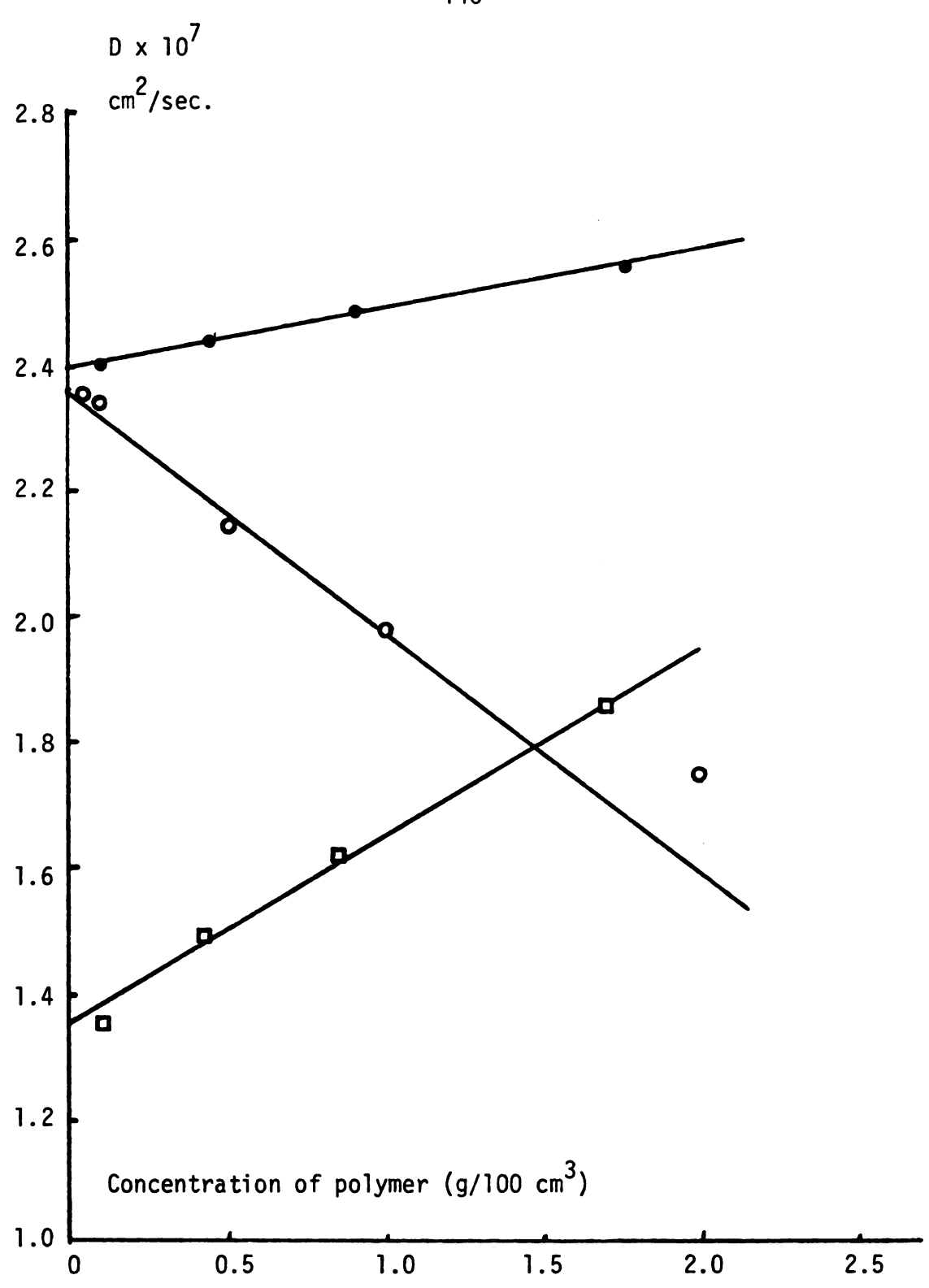


Figure 6-3.--Concentration dependence of diffusion coefficients obtained from light beating for SAN-1 in dimethyl formamide (□), methyl ethyl ketone (♠) and benzene (♠) at 25°C.

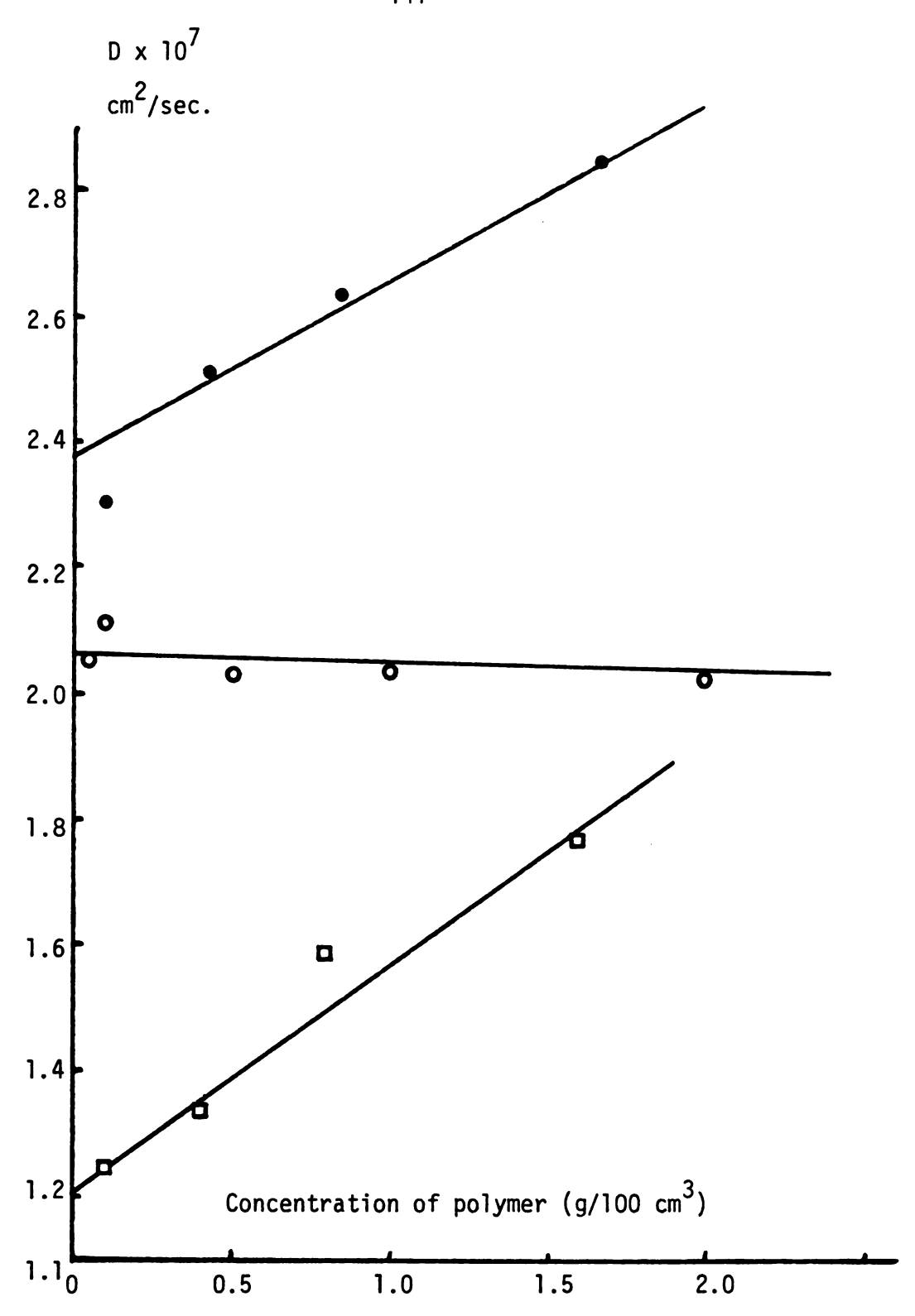


Figure 6.4.--Concentration dependence of diffusion coefficients obtained from light beating for SAN-2 in dimethyl formamide (□), methyl ethyl ketone (▶), and benzene (♠) at 25°C.

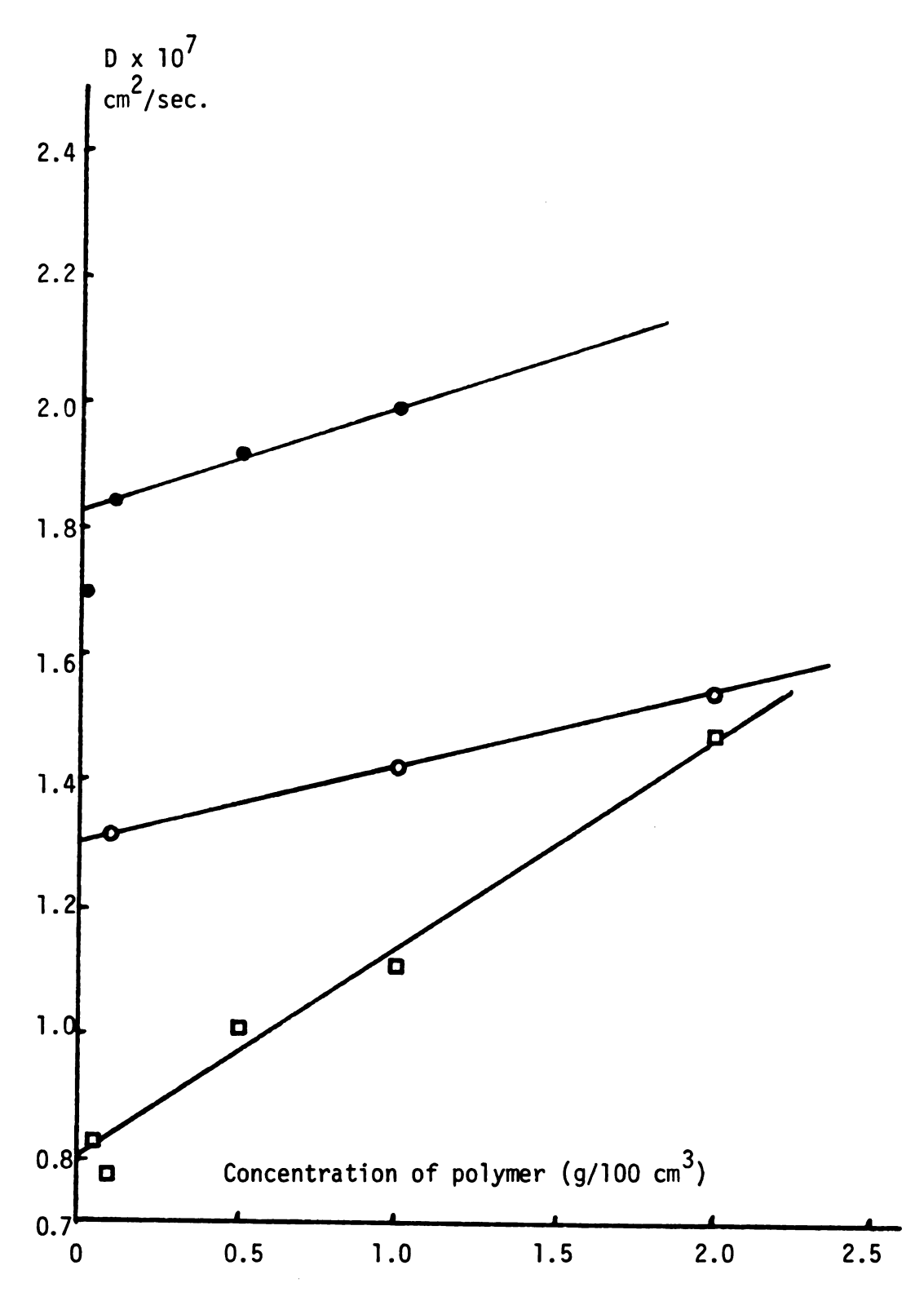


Figure 6-5.--Concentration dependence of diffusion coefficients obtained from light beating for SAN-3 in benzene (•), methyl ethyl ketone (•), and dimethyl formamide (•) at 25°C.

TABLE 6.1.--Values of \mathbf{D}_{o} and \mathbf{k}_{d} calculated from light beating data.

Polymer	Solvent	$D_0 \times 10^7 \text{ cm}^2/\text{sec}$	k _d , cm ³ /gram
PS-1	Decalin	1.688 ± 0.042	-11.845 ± 2.17
PS-2	Decalin	1.159 ± 0.004	8.450 ± 0.28
PS-1	Benzene	3.505 ± 0.011	- 5.960 ± 0.29
PS-2	Benzene	1.911 ± 0.013	20.840 ± 0.61
SAN-1	Benzene	2.338 ± 0.032	-13.350 ± 1.33
SAN-1	Dimethyl Formamide	1.342 ± 0.023	23.050 ± 1.72
SAN-1	Methyl Ethyl Ketone	2.393 ± 0.005	4.320 ± 0.22
SAN-2	Benzene	2.073 ± 0.021	- 1.540 ± 1.00
SAN-2	Dimethyl Formamide	1.205 ± 0.036	31.400 ± 3.63
SAN-2	Methyl Ethyl Ketone	2.312 ± 0.049	14.480 ± 2.22
SAN-3	Benzene	1.302 ± 0.003	9.410 ± 1.82
SAN-3	Dimethyl Formamide	0.789 ± 0.028	43.41 ± 3.49
SAN-3	Methyl Ethyl Ketone	1.759 ± 0.053	14.56 ± 5.08

was also observed. Our data do not yield any evidence suggesting a more complicated behavior with a concentration independent region at very low concentration (3B-1). The relative change of the diffusion coefficient with concentration is represented by the single parameter \mathbf{k}_{d} .

The diffusion coefficients of polystyrene polymers in decalin were consistently lower than those recorded in benzene. For the low molecular weight polystyrene the diffusion coefficients decreased with increase in concentration, for high molecular weights the diffusion coefficient increased with increase in concentration. This was observed in both solvents used for polystyrene.

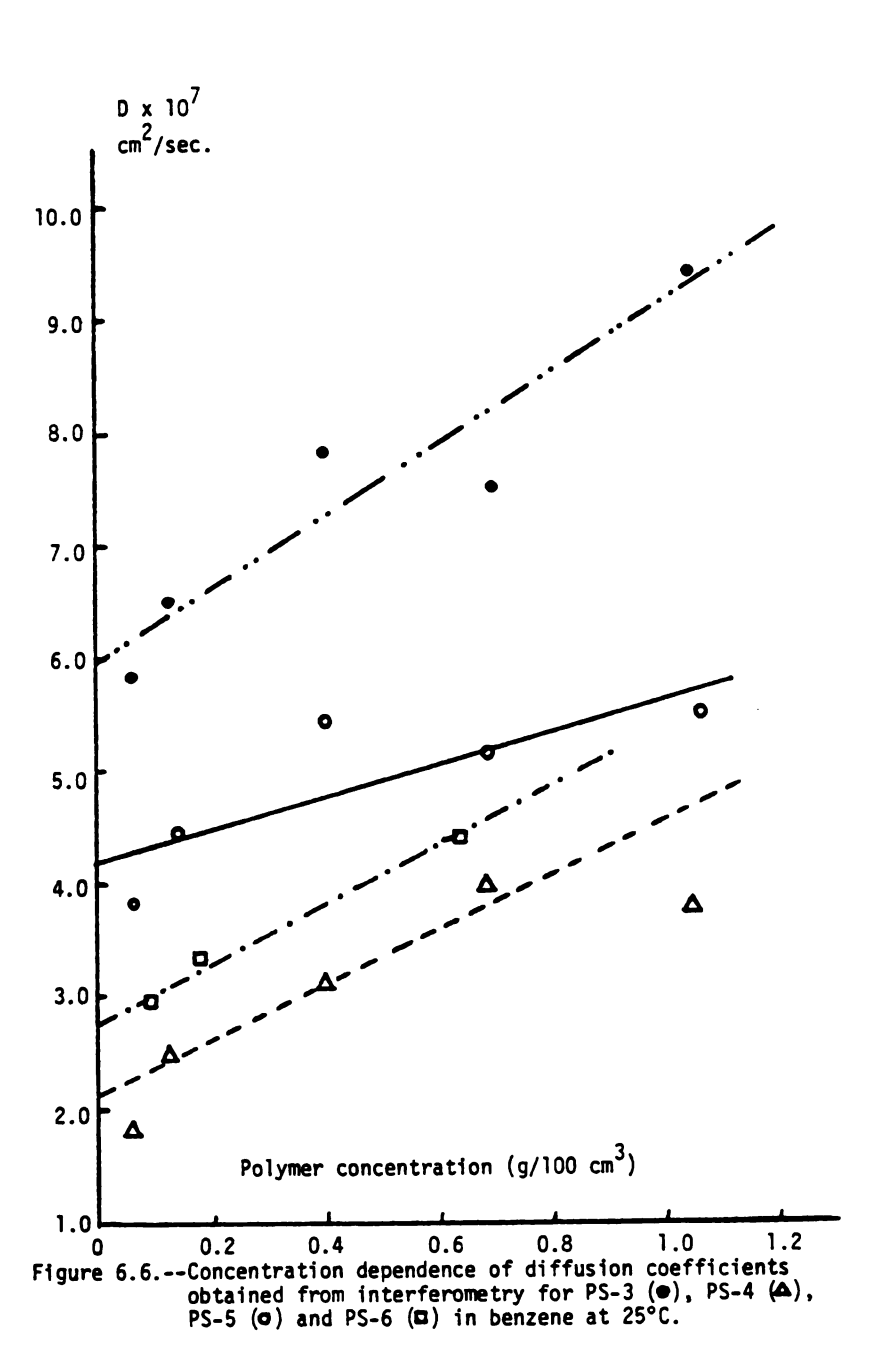
For copolymers, the diffusion coefficients in dimethyl formamide always increased with increase in concentration for all the molecular weights. The same phenomena as in dimethyl formamide is also observed in methyl ethyl ketone. The results in benzene are a classical example of concentration dependence. At low molecular weights the diffusion coefficient decreased with increase in concentration, at medium molecular weights, the diffusion coefficients are approximately concentration independent, and at high molecular weights diffusion coefficients increased with increasing concentration.

<u>Interferometry</u>

The average value of the diffusion coefficients measured by interferometry for the polymer-solvent systems studied in this work are presented in Appendix E. The concentration dependence of the

diffusion coefficients is illustrated in Figures 6-6 through 6-10. It was mentioned earlier that the diffusion coefficients measured by this method are accurate to within 2.5%. The main purpose of obtaining data by interferometry was to measure diffusion coefficients in the intermediate concentration range. We were not very successful in obtaining data at higher concentrations because of flow problems encountered in the diffusion cell at high concentrations. For the low molecular weights data were obtained up to a concentration of ten grams of polymer in one hundred cm³ of solution. For the intermediate molecular weights the experiments could be performed only up to a concentration of five grams of polymer in one hundred cm³ of solution, and for high molecular weights only up to two grams of polymer in one hundred cm³ of solution.

Diffusion coefficients of monodisperse polystyrenes and mixtures of these monodisperse samples were obtained over a concentration range to check the validity of equation 5-45. The results of these experimental runs are shown in Figure 6-6. For these polymers diffusion coefficients were obtained at low concentrations in order that linear extrapolations can be performed to zero polymer concentrations. The data show significant scatter, which might be due to small concentration gradients producing relatively few fringes. It is not advisable to measure diffusion coefficients at such low concentrations with interferometry. Linear extrapolations were performed for all the polymers in Figure 6-6, and the values of $k_{\rm d}$ and $D_{\rm o}$ obtained from a least-squares fit are displayed in Table 6-2.



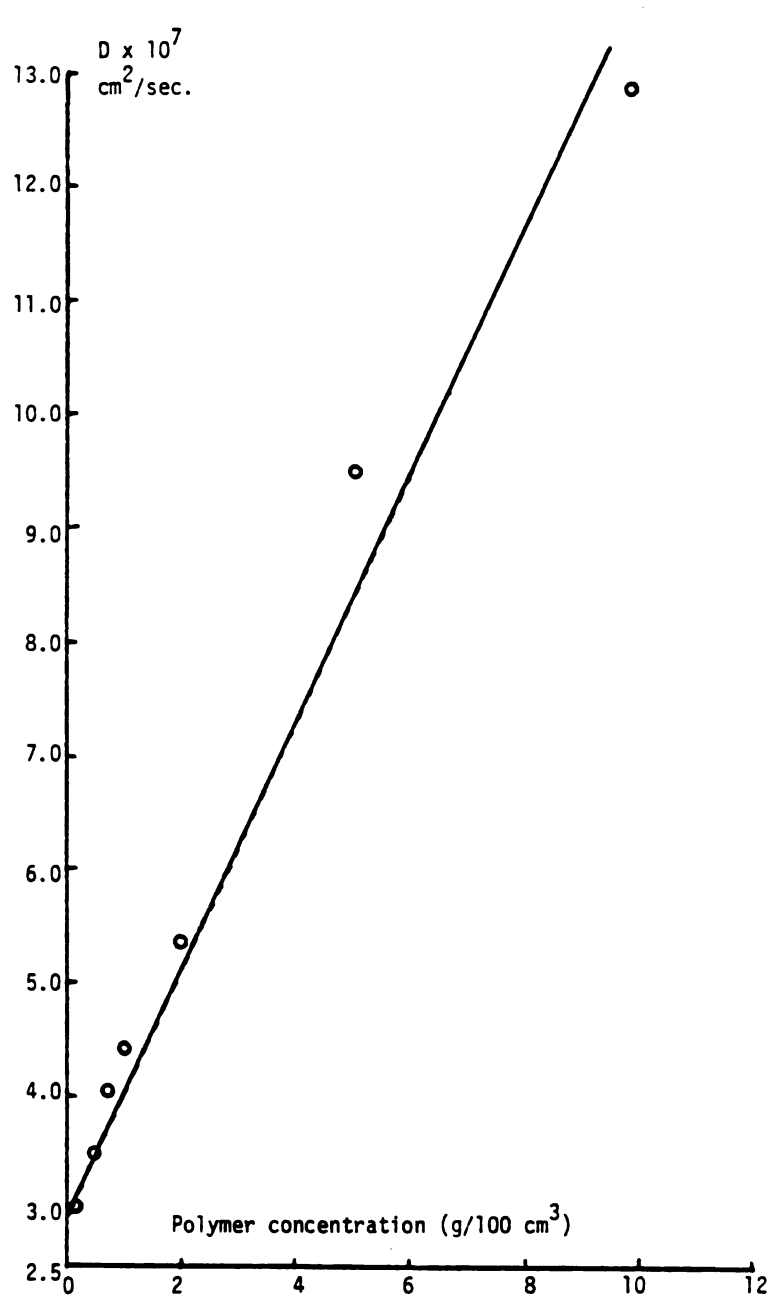


Figure 6-7.--Concentration dependence of diffusion coefficients obtained from interferometry for PS-2 in benzene (\circ) at 25°C.

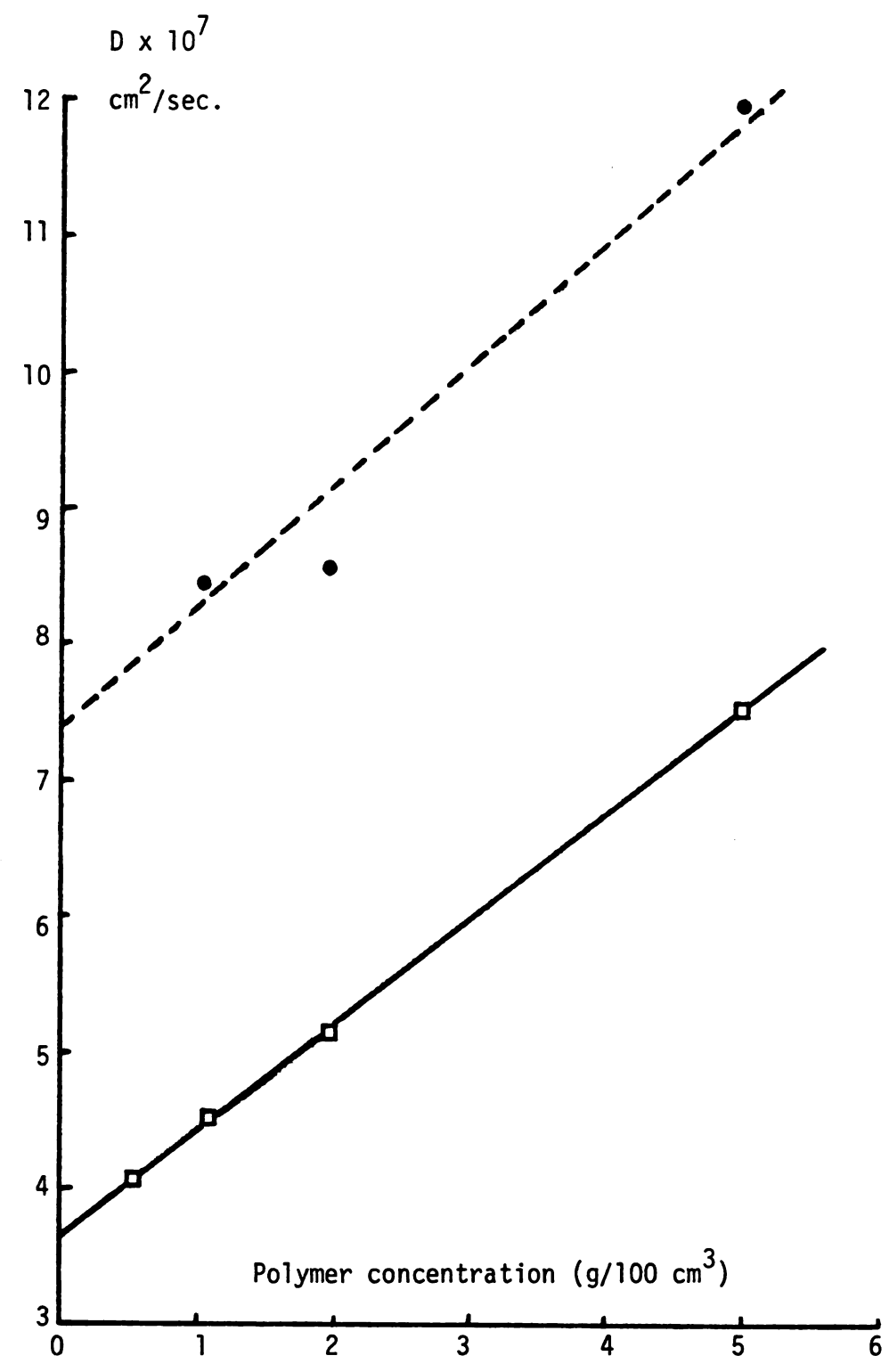


Figure 6-8.--Concentration dependence of diffusion coefficients obtained from interferometry for SAN-1 in dimethyl formamide (a), and methyl ethyl ketone (•) at 25°C.

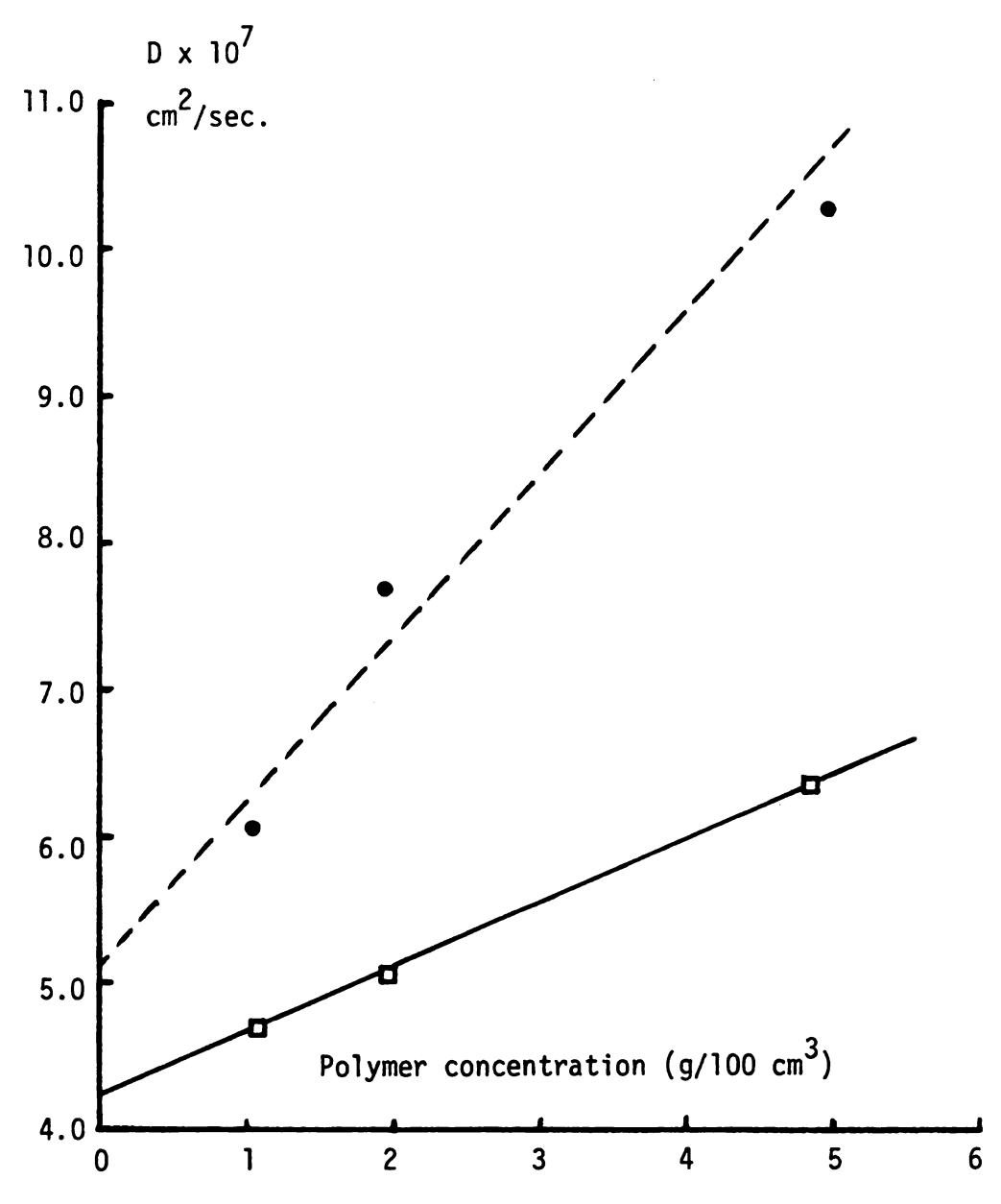


Figure 6-9.--Concentration dependence of diffusion coefficients obtained from interferometry for SAN-2 in dimethyl formamide (□), and methyl ethyl ketone (●) at 25°C.

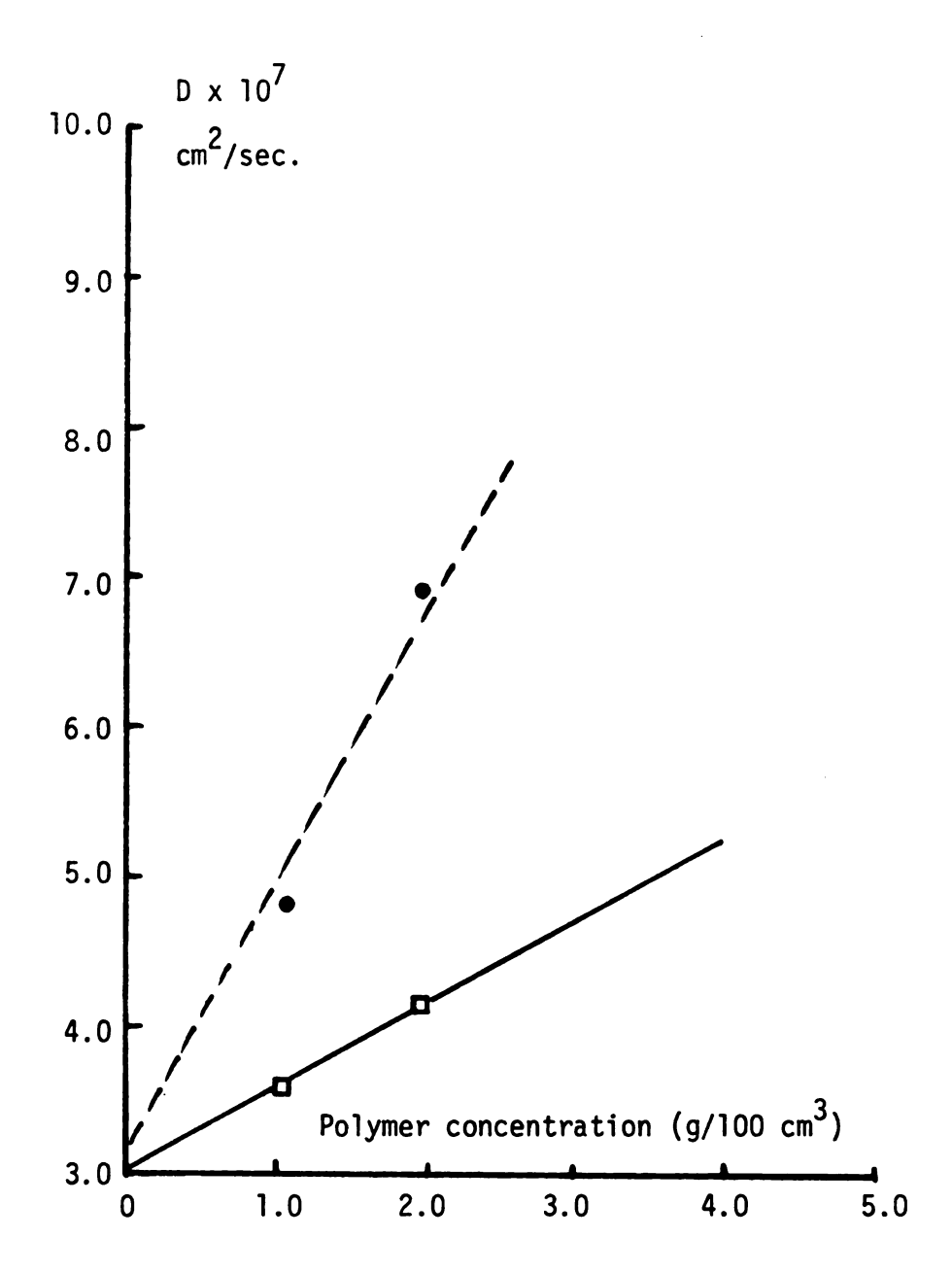


Figure 6-10.--Concentration dependence of diffusion coefficients obtained from interferometry for SAN-3 in dimethyl formamide (□), and methyl ethyl ketone (●) at 25°C.

TABLE 6-2.--Values of D_0 and k_d obtained from interferometric data for monodisperse polystyrenes and their mixtures.

Polymer	Solvent	$D_0 \times 10^7$, cm ² /sec.	k _d , cm ³ /gram.
PS-3	Benzene	5.998 ± 0.399	51.755 ± 11.13
PS-4	Benzene	2.173 ± 0.339	89.546 ± 26.21
PS-5	Benzene	4.234 ± 0.336	33.230 ± 13.26
PS-6	Benzene	2.818 ± 0.107	90.659 ± 9.82

Figure 6-7 is a concentration dependence plot of diffusion coefficient for polydisperse polystyrene. Figures 6-8 to 6-10 are the plots for the copolymers. If the diffusion coefficients for a particular concentration (1 or 2 grams per 100 cm³) of polymer obtained both by light beating and interferometry are compared, it can be concluded that the diffusion coefficients obtained from interferometry are at least 2 to 3 times greater than the values obtained from light beating. This discrepancy will be discussed in a detailed fashion in the next chapter.

CHAPTER VII

COMPARISON WITH THEORY

It is of interest to compare the experimental values of diffusion coefficients obtained in different laboratories on a particular system, before the results obtained in this work are discussed. This was necessitated by the fact that several authors have noted lack of precision of diffusion data reported in the literature (3B-10, 5A-16). Relatively few data on well characterized flexible polymers have been reported, and in the very few cases where comparisons can be made serious disagreement exists. This chapter discusses both comparisons of the data of other investigators and the data obtained in this work, as follows. In the section on "Comparison of Light Beating Data for Polystyrene in Methyl Ethyl Ketone" the data of Ford, et al. (3A-15) are compared with those of King, et al. (3A-14) for the polystyrene-2-butanone system. The section on "Comparison of Light Beating Data for Polystyrene in Tetrahydrofuran" contains a comparison of the Jamieson, et al. (3B-10) data with those of Mandema, et al. (3B-11) for polystyrene in tetrahydrofuran. The above mentioned comparisons were for systems where data were obtained by light beating measurements. The section on "Comparison of Interferometry

Data for Polystyrene in Toluene" describes the data obtained from interferometry for polystyrene in toluene with different optical setups by two investigators. In the section on "Comparison of Data Obtained from Interferometry with the Data Obtained from Light Beating for Polystyrene in Toluene" the data obtained from interferometry are compared with those obtained from light beating for polystyrene in toluene. The section on "Discussion of the Results Obtained from Light Beating Spectroscopy" discusses the data obtained in this work from light beating spectroscopy. The section on "Discussion of the Results Obtained from Interferometry" contains the discussion of the interferometric data obtained in this work. In the section on "Comparison of Light Beating and Interferometry Data" the data obtained from light beating and interferometry in this work are compared. Finally, in the section on "Comparison of Thermodynamic Parameters" the thermodynamic parameters obtained from the two parameter theory in this work are compared to the values on similar systems obtained from the literature.

Comparison of Light Beating Data for Polystyrene in Methyl Ethyl Ketone

King, et al. (3A-14) studied the diffusion of linear polystyrene under non-theta conditions in methyl ethyl ketone using a homodyne spectrometer, for polymers with a molecular weight range of 2.08×10^4 to 8.7×10^6 , as a function of concentration of polymer. By extrapolation of diffusion coefficient values to zero polymer concentration they obtained a relation between D_0 and molecular weight. In the concentration range investigated by King

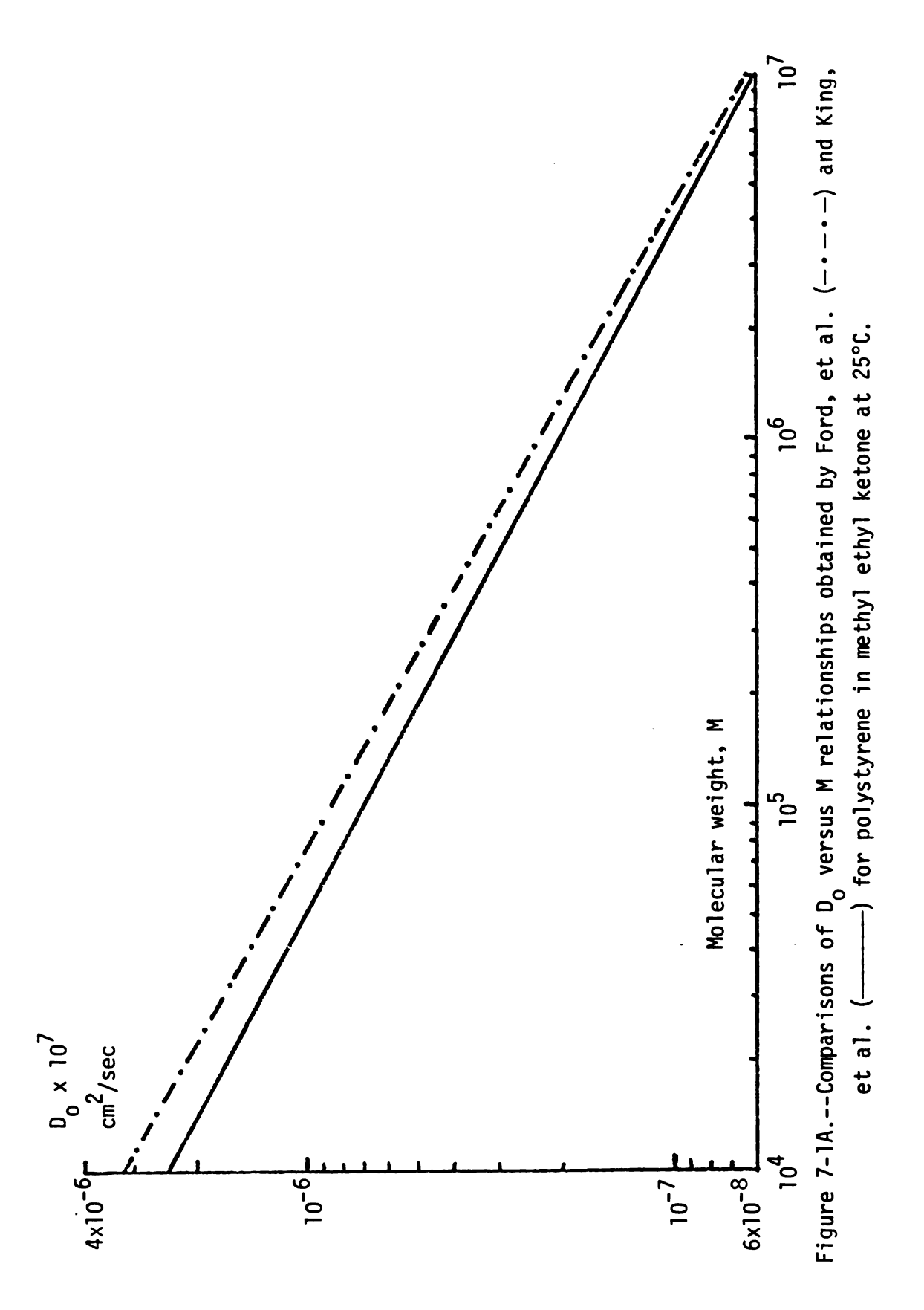
the D(c) versus c curve may be represented by a linear equation of the form 3-10. From the linear extrapolations values of k_d were obtained. Measurements of the diffusion coefficients were made at room temperature and results corrected, by at most 4%, to 25°C.

Ford, et al. (3A-15) used a laser homodyne spectrometer to study the power spectrum of light scattered from dilute polystyrenemethyl ethyl ketone solutions. From the measurements the translational diffusion coefficients for the macromolecules were determined as a function of molecular weight and polymer concentration. The molecular weight range investigated was 2 x 10^4 to 1.7 x 10^6 . Linear extrapolations were performed to obtain the parameters D_0 and k_d . In their study Ford, et al. found that D(c) was approximately constant above a polymer concentration of about 3 x 10^{-3} grams per cubic centimeter. Below this, D(c) could be expressed in the linear form of equation 3-10. From this latter linear region values of k_d were obtained. The experiments were performed at 25°C.

Both Ford and King obtained their monodisperse polystyrene polymers from Pressure Chemicals Co. To remove dust, King, et al. centrifuged their samples and Ford, et al. filtered their solutions through ultra-fine sintered glass filters. The results obtained in both of these works are shown in Table 7-1. The blanks in the table for Ford's data correspond to polymers where data were not reported. The two different relations for D_0 versus M reported by Ford and King are incompatible except when M is equal to 10^6 or higher. This point is further illustrated by the comparison of the two relations in Figure 7-1A.

TABLE 7-1.--Comparison of King, et al. and Ford, et al. data for polystyrene in methyl ethyl ketone at 25°C, obtained by light beating spectroscopy.

	Daí	Data of King, et	ng, et al.			Dat	Data of Ford, et al.	
Σ	M/W	D _o ×10 ⁷ ,	$M_{\rm w}/M_{\rm n}$ $D_{\rm o} \times 10^7$, cm ² /sec	k _d , cm ³ /gram	₩ M	M/W	$M_{\rm w}/M_{\rm h}$ $D_{\rm o}$ x10 ⁷ , cm ² /sec $k_{\rm d}$, cm ³ /gram	k _d , cm ³ /gram
20,800	1.06	22.5 ± 1	+1	-25 ± 5	20,800		1	-10.0
33,000	1.06	16.0	16.0 ± 0.6	-26 ± 5	20,500	ı	1	1
111,000	1.06	8.1	± 0.3	-11 ± 4	160,000	ı	ı	1
200,000	1.06	5.95	5.95 ± 0.1	- 2 ± 3				
392,000	1.1	3.95	3.95 ± 0.15	4 4	179,000	ı	ı	1
507,000	1.2	3.3	3.3 ± 0.01	19 ± 4				
670,000	1.1	2.9	2.9 ± 0.01	27 ± 4	670,000	1.1	1	190.0
$D_0 = (3.1 \pm 0.2) 10^{-4} \text{M}^{-0.53 \pm}$	1 ± 0.2)	10-4 M-0	.53 ± 0.02	0.02 cm ² /sec	$D_0 = (5.5)$	± 0.2)	$D_0 = (5.5 \pm 0.2) 10^{-4} M^{-0.561 \pm 0.005} cm^2/sec$	005 cm ² /sec



The relation between the diffusion coefficient at infinite dilution, $\mathbf{D}_{\mathbf{0}}$, and molecular weight of polymer is given by

$$D_0 = K_d M^{-b}$$

The relation between intrinsic viscosity and molecular weight of polymer is given by the Mark-Houwink relation

$$[\eta] = K_v M^a$$

where K_d , K_v , b and a are all constants for a polymer-solvent pair. Flory (2A-1) showed that the exponents a and b are related by

$$3 b = a + 1$$
 (7-1)

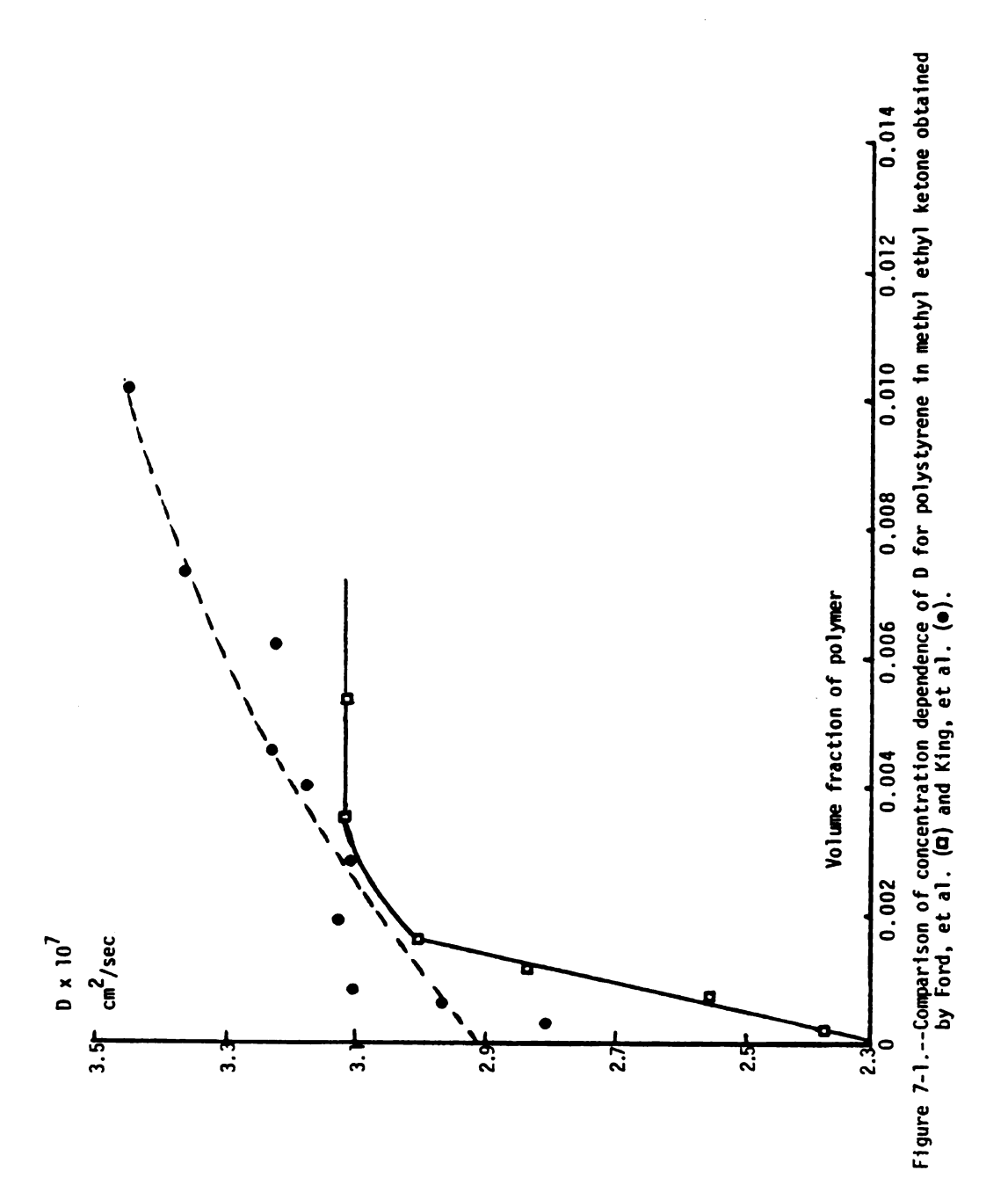
If values of D_0 are obtained over a large molecular weight range by diffusion measurements, the values of K_d and b can be calculated. Once the value of b is thus determined, it is possible to calculate the Mark-Houwink exponent a from the above relation and compare it with the value available in the literature from intrinsic viscosity measurements.

The intrinsic viscosity of the polystyrene-methyl ethyl ketone system at 25°C has been studied by several investigators with results for a ranging from 0.58 to 0.63. The value of b observed by Ford resulted in a calculated a in good agreement with the intrinsic viscosity result while that obtained by King did not.

Furthermore the values of k obtained in the two studies differ significantly. This was pointed out while comparing

experimental data with the two parameter theory in Chapter III in the section on "Comparison of Predicted Values of $\mathbf{k}_{\mathbf{d}}$ with Experimental Data." At low molecular weights the value of k_d obtained by Ford agrees very well with the predictions from theory, while at high molecular weights the value of King agrees well with theory. To shed additional light on the results in the two cases the D versus c curves for the polymer with molecular weight 670,000 are shown in Figure 7-1. Much emphasis cannot be placed on the accuracy of Figure 7-1, because all the points shown were obtained from small graphs in the original publications of the authors. Although the points might not be exact, the shape of the curves is accurately represented. The smooth lines through the points are the extrapolations as performed by the two sets of authors. The accuracy of the data reported by Ford, et al. is claimed as 3%, and for King, et al., calculated from their error bars, is around 3.5%. The main discrepancy arises from the conclusion by Ford, et al. that the linear relationship is valid only up to a concentration of 3 \times 10^{-3} grams per cubic centimeter. This gives rise to the high value of k_d reported by them. It is astonishing that the same polymer-solvent pair studied under nearly identical conditions can give rise to such a difference in results of the two laboratories.

In the author's opinion this discrepancy may be an outcome of either inaccurate data analysis or insufficient dust removal techniques. It is very hard to remove the dust particles completely from the polymer solutions. Even monodisperse polymer solutions may exhibit non-Lorentzian spectra due to the presence of minute amounts



of dust. A data analysis procedure that recognizes this aspect must be used to obtain the halfwidth of the spectrum. With the available information it is not possible to resolve this discrepancy. A conclusion on whose data is valid cannot be reached, without a critical analysis of the experimental methods.

Comparison of Light Beating Data for Polystyrene in Tetrahydrofuran

Mandema, et al. (3B-11) studied the diffusion of polystyrene in tetrahydrofuran by laser light beating spectroscopy. The diffusion coefficients were obtained as a function of concentration for polymers with a molecular weight range of 2.04 x 10^4 to 1.8 x 10^6 . At low concentrations the relationship between D and c was linear to a very good approximation. The molecular weight dependence of D₀ was also determined. The accuracy claimed for this data is 1%. All of the diffusion coefficients were corrected to a reference temperature of 24°C .

Jamieson, et al. (3B-10) determined diffusion coefficients of narrow molecular weight polystyrenes at infinite dilution in various solvents including tetrahydrofuran using light beating spectroscopy. The concentration dependence of the diffusion coefficient was found to be linear in the entire concentration range studied. From linear extrapolations values of k_d and D_o were obtained. The molecular weight dependence of D_o was also determined. An accuracy of 3% was claimed and the diffusion coefficients were corrected to a reference temperature of 25°C.

Mandema, et al. used millipore filtration for removing the Jamieson, et al. did not mention what type of procedure they used for removing the dust. The data from both laboratories are compared in Table 7-2. Here the data seem to be in reasonable agreement. The Mark-Houwink exponent a for this system reported by Coleman and Fuller (7B-1) was 0.638, as determined by intrinsic viscosity measurements. The exponent in the D_0 versus M relationship obtained by both Mandema and Jamieson are in agreement with the values calculated from equation 7-1 using the intrinsic viscosity result. The only discrepancy appears to be in the value of $\mathbf{k}_{\mathbf{d}}$ at the molecular weight of 19,800. Jamieson, et al. in their work concluded that the extremely large value of k_d for the 19,800 sample was an artifact since the data at low molecular weights may have a significant heterodyne component and the concentration dependence may be due to a transition from homodyne to heterodyne scattering as the polymer molecular weight was lowered. The heterodyne component arises from the light scattered by particles other than the polymer in solution. These may be either dust or inhomogeneties in the glass sample cell. Any scattering from particles other than the polymer will contribute to the spectrum to a greater extent for low molecular weight polymer because the low molecular weight polymer scatters much less light compared with the high molecular weight polymer. The value of k_d obtained by both investigators, except for the 19,800 sample, appear to be in good agreement with the predictions from two parameter theory, as was pointed out in Chapter III

TABLE 7-2.--Comparison of Mandema, et al. and Jamieson, et al. data for polystyrene in tetrahydro-furan.

	Data of Mandema, et al.	al.		Data of Jamieson, et al.	: al.
$\mathbf{\Sigma}^{\mathbf{X}}$	$D_0 \times 10^7$, cm ² /sec	k _d , cm ³ /gram	Σ ^M	D _o ×10 ⁷ , cm ² /sec	k _d , cm³/gram
20,400	12.7	7.0	19,800	13.41	76.0
51,000	7.65	16.0	37,000	8.81	24.0
97,200	5.43	28.0	51,000	8.02	14.9
160,000	3.99	44.0	110,000	4.92	32.0
411,000	2.35	91.0	411,000	2.51	75.0
860,000	1.59	136.0			
1,800,000	1.01	264.0			
$D_0 = (3.45x)$	$D_0 = (3.45 \times 10^{-4}) \text{ M}^{-0.564} \text{ cm}^2/\text{sec}$	U	D ₀ = (3.0±	$D_0 = (3.0\pm0.4) 10^{-4} M^{-0.549\pm0.013} cm^2/sec$	013 cm ² /sec

in the section on "Comparison of Predicted Values of \mathbf{k}_{d} with Experimental Data."

This analysis leads to a critical point which must be taken into account when making light beating measurements: What is the size and concentration of the smallest particles that can be studied without significant experimental errors on a particular experimental apparatus? The answer to this question can be obtained by good calibration measurements. This aspect is further discussed in Chapter VIII under recommendations.

Comparison of Interferometry Data for Polystyrene in Toluene

Rehage, et al. (5B-6) studied diffusion of polystyrene in toluene up to a concentration of 30 grams of polymer in 100 cm³ of solution. The polystyrene had an M_n of 180,000. They neither disclosed the polydispersity ratio nor did they mention about molecular weight distribution of the polymer. For the sake of simplicity we may assume that the polymer was monodisperse. The diffusion coefficients were measured at 29.9°C, using an interferometric method, for two solutions differing by about 2% in concentration. The optical arrangement in the interferometer was that of Jamin (5B-6). The diffusion data at 29.9°C was converted to a reference temperature of 25°C by the author. These data are plotted in Figure 7-2. Once again, not much emphasis can be placed on the plot because the data were obtained from a small figure in the original paper.

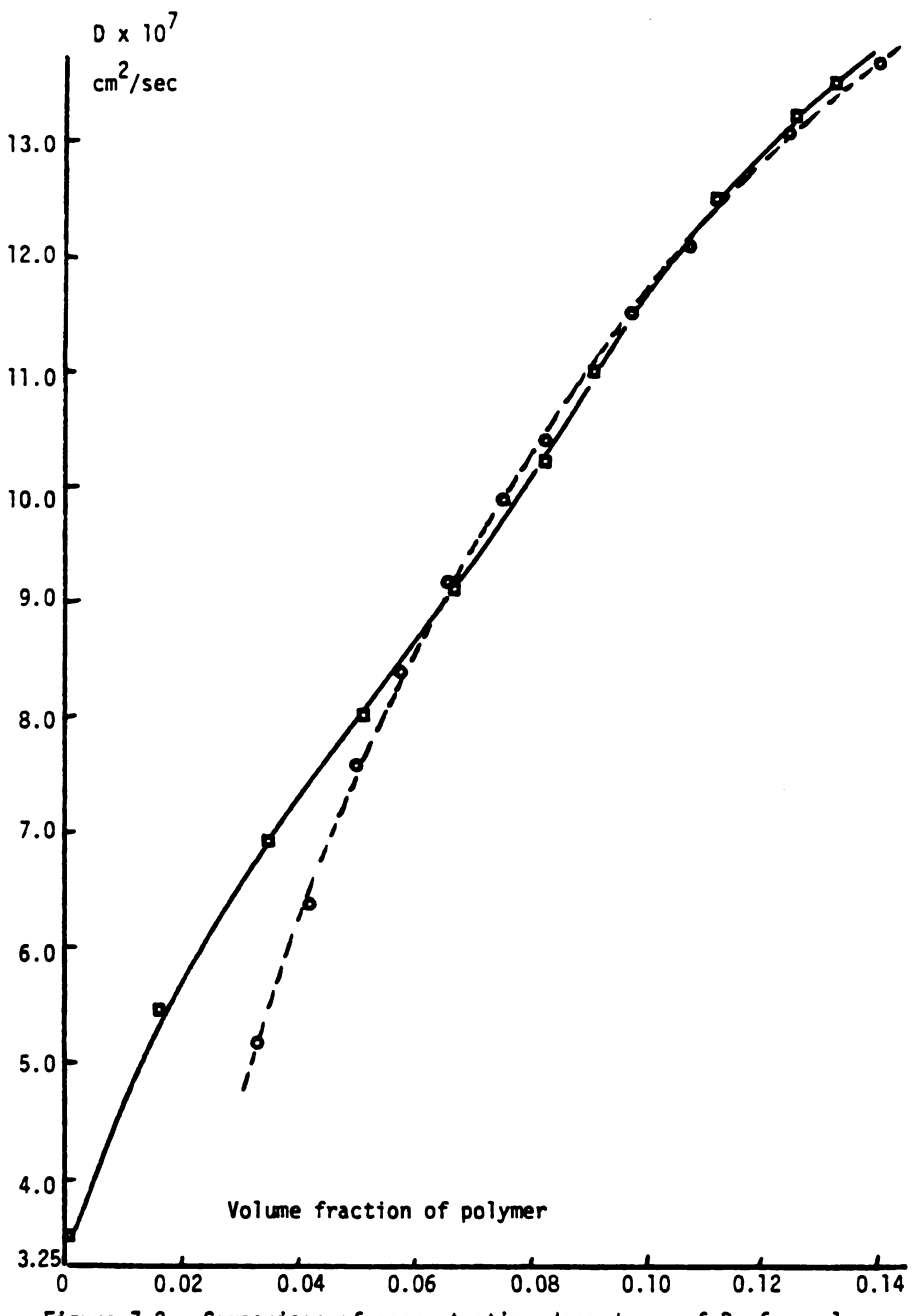


Figure 7-2.--Comparison of concentration dependence of D, for polystyrene in toluene obtained by Rehage, et al. (\Box) and Chitrangad (O).

Chitrangad (7C-3) measured diffusion coefficients of polystyrene in toluene at ambient temperature, using an interferometric technique. A Schlieren optics arrangement was used in conjunction with a Tiselius cell and a newly modified Claesson cell. The molecular weight of the polystyrene was 200,000, with a polydispersity ratio of less than 1.06. All the diffusion data were converted to a reference temperature of 25°C. The diffusion data are plotted in Figure 7-2, for comparison with data of Rehage, et al.

It can be concluded from Figure 7-2 that the diffusion coefficients are in good agreement above a polymer volume fraction of 0.06. Below this volume fraction the diffusion coefficients differ, the difference becoming quite large as the volume fraction of the polymer is decreased.

with the Data Obtained from Light Beating for Polystyrene in Toluene

Pusey, et al. (7D-4) studied the diffusional behavior of three polystyrenes in toluene using light beating spectroscopy. The apparent diffusion coefficient increased with increasing concentration of polymer. Variation of D with concentration and molecular weight was reported. The polystyrene had an $\rm M_{\rm W}$ of 200,000 and an $\rm M_{\rm D}$ of 193,000; thus it was essentially monodisperse. Pusey, et al. centrifuged their samples to minimize scattering from dust particles. The variation of D with concentration was linear for low concentrations. At higher concentrations the linear dependence was

not observed. Their data are plotted in Figure 7-3. These data are compared with the data obtained by Rehage, et al. discussed in the last section for the same system under the same conditions but obtained from an interferometer.

The agreement in the diffusion coefficients obtained from the two different methods seems to be fair up to 0.02 volume fraction of polymer. Above this volume fraction, the discrepancies become large as the polymer volume fraction increases. The outcome of this comparison is that even though the data from the two methods do not show numerical agreement, at least the same trends in D(c) are shown.

In summary, what has been described in this chapter thus far is that in the few cases where comparisons can be made, serious disagreement exists in both numerical values and in D(c) behavior. The resolution of these discrepancies would involve critical analysis of all the experimental work discussed and is beyond the scope of this thesis. A point to be noted here is that all the polymers used for comparisons were monodisperse. With the disagreements observed for the monodisperse polymers one wonders how comparisons would look if the polymers were polydisperse. The rest of the chapter discusses the data obtained in this work.

Discussion of the Results Obtained from Light Beating Spectroscopy

All the diffusion data obtained in this work from light beating spectroscopy were given graphically in Chapter VI in the section on "Light Beating Spectroscopy." It was also stated that in



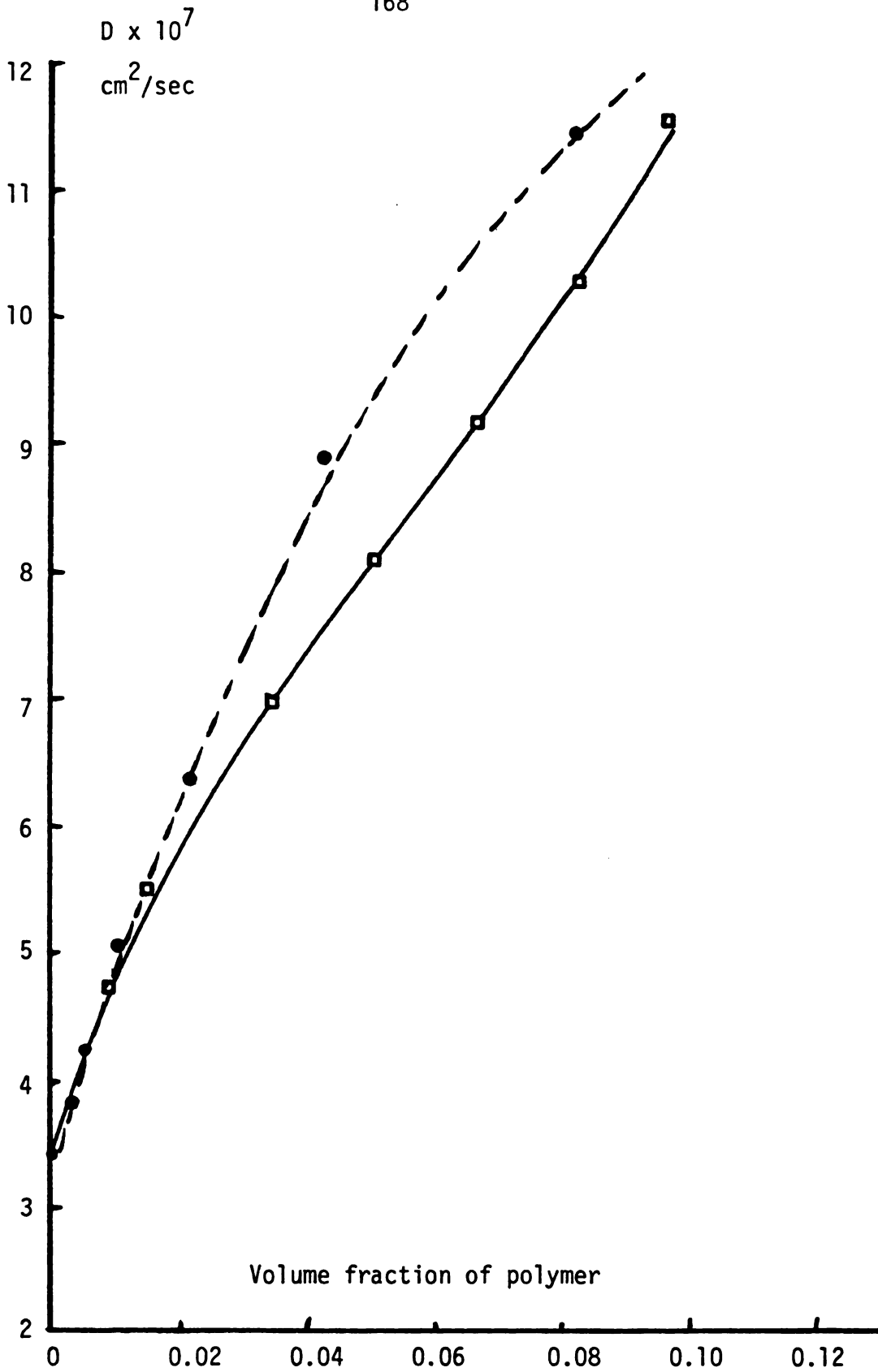


Figure 7-3.--Comparison of concentration dependence of D, obtained from light beating by Pusey, et al. (●), and from interferometry by Rehage, et al. (□).

the concentration range employed the concentration dependence of D was linear. This was in agreement with results obtained by others on similar systems. The values of D_0 and k_d obtained from linear extrapolations were shown in Table 6-1. In this section experimental values are compared with predictions from theory. First the values for polystyrene are compared, and then the copolymer data are analyzed.

Polystyrene in Various Solvents

Polystyrene was studied in two solvents, benzene (good solvent) and decalin (poor solvent). The values of D_0 obtained experimentally will be compared with the predictions from the theory, using both Johnston's theory and the semi-empirical relation suggested in this work. Two methods were used because all the values of D could not be predicted by Johnston's theory alone, due to the unavailability of viscosity-molecular weight relationships for all the polymer-solvent pairs used in this study. The viscositymolecular weight relationships used in Johnston's theory are shown in Appendix B. The other quantity needed for predicting D_0 is the parameter A, which contains the unperturbed dimension of the polymer chain. The value of A used for polystyrene was 700×10^{-11} cm (3A-9). The values of $\mathbf{D}_{\mathbf{O}}$ predicted from theory for polystyrene in the two solvents are compared with those obtained from the experimental data in Table 7-3. For predicting D_0 by equations 3-9 and 3-10, M_{W} was used in place of both M_{U} and M. Use of M_{W} as the characteristic molecular weight is justified later in this section.

TABLE 7-3.--Comparison of experimental and theoretical values of $\mathbf{D}_{\mathbf{0}}$.

Polymer	Solvent	Expt $D_0 \times 10^7$ cm ² /sec	Johnston's theory for $D_0 \times 10^7$ cm ² /sec	Semi-empirical theory for ${\rm D_o} \times {\rm 10}^7$ cm $^2/{\rm sec}$
PS-1	Decalin	1.688 ± 0.042	ı	1.787
PS-2	Decalin	1.159 ± 0.004	ı	0.871
PS-1	Benzene	3.505 ± 0.011	4.299	3,563
PS-2	Benzene	1.911 ± 0.013	1.877	1.736

It is clear from Table 7-3 that both the methods for predicting D_0 give excellent results. From this and the previous comparisons in Chapter III it can be concluded that both Johnston's theory and the semi-empirical relation developed by the author can be satisfactorily used for predicting D_0 for homopolymers.

The next step is to compare the values of $k_{\mbox{\scriptsize d}}$ obtained from theory with experimental results. Prediction of \mathbf{k}_{d} was thoroughly discussed in Chapter III in the section on "Diffusion in Dilute and Moderately Concentrated Polymer Solutions," using a combination of two parameter theory and modified Pyun and Fixman theory. A fundamental difficulty in using this method is that the excluded volume parameter, B, is not directly observable nor may it be estimated from molecular theory. It is therefore impossible to make an explicit comparison of theory with experiment. To circumvent this problem the following procedure was used. For a polymer-solvent pair a value of B was obtained from plots similar to those of 3-9 to 3-11, which show the molecular weight dependence of k_d in the molecular weight range of interest. This value of B is compared with the value of B in the literature for similar systems obtained from viscosity plots. The procedure for obtaining B from viscosity plots is described in detail by Yamakawa (3B-5e). The other check on the values of B is to examine the change in magnitude and direction of B with respect to the quality of different solvents used. In Table 7-4, experimental values of $\mathbf{k}_{\mathbf{d}}$ are compared with predictions. In the last column of the table the value of B used for the polymer-solvent pair to obtain $\boldsymbol{k}_{\boldsymbol{d}}$ is shown. It is to be noted

TABLE 7-4.--Comparison of experimental and theoretical values of ${\sf k}_{\sf d}.$

Polymer	Solvent	Value of k _d from expt. cm ³ /gram	Value of k _d from theory cm ³ /gram	Value of B used to predict k _d cm ³
PS-1	Decalin	-11.845 ± 2.17	-5.0	0.5×10^{-27}
PS-2	Decalin	8.45 ± 0.28	5.0	0.5×10^{-27}
PS-1	Benzene	- 5.96 ± 0.29	-1.0	1.0×10^{-27}
PS-2	Benzene	20.84 ± 0.61	22.0	1.0×10^{-27}

that in Table 7-4 one value of the parameter B was used for a polymer-solvent pair over the whole molecular weight range of interest (using M_{ω} for M).

It can be seen that the value of B is smaller for the polystyrene-decalin system than for the polystyrene-benzene system. This is expected because benzene is a thermodynamically good solvent for polystyrene compared with decalin. The values of B from this work compare well to those obtained from viscosity plots reported in the literature (see Table 7-5).

All the values of B obtained from the literature were determined at a temperature of 30°C. The values of B obtained in this work correspond to a temperature of 25°C. It is known that the value of B decreases with decrease in temperature (3B-5); however, a quantitative correction for this effect is not possible. The values of k_d obtained from theory do not agree numerically to those obtained from experiment, but they are in the right order with respect to solvent power and are also of the right order of magnitude.

All the values reported in this section were calculated using M_W , the weight average molecular weight, in place of M_V , since, as pointed out in the light beating section of Chapter V, the average diffusion coefficient obtained by the method of analysis used in this work corresponds to that of a polymeric species whose molecular weight is equal to the weight average molecular weight, M_W .

TABLE 7-5.--Comparisons for the values of B for polystyrene.

Polymer	Solvent	Value of B from this work cm ³	Value of B from literature cm ³
Polystyrene	Benzene	1.0 × 10 ⁻²⁷	1.4 to 2.55×10^{-27} (3A-5e)
Polystyrene	Decalin	0.5×10^{-27}	0.203×10^{-27} (70-6)

It can now be concluded that the prediction scheme for k_d which was first proposed by Duda, et al. (3B-3) provides a useful method for obtaining a reasonable estimate of k_d .

Styrene-Acrylonitrile Copolymers in Various Solvents

One of the objectives of this work was to test the applicability of the theories for prediction of D_0 and k_d for homopolymers to copolymers. Difficulties in copolymer studies might arise from the fact that there are at least two extra factors to consider compared with homopolymer solutions; the monomeric composition of the copolymer and the specific mode of monomer arrangements along a copolymer chain. In addition the heterogeneities with respect to these two factors would further complicate the problem. These factors were minimized in this work by preparing copolymers of the single azeotropic composition, which results in random arrangement of the monomers in the copolymer (4A-1).

In the absence of chemical heterogenity and any particular mode of monomer arrangement, the copolymer might be treated as a homopolymer for the purposes of diffusion measurements. The validity of this assumption is checked by predicting D_0 and k_d for copolymers by the same theories used for homopolymers, but using the copolymer values for the parameters A, V_{20} and b_1 . The value of A used for the copolymer was 843.8 x 10^{-11} (7E-1). The Mark-Houwink relations used for the copolymers are shown in Appendix B. The calculated values for D_0 for the copolymers using Johnston's theory and the semi-empirical relation are compared with the values obtained from

experimental extrapolations in Table 7-6. It can be seen from the results in Table 7-6 that the homopolymer theory for D_0 predicts values of D_0 for the copolymers reasonably well.

Given that D_0 can be predicted satisfactorily for copolymers, the next task is to obtain reasonable estimates for k_d . The values of k_d obtained for the copolymers from homopolymer theory, using the copolymer values for parameters A, V_{20} and b_1 are shown in Table 7-7. The table also contains the values of k_d obtained from experimental data.

The values of B obtained for the copolymers are in the right order with respect to the thermodynamic quality of the solvent. Since dimethyl formamide is a very good solvent for the copolymer, B is the largest compared with values for the other solvents used. Benzene is a poor solvent for the copolymer and correspondingly the value of B is the smallest. Methyl ethyl ketone is an intermediate solvent and the value of B lies between the values for dimethyl formamide and benzene. For the azeotropic styrene-acrylonitrile copolymer the only value of B available from viscosity plots is for solutions of the copolymer in dimethyl formamide. This literature value 1.76 to 2.7×10^{-7} at 30° C (7E-1) compares well with the one obtained in this work.

It can be concluded from the results in Table 7-7 that the combination of two parameter theory and modified Pyun and Fixman theory does provide a useful method for obtaining a reasonable estimate of $k_{\rm d}$ for copolymers when chemical heterogenity is absent. The final outcome of this analysis is that the existing homopolymer

TABLE 7-6.--Comparisons of experimental and theoretical values of ${
m D_0}$ for the copolymers.

Polymer	Solvent	Experimental $D_0 \times 10^7$ cm ² /sec	Johnston's theory for ${\rm D_o} \times {\rm 10}^7$ cm ² /sec	Semi-empirical relation for $D_0 \times 10^7$ cm ² /sec
SAN-1	DMF	1.342 ± 0.023	1.67	1.386
SAN-1	MEK	2.393 ± 0.005	1	3.316
SAN-1	BEN	2.338 ± 0.032	ı	3.216
SAN-2	DMF	1.205 ± 0.036	1.16	1.010
SAN-2	MEK	2.312 ± 0.049	ı	2.417
SAN-2	BEN	2.073 ± 0.021	ı	2.345
SAN-3	DMF	0.789 ± 0.28	0.806	0.736
SAN-3	MEK	1.759 ± 0.053	1	1.763
SAN-3	BEN	1.302 ± 0.003	ı	1.710

DMF- dimethyl formamide; MEK - methyl ethyl ketone; BEN - benzene

TABLE 7-7.--Comparisons of experimental and theoretical values of $k_{f d}$ for the copolymer.

0.65×10^{-27}	12.5	9.41 ± 1.82	BEN	SAN-3
0.9×10^{-27}	36.5	14.56 ± 5.08	MEK	SAN-3
1.4×10^{-27}	77.0	43.41 ± 3.49	DMF	SAN-3
0.65×10^{-27}	- 3.7	- 1.54 ± 1.00	BEN	SAN-2
0.9×10^{-27}	10.0	14.48 ± 2.22	MEK	SAN-2
1.4×10^{-27}	33.0	31.4 ± 3.63	DMF	SAN-2
0.65×10^{-27}	-11.0	-13.35 ± 1.33	BEN	SAN-1
0.9×10^{-27}	- 1.0	4.32 ± 0.22	MEK	SAN-1
1.4×10^{-27}	11.5	23.05 ± 1.72	DMF	SAN-1
Value of B used for predicting k _d , cm ³	k _d from theory cm ³ /gram	k _d from experiment cm ³ /gram	Solvent	Polymer

DMF - dimethyl formamide; MEK - methyl ethyl ketone; BEN - benzene

theories can be used for copolymers for predicting the concentration dependence of the diffusion coefficient in the dilute solution range.

Discussion of the Results Obtained from Interferometry

The diffusion coefficients measured in the intermediate and dilute concentration range by interferometry are tabulated in Appendix E, and are presented graphically in Chapter VI in the section on "Interferometry."

Monodisperse Polystyrene in Benzene

In Chapter V, in the section on "Interferometry," a relation between the average diffusion coefficient measured by interferometry and the diffusion coefficient of individual species of a polydisperse polymer was determined:

$$\frac{1}{\sqrt{D_{avg}}} = \sum_{i=1}^{N} \frac{w_i}{\sqrt{D_i}}$$
 (5-45)

where w_i and D_i are the weight fraction and the diffusion coefficient of the individual species of molecular weight M_i. To test the validity of equation 5-45, diffusion coefficients for monodisperse polystyrenes (PS-3 and PS-4) were measured as a function of concentration. Then two polydisperse polymers (PS-5 and PS-6) were prepared by mixing different proportions of the monodisperse polymers. PS-5 was obtained by mixing equal parts by weight of the two monodisperse polymers PS-3 and PS-4. PS-6 was obtained by mixing 28% by

weight of PS-3 and 72% by weight of PS-4. The diffusion coefficients of these polydisperse polymers PS-5 and PS-6 were measured as a function of polymer concentration. The results of these experiments are displayed in Table 7-8. The first two columns in the table are the experimentally measured diffusion coefficients for the two monodisperse polymers. The third and the sixth columns contain the experimentally measured average diffusion coefficients for the polydisperse polymers PS-5 and PS-6 respectively. The fourth and the seventh columns contain the diffusion coefficients calculated by using equation 5-45 with the experimental $D_{\bf j}$'s for the monodisperse polymers.

Comparing columns 3 and 4, and columns 6 and 7 in Table 7-8, it is concluded that there is good agreement, at higher concentrations. However, at lower concentrations the agreement is not as good. This might be due to the fact that at low concentrations the accuracy of the interferometric experimental method decreases rapidly because of the small number of fringes obtained. Therefore it appears that equation 5-45 is a valid relation for the average diffusion coefficient measured by interferometry. Linear extrapolations were performed on the experimental data for the polymers PS-3, PS-4, PS-5, and PS-6. The values of $k_{\rm d}$ and $D_{\rm o}$ are shown in Table 6-2. It is of interest to compare these values with those predicted from theory. One point that should be clear is that it was mathematically shown in Chapter V in the section on "Extension to Polymer Solutions" that the average diffusion coefficient measured for a mixture by this technique will correspond to a coefficient of

TABLE 7-8.--Concentration dependence of D, for monodisperse polystyrenes and their mixtures

	obtained from interferometry.	interferometry.				
For PS-3 Exptl. D x 10^7 cm ² /sec	For PS-4 Exptl. D x 10 ⁷ cm ² /sec	For PS-5 Exptl. D x 10 ⁷ cm ² /sec	Theo. D x 10 ⁷ for PS-5 using Eq. 5-45, cm ² /sec	Avg. Conc. gms/100 cm ³	For PS-6 Exptl. D x 10 ⁷ cm ² /sec	Theo. D x 10 ⁷ for PS-6 using Eq. 5-45 cm ² /sec
9.44	3.818	5.558	5.706	1.05	1	•
7.56	4.036	5.138	5.389	0.7	4.443	4.721
7.88	3.152	5.437	4.731	0.4	1	1
6.528	2.546	4.489	3.859	0.12	3.362	3.179
5.877	1.854	3.869	3.041	90.0	2.972	2.409

a sample with M = M_n , the number average molecular weight of the mixture. In Table 7-9 are displayed the values of D_0 from experiment and those obtained from Johnston's theory using $M_u = M_w$ and $M_u = M_n$. It is evident from the comparisons in Table 7-9 that the interferometric method of analysis does give a diffusion coefficient corresponding with an average value typical of a polymeric species with molecular weight M_n .

<u>Polydisperse Polystyrene</u> in Benzene

Only one polydisperse polystyrene (PS-2) with a continuous distribution of molecular weights was studied by interferometry. The concentration dependence of the diffusion coefficient of the polymer in benzene is shown in Figure 6-7. The polymer was studied in the concentration range of 0.2113 to 9.93 grams of polymer in $100~{\rm cm}^3$ of solution. The concentration dependence appears to be linear. A linear least squares fit and extrapolation of these data were performed to zero polymer concentration. From the analysis the values of D_0 and k_d were obtained. The value of D_0 compares well with the prediction from Johnston's theory with $M_u = M_n$ as shown in Table 7-10.

This further indicates that the average D_o obtained from interferometry corresponds with a value characteristic of a sample molecular weight M_n , the number average molecular weight. Next the value of k_d obtained is compared with the theoretical prediction. The value of the parameter B used for obtaining k_d from theory was 1.0×10^{-27} . This was the same value of B that was used for the

TABLE 7-9.--Comparison of experimental and theoretical values of D₀ for the monodisperse polystyrenes and their mixtures obtained by interferometry.

	styrenes and	d their mixtares obtained by interierometry.	ed by interierometry.	
Polymer	Solvent	D _o x 10 ⁷ cm ² /sec from experimental data	$D_0 \times 10 \text{ cm}^2/\text{sec}$ from Johnston's theory with $M_0 = M_0$	$D_0 \times 10^7 \text{ cm}^2/\text{sec}$ from Johnston's theory with $M_u = M_w$
PS-3	Benzene	5.998 ± 0.399	5.3	5.2
PS-4	Benzene	2.173 ± 0.339	1.7	1.65
PS-5	Benzene	4.234 ± 0.336	3.8	2.3
PS-6	Benzene	2.818 ± 0.107	3.05	1.85

TABLE 7-10.--Comparison of experimental and theoretical values of D_0 for polydisperse polystyrene (PS-2) obtained from interferometry.

D _o from experiment x 10 ⁷ , cm ² /sec	D_0 from Johnston's theory with $M_u = M_n$ $cm^2/sec \times 10^7$	D_0 from Johnston's theory with $M_u = M_w$ $cm^2/sec \times 10^7$
3.326 ± 0.295	2.943	1.736

polystyrene-benzene system for comparing light beating data with theory. The values of \mathbf{k}_{d} are compared in Table 7-11.

TABLE 7-11.--Comparison of experimental and theoretical values of \mathbf{k}_d for polydisperse polystyrene (PS-2) obtained from interferometry.

k _d obtained from experiment cm ³ /gram	k _d obtained from theory with M = M _n cm ³ /gram	k _d obtained from theory with M = M cm ³ /gram
30.568 ± 2.061	3.0	23.0

The values of k_d were predicted from theory using M_w and M_n in place of M. The value of k_d predicted by using M_w comes very close to the experimental value. This is a very significant piece of information, because in the interferometric data for diffusion it was found that D_o is biased towards M_n , whereas here k_d appears to be biased towards M_w . This analysis suggests that the characteristic molecular weight

to be used for predicting $\mathbf{k}_{\mathbf{d}}$ for polydisperse systems is $\mathbf{M}_{\mathbf{W}}$. However, there is no theoretical justification for this observation.

Therefore, another way to look at this point is that the value of the parameter B obtained from light beating may not be the same as the value obtained from interferometry. A possible justification for this is the fact that in polymer solutions the second virial coefficient, A_2 , obtained from osmotic pressure measurements is greater than A_2 obtained from light scattering for polydisperse polymer solutions. The parameters A_2 and B are directly related by equation 3-12. There is both experimental (7F-1) and theoretical evidence (3B-5c) for the difference in values of A_2 so obtained. It is also well established that the molecular weight of a polymer obtained from osmotic pressure measurements is biased towards small molecules and is equal to M_n , the number average molecular weight, whereas from light scattering measurements one obtains $M_{\mathbf{w}}$, the weight average molecular weight. Since the values of A_2 obtained from osmotic pressure measurements are greater than the values obtained from light scattering, it may not be surprising if interferometry could give a value of B greater than that obtained from light beating spectroscopy. For polystyrene if a higher value of B is used, the results of the comparison are shown in Table 7-12. Table 7-12 shows that if the assumption is made that the value of B obtained from interferometry is greater than the value obtained from light beating, then the concentration dependence of the diffusion coefficient can be predicted from theory using only one molecular

weight M_n , the number average molecular weight for predicting both D_0 and k_d for interferometry results in polydisperse systems. This value of B is still within the range of values for B obtained from viscosity plots in the literature for the same system (refer to Table 7-5).

TABLE 7-12.--Comparison of experimental and theoretical values of k_d for polystyrene (PS-2) in benzene using higher values of B.

Experimental value of k _d cm ³ /gram	k _d obtained from theory with M = M _n cm ³ /gram	Value of B used for obtaining k _d
30.586 ± 2.06	22.0	2.5 x 10 ⁻²⁷

<u>Styrene-Acrylonitrile Copolymer</u> <u>in Various Solvents</u>

The concentration dependence of the diffusion coefficients obtained by interferometry for solutions of copolymer in methyl ethyl ketone and dimethyl formamide are shown in Figures 6-8 through 6-10. None of the theories discussed in this work for predicting D_0 are able to predict the value of D_0 obtained from linear extrapolations of these copolymer data using literature values for polymer dimensions, A. The values of D_0 obtained from experimental data are approximately twice the values predicted by either Johnston's theory or by the semi-empirical relation. Such a large difference in the values of D_0 obtained from theory and experiment

can not be explained with the available theory of copolymer behavior in solution. This is surprising because the copolymer data obtained from light beating spectroscopy could be described adequately with existing theory. A discussion of these discrepancies follows.

It has been shown that the diffusion coefficient for a polydisperse system, obtained by interferometry, corresponds to a value characteristic of a species whose molecular weight is equal to M_n . The diffusion data for SAN-1 in dimethyl formamide, where the data was obtained at low concentrations, were extrapolated to zero polymer concentration. Using this experimental value of D_0 and the semi-empirical relation with M_n , the value of the parameter A was calculated using equation 3-10. The value of A obtained in this fashion is 403.4×10^{-11} cm. This value of A is roughly half the value of A, 843.8×10^{-11} cm, reported in the literature, obtained by light scattering (7E-1). It has been well established that light scattering yields information corresponding to species with molecular weight equal to M_w . The parameter A defined in equation 3-15 is

$$A = \left(\frac{\langle R_0^2 \rangle}{M}\right)^{1/2}$$

where M is a characteristic molecular weight. The interferometric diffusion data for copolymer solutions indicate that the value of the parameter A that should be used corresponds with a species where $M = M_n$. The value of parameter A should be independent of M_w

or M_n . The diffusion data obtained by interferometry for the copolymers indicate that the value of A is smaller than the one reported in the literature. There is no theoretical evidence supporting the above observation. Due to the lack of any other methods the value of $A = 403.4 \times 10^{-11}$ was used to predict D_0 for the other copolymer solution data. The predicted values of D_0 for the copolymers are compared with those obtained from linear extrapolations, for SAN-1 and SAN-2, in Table 7-13. The copolymer SAN-3 was

TABLE 7-13.--Comparison of experimental and theoretical values of ${\bf D_0}$ for the copolymers obtained from interferometry.

Polymer	Solvent	D _o x 10 ⁷ obtained from semi-empirical relation, cm ² /sec	D _o x 10 ⁷ obtained from experimental extrapolations, cm ² /sec
SAN-1	methyl ethyl ketone	8.682	7.06
SAN-2	dimethyl formamide	2.721	4.212
SAN-2	methyl ethyl ketone	6.51	5.31

not used in any of the comparisons, because there were not enough experimental data to perform reasonable extrapolations. For the same copolymers the values of k_d obtained from linear extrapolation are compared with the values obtained from theory with $M=M_W$, in Table 7-14. The values of B used in Table 7-14 for predicting k_d were the same values that were used for the polymer-solvent pair for

TABLE 7-14.--Comparisons of experimental and theoretical values of \mathbf{k}_d for copolymers obtained from interferometry.

Polymer	Solvent	k _d obtained from theory cm ³ /gram	k _d obtained from experiment cm ³ /gram	Value of B used to predict k _d cm ³
SAN-1	DMF	13.0	21.28 ± 0.442	1.4×10^{-27}
SAN-1	MEK	1.0	14.01 ± 2.97	0.9×10^{-27}
SAN-2	DMF	35.0	10.48 ± 0.03	1.4×10^{-27}
SAN-2	MEK	15.0	19.33 ± 3.13	0.9×10^{-27}

DMF - dimethyl formamide; MEK - methyl ethyl ketone

comparing light beating results. It was shown in the previous section for polystyrene that another method of comparison is possible. If the value of B from interferometric experiments is greater than the value obtained from light beating, the concentration dependence of the diffusion coefficient can be predicted using only M_n . These results are tabulated in Table 7-15.

From Tables 7-13 to 7-15 it can be concluded that the predictions from theory are not in good agreement with the experimental values for copolymer solutions. However, the assumption that the values of B obtained from interferometry may be greater than the values obtained from light beating appears to be justified by the results in Table 7-15.

One of the reasons for such difference in experimental and theoretical values might be that the extrapolations of the interferometric data were performed from higher concentrations compared to the light beating data, and may therefore be inaccurate. The diffusion of the copolymers studied by interferometry could be explained by theory with the value of the parameter A obtained from one of the diffusion measurements. To justify the use of such a small value of the parameter A requires further work in understanding copolymer theory. The basic question on whether the value of B could be greater for interferometric measurements cannot be answered without further study of copolymer solutions.

TABLE 7-15.--Comparison of experimental and theoretical values of \mathbf{k}_{d} for copolymers obtained from interferometry with higher values of B.

		boniet+40 7	bonic 4	
Polymer	Solvent	from theory cm ³ /gram	from experiment cm ³ /gram	Value of B used to predict k _d cm ³
SAN-1	DMF	20.0	21.28 ± 0.442	2.5 × 10 ⁻²⁷
SAN-1	MEK	11.0	14.01 ± 2.97	1.5×10^{-27}
SAN-2	DMF	48.0	10.48 ± 0.03	2.5×10^{-27}
SAN-2	WEK .	20.0	19.33 ± 3.13	1.5×10^{-27}

DMF - dimethyl formamide; MEK - methyl ethyl ketone

Comparison of Light Beating and Interferometry Data

All the polymer solutions studied in this work exhibit the same trends when comparing the light beating data with the interferometry data. Therefore only one polymer-solvent pair, PS-2 in benzene, will be discussed in this section, as an example. This system was chosen because of the availability of data over the widest concentration range. The data for PS-2 in benzene obtained from interferometry and light beating are shown in Figure 7-4. The dotted lines are the predictions from theory as discussed previously. The two experimental methods do not give the same values for diffusion coefficients in the concentration range where they overlap. This was the discrepancy that was discussed in the last two sections of this chapter. The following are possible reasons for the difference in diffusion coefficients obtained by the two methods:

- l. The data analysis method used in this work for interpreting the light beating experiment gives an average diffusion coefficient corresponding to the species with a weight average molecular weight, $M_{\rm w}$.
- 2. It was shown theoretically and experimentally that the average diffusion coefficient measured by the interferometric technique corresponds to the species with a number average molecular weight, $\mathbf{M_n}$.
- 3. Since for all the polymers used in this work the ratio of $M_{\rm w}/M_{\rm n}$ lies in the range of 1.5 to 2.9 the diffusion results obtained by the two methods do not match in the concentration range where they overlap.

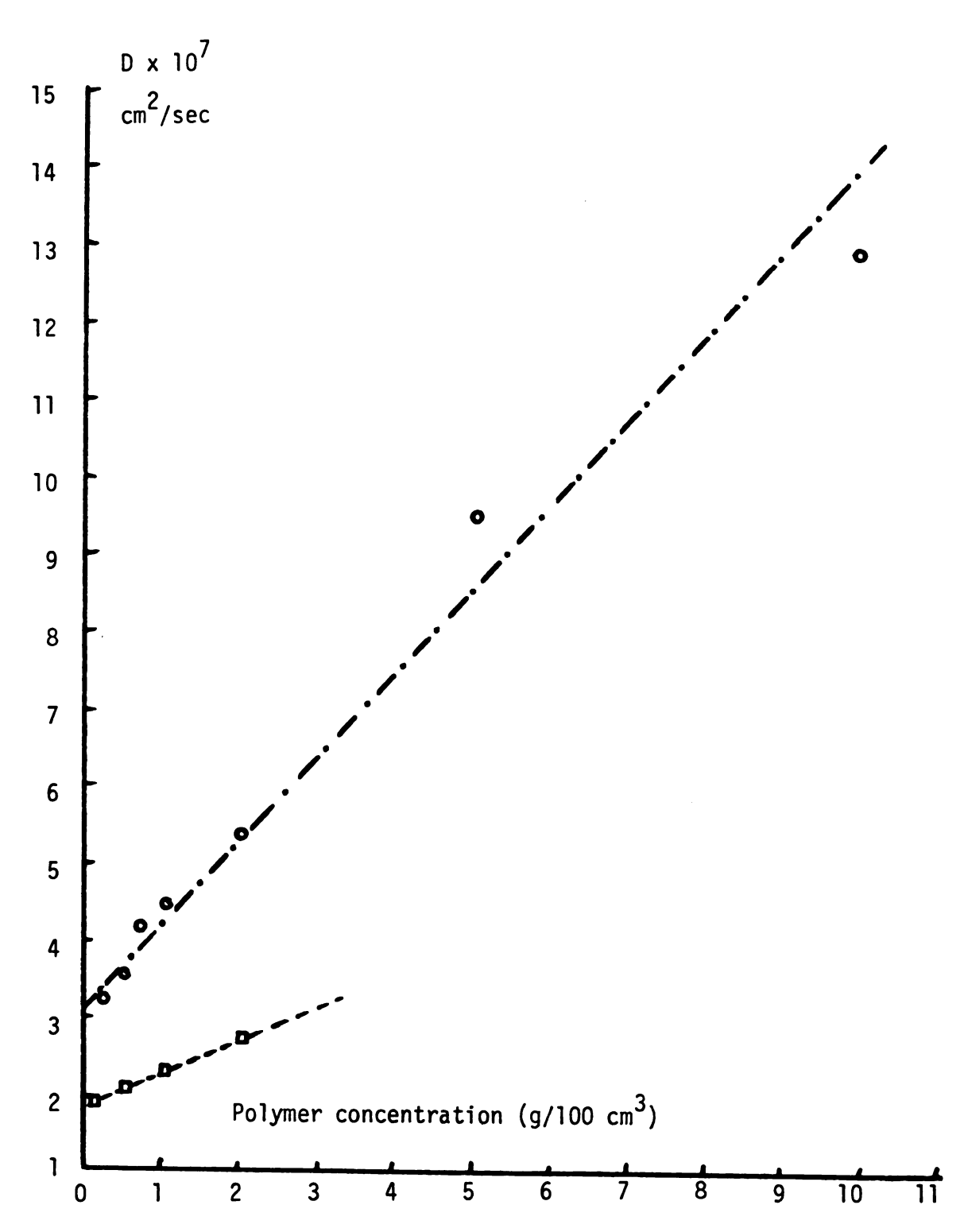


Figure 7-4.--Comparison of experimental data obtained from light beating (\square) and interferometry (\circ) for PS-2 in benzene at 25°C.

Monodisperse polymers should give the same values for diffusion coefficients obtained from these two methods. Additional data would be required to verify this hypothesis.

Comparison of Thermodynamic Parameters

Using two parameter theory the value of B was obtained which gave the best fit to the values of $\boldsymbol{k}_{\boldsymbol{d}}$ observed. The values of B obtained for the various polymer-solvent pairs in this work were compared with those obtained from viscosity plots in the literature. The agreement was satisfactory. With the resulting value of B for a polymer-solvent pair, the thermodynamic parameters A_2 , the second virial coefficient, and α , the linear expansion factor may be predicted by the two parameter theory. These thermodynamic parameters are then compared with the values that were obtained experimentally for similar systems by Shah (4A-4). The comparisons are made in Table 7-16. Both the values of A_2 and α obtained from theory are not in numerical agreement with the experimental values, but are of the right order of magnitude. In the case of copolymer in benzene the experimental values have negative values for A_2 and expansion factors of less than one. This type of behavior is only possible for copolymers, and not for homopolymers. Since the theory was basically developed for homopolymers, and then extended to copolymers, this type of behavior will not be predicted by the available theory.

TABLE 7-16.--Comparison of experimental and theoretical values of the thermodynamic parameters.

Mole wei	Molecular weight	Solvent	Predicted values $A_2 \times 10^4 \alpha$	d values 0^4 α	Experimental values ${\rm A_2 \times 10^4} \alpha$	al values t α
PS	185,000	BEN	1.75	1.16	5.64	1.278
PS	501,000	BEN	ı	1.23	ı	1.38
SAN	203,000	DMF	2.75	1.14	6.92	1.185
SAN	203,000	MEK	2.05	1.1	5.7	1.128
SAN	203,000	BEN	1.4	1.04	-0.66	0.952
SAN	635,000	DMF	2.25	1.22	97.9	1.287
SAN	635,000	MEK	1.72	1.17	5.3	1.215
SAN	635,000	BEN	1.2	1.07	-0.68	0.910

PS - polystyrene; SAN - styrene-acrylonitrile copolymer; DMF - dimethyl formamide; MEK - methyl ethyl ketone; BEN - benzene

CHAPTER VIII

CONCLUSIONS AND RECOMMENDATIONS

The results obtained in this work can be summarized as follows:

- l. Light beating spectroscopy. Diffusion coefficients in dilute polymer and copolymer solutions can be obtained reliably by the light beating spectroscopic technique. One must be careful in choosing the procedure used for data analysis when solutions of polydisperse polymers are being investigated. It is evident from the experimental results obtained from light beating that the concentration dependence of D may be approximated by a linear relationship over the entire concentration range examined in this work. The diffusion coefficient of polymer at infinite dilution, $\mathbf{D_0}$, obtained from linear extrapolation of the experimental data, both for the homopolymer and copolymer solutions, compare quite well with theoretical predictions. The relative change of diffusion coefficient with concentration, represented by the value of the parameter $\mathbf{k_d}$ obtained from the curve fit of experimental data, could be estimated reasonably well with the existing theories.
- 2. <u>Interferometry</u>. Diffusion coefficients in the moderately concentrated range can be obtained reliably and accurately with the interferometric technique. At low polymer concentrations or in

dilute polymer solutions, the accuracy of the method for obtaining diffusion coefficients falls off rapidly. In order to obtain the desired accuracy of 2%, at least thirty to forty fringes are necessary. The number of fringes measured for solutions of low concentration are less than this. When polydisperse polymers are used, the average diffusion coefficient obtained from the experimental method used in this work correspond to species with a molecular weight of $\mathbf{M}_{\mathbf{n}}$, the number average molecular weight. The diffusion coefficients obtained for homopolymers could be predicted by existing theories. However, for copolymers, the diffusion coefficient at infinite dilution $\mathbf{D}_{\mathbf{0}}$ obtained by linear extrapolation of experimental data could not be predicted by any existing theories. This does not necessarily reflect on the adequacy of the method for obtaining the diffusion coefficients.

- 3. Theories for predicting D_0 . Both Johnston's theory and the semi-empirical relation developed here are acceptable methods for estimating the diffusion coefficient at infinite dilution for homopolymers. Much cannot be said about the reliability of these methods for copolymers. More experimental data are needed for diffusion of copolymers in solution in order to understand the behavior of such systems. However, the two methods do predict the values of D_0 for copolymers within reasonable limits.
- 4. Theories for predicting k_d . Combination of the two parameter theory and the modified Pyun and Fixman theory are quite adequate in predicting the concentration dependence of diffusion coefficients, both for homopolymers and copolymers. One disadvantage

of the theory as pointed out by previous investigators (3A-14, 3A-15) is that the values of k_d at low molecular weights are not reliably predicted. Before final conclusions on the adequacy of this theory can be reached, a thorough analysis of data obtained at low molecular weights must be performed. The method as proposed by Duda, et al. (3B-3) seems to be the only available way for using these theories, until the value of the excluded volume parameter B can be determined for a particular polymer-solvent pair from statistical mechanics arguments.

From the analysis of the various aspects of this investigation, the following are the recommendations for future work:

- l. The light beating spectrometer should be calibrated with polystyrene spheres of the same size and concentration as the smallest polymer molecule to be investigated. This would give rise to the smallest signal to noise ratio which might be expected in experiments with polymer solutions, and would indicate the lowest concentration of the smallest polymer molecule that could be used to obtain an accurate diffusion coefficient for a given set of experimental conditions. Once the lowest concentration of the smallest polymer molecule is found, corresponding to a reasonably acceptable signal to noise ratio, a lower limit on the polymer solutions that can be investigated with this apparatus would be obtained.
- 2. The data analysis of the interferometric technique could be changed to give an average diffusion coefficient corresponding to species with molecular weight equal to M_{ω} . This could

be achieved if D_{2m} is defined as

$$D_{2m} = \frac{1}{2t\Delta n} \int_{-\infty}^{\infty} x^2 \left(\frac{\partial n}{\partial x} \right) dx$$
 (8-1)

The value of $\frac{\partial n}{\partial x}$ for a multicomponent system was defined in equation 5-44. If this value is substituted into equation 8-1 and the integration performed we obtain

$$D_{2m} = \sum w_i D_i$$

Where $\mathbf{w_i}$ and $\mathbf{D_i}$ are weight fraction and diffusion coefficient of the ith species. This analysis could not be used in this work because to obtain an adequate value of $\mathbf{D_{2m}}$ from equation 8-1 numerical integration of equation 8-1 must be performed. This requires at least one hundred fringes to obtain reasonable accuracy. To obtain that many fringes, larger concentration differences must be established in the interferometric cell. When large concentration differences exist the assumption of D being independent of c used in this analysis is not valid. However, some type of relation such as linear dependence of D on concentration could be incorporated into the data analysis and this method could then give $\mathbf{D_{2m}}$, the average diffusion coefficient for weight average species.

3. The cell used in the interferometric experiments should be redesigned so that solutions of higher concentrations could be

used to obtain diffusion coefficients at higher concentrations. The existing cell has some flow problems when polymer solutions of high concentrations are used.

- 4. The concentration dependence of the diffusion coefficient should be studied for monodisperse polymers over a wide molecular weight range by both light beating and interferometry to determine whether the data obtained from the two methods agree within experimental error.
- 5. The light beating spectrometer should not be used for any other studies once it is calibrated for diffusion measurements.
- 6. It will be of interest to study why the value of the excluded volume parameter obtained from interferometry and light beating differ. A clue to the solution of the above problem may be obtained from taking a closer look at the theory and experimental data which indicate that the values of A_2 obtained from osmotic pressure and light scattering measurements also differ.

NOMENCLATURE

Sometimes the same notation is used for different quantities to preserve the already well established nomenclature in the literature.

a	Mark-Houwink exponent defined in eq. 3-8
a _o	Diameter of sphere defined in eq. 3-26, cm
Α	Parameter defined in eq. 3-3, cm
°A	° Angstrom unit, 10 ⁻⁸ cm
A ₁	Constant defined in eq. 3-21
A ₂ , A ₃	Second and third virial coefficients
A*	Quantity defined in 3-25
В	Excluded volume parameter, cm ³
c, c ₁ , c ₂	Concentration of polymer, g/cm ³
C (τ)	Autocorrelation function of scattered light
D	Translational mutual diffusion coefficient
D _o	Value of D at infinite dilution of polymer, cm ² /sec
(D _o) ₀	Value of D _o at theta condition,cm ² /sec
D _{2m}	Weight average diffusion coefficient obtained from interferometry
Dav	Average diffusion coefficient obtained from light beating spectroscopy for a polydisperse polymer, ${\rm cm}^2/{\rm sec}$
Davg	Average diffusion coefficient obtained from interferometry, cm ² /sec

D _i	Diffusion coefficients for the individual
	species of a polydisperse polymer, cm ² /sec
D(M _W)	Diffusion coefficient of the weight average species obtained from light beating spectroscopy, cm ² /sec
E(t)	Time dependent electric field associated with
	the spectrum of scattered light
f, f ₁₂	Friction coefficients
f _o , (f ₁₂) _o	Values of f and f_{12} , respectively at limit of zero polymer concentration
f ₁ , f ₂	Mole fraction of monomers 1 and 2, in monomer mixture
g(r)	Pair correlation function
$g^{(1)}(\tau), g^{(2)}(\tau)$	Correlation functions of scattered light and photocurrent, respectively
ΔG_{m}	Change in free energy of mixing
G(r)	Distribution function, for a polydisperse polymer
h	Schulz distribution parameter defined in eq. 5-25
h _o (z̄)	Function defined in eq. 3-17
i(t)	Output current of photomultiplier tube
[1]	Concentration of initiator, mole/cm ³
I	Time average intensity of the scattered light
k	Boltzman constant
k _o	Wave vector for incident light
^k d	Parameter that describes the concentration dependence of the diffusion coefficient, defined in eq. 3-10, cm ³ /g
k _e	Wave vector for scattered light

k _s	Friction constant defined in eq. 3-11A
k ₁₁ , k ₁₂ , k ₂₁ , k ₂₂	Copolymerization propagation constants for a radical of the type indicated by the first subscript with a monomer indicated by the second
k _{de}	Reaction rate constant for initiator decomposition
k _{t11} , k _{t22} , k _{t12}	Termination rate constants for a radical of the type indicated by the first subscript with the radical of the type indicated by the second subscript
k _{t(12)}	Termination rate constant in diffusion controlled copolymerization
k(A)	Integral defined in eq. 3-21
k(A*)	Integral defined in eq. 3-24
K	Constant in eq. 5-47
K	Scattering vector
K _f	Constant defined in eq. 3-4
K _v	Constant defined in eq. 3-8
L	Effective bond length
m	Ratio of molar volumes of polymer and solvent
M, M ₂	Characteristic molecular weight of the polymer
M ₁ , M ₂ , [M ₁], [M ₂]	Monomers 1 and 2, respectively, and their compositions
M ₁ , M ₂	Chain radicals of type 1 and 2, respectively
M _n , M _w , M _u , M _z	Number, weight, viscosity, and the Z-average molecular weights of the polymer, respectively
M _s	Molecular weight of the segment
n	Number of effective bonds
n	Refractive index

Δn	Total change in refractive index in the diffusion cell
n _i	Moles of component i
N _O	Avogadro's number
Р	Universal constant defined in eq. 3-5
P(w)	Power spectrum of scattered light
r	Separation at infinite dilution
r ₁ , r ₂	Monomer reactivity ratios in copolymerization
R	Differential refractive index increment
R	Gas constant
R _a	Radius of spherical molecule
R _i , R _p	Rates of initiation and propagation
$< R^2 > 1/2$ $< R_0^2 > 1/2$	Root mean square end-to-end distance
$< R_0^2 > 1/2$	Value of $\langle R^2 \rangle^{1/2}$ at the theta condition
t	Time, sec
Т	Absolute temperature
u ₁ , u ₂	Velocity of solvent and polymer
^v e	Volume of hydrodynamic sphere
v _f	Average velocity of untrapped solvent
v _p	Specific volume of polymer
v _s	Molar volume of solvent
v _s	Average velocity of spherical polymer cloud
νη	Partial specific volume of solvent
v ₁₀	Value of V_1 at infinite dilution of polymer
w _o	Frequency of incident light
w ₁ , w ₂	Frequencies of components 1 and 2, respectively

^{∆w} 1/2	Half width of the light beating spectrum
x	Distance, cm
X	Measure of hydrodynamic interactions between polymer and solvent
X _n	Number average degree of polymerization
Z	Excluded volume parameter
ž	Parameter related to z, defined in eq. 3-13
α	Linear expansion factor
α	Exponent in eq. 5-47
β	Binary cluster integral
δε	Fluctuations in dielectric constant
δc	Fluctuations in concentration
ε	Excess dielectric constant
ζ	Translational friction coefficient
ξ	Friction coefficient
π	Osmotic pressure
ηο	Viscosity of solvent
[n]	Intrinsic viscosity
θ	Scattering angle
λ ₁ , λ ₂	Parameters in eq. 4-10
λ_0 , λ_s	Wave length of incident and scattered light, respectively
ф	Universal constant defined by eq. 3-5
Φi	Volume fraction of component i
φk	Parameter in eq. 4-10
$\Phi_{\mathbf{v}}$	Volume fraction of polymeric species
χ	Flory's polymer-solvent interaction parameter

APPENDICES

APPENDIX A

SAMPLE CALCULATION

Experimental run number: R18

Date: May 16, 1977

Solution B (for lower level of diffusion cell)

2.2 grams of styrene-acrylonitrile copolymer SAN-l
in 100 cm³ of methyl ethyl ketone

Solution A (for upper level of diffusion cell) $60~{\rm cm}^3$ of solution B + 15 cm 3 of pure methyl ethyl ketone

Photographic plate:

Exposure Nu	mber Time,	Seconds
1		0
2		300
3		600
4	1	200
5	1	800
6	2	400
7	2	700
8	3	000
9	3	300
10	3	600

Total fringes, J = 43

	_	
	đ	ļ
	٤	5
	Ξ	
	۲	?
	č	Ź
	>	(
ı	•	J

t = 0 seconds

(For definition of measurements see Figure 5-17.)

$[(x_0' + x_k') - (x_0' - x_j')]$, cm	0.2227 0.2133 0.2105 0.2132 0.2203	t = 600 seconds	0.2377 0.2293 0.2245 0.2267 0.2357	t = 1200 seconds	0.2514 0.2424 0.2381 0.2415 0.2506	t = 1800 seconds	0.2652 0.2612 0.2509 0.2544 0.2651
$(x_0' + x_k')$, cm	1.5923 1.6128 1.6351 1.6596 1.6889		1.5925 1.6147 1.6378 1.6642 1.6952		1.5952 1.6184 1.6430 1.6723 1.7052		1.5986 1.6289 1.6492 1.6800
*	28 32 34 36		28 32 34 36 36		33 33 34 36 36		28 30 34 34
$(x_0' - x_j')$, cm	1.3696 1.3995 1.4246 1.4464	Exposure 3	1.3548 1.3854 1.4133 1.4375	Exposure 4	1.3438 1.3760 1.4049 1.4308 1.4546	Exposure 5	1.3334 1.3677 1.3983 1.4256 1.4502
.c.	7 11 15		7 9 11 15		7 11 15		7 9 11 13

				1 + B	1.0311 1.0661 1.0774 1.0661
t = 2400 seconds	0.2771 0.2692 0.2646 0.2670 0.2770	t = 2700 seconds	0.2847 0.2776 0.2737 0.2748 0.2849	$\frac{B}{erf^{-1}} \frac{2 k - J}{J}$	0.2747 0.3661 0.4641 0.5719 0.6951
	.6011 .6270 .6546 .6852 .7217		.6011 .6274 .6578 .6890 .7262	2 k - J	0.30233 0.39535 0.48837 0.58139 0.67442
	99997		9.0.0.0	~	28 32 34 36 36
e 6	28 30 34 36	e 7	30 34 34 36	A erf ⁻¹ <u>ا - 2 غ</u>	0.6951 0.5719 0.4641 0.3661
Exposure	1.3240 1.3578 1.3900 1.4182 1.4447	Exposure 7	1.3164 1.3498 1.3841 1.4142 1.4412	J -2 j	0.67442 0.58139 0.48837 0.39535 0.30233
	7 11 13		7 9 11 13	·D	7 11 13

	$\begin{pmatrix} x_k + x_j \\ A + B \end{pmatrix}$, cm	0.24510 0.24445 0.24186 0.24168 0.24304 0.24323		0.27346 0.27846 0.27031 0.27122 0.27336		0.29356 0.29595 0.29487 0.29296 0.29377 0.29422
Exposure 3	$(x_k + x_j)$, cm	0.2377 0.2293 0.2245 0.2267 0.2357 Average	Exposure 5	0.2652 0.2612 0.2509 0.2544 0.2651 Average	Exposure 7	0.2847 0.2776 0.2737 0.2748 0.2849 Average
Exposure 1	$(x_k + x_j)$ (A + B), cm	0.22963 0.22739 0.22678 0.22729 0.22765	Exposure 4	0.25923 0.25842 0.25652 0.25746 0.2580	Exposure 6	0.28573 0.28699 0.28507 0.28465 0.28563
	$(x_k' + x_j')$, cm	0.2227 0.2133 0.2105 0.2132 0.2203 Average		0.2514 0.2424 0.2381 0.2415 0.2506 Average		0.2771 0.2692 0.2646 0.2670 0.2770 Average

Exposure	$\frac{(x_k + x_j)^2}{(A + B)^2}$, cm ²
1	0.051826
3	0.059161
4	0.066567
5	0.074726
6	0.081575
7	0.086568

Slope of the plot of
$$\frac{(x_j' + x_k')^2}{(A + B)^2}$$

versus time, t is $1.2745 \times 10^{-5} \text{cm}^2/\text{sec.}$ (See Figure A-1 for plot.)

$$D_{avg} = \frac{Slope}{4M^2} = \frac{1.2745 \times 10^{-5}}{14.884}$$
$$= 8.56 \times 10^{-7} \text{ cm}^2/\text{sec}$$

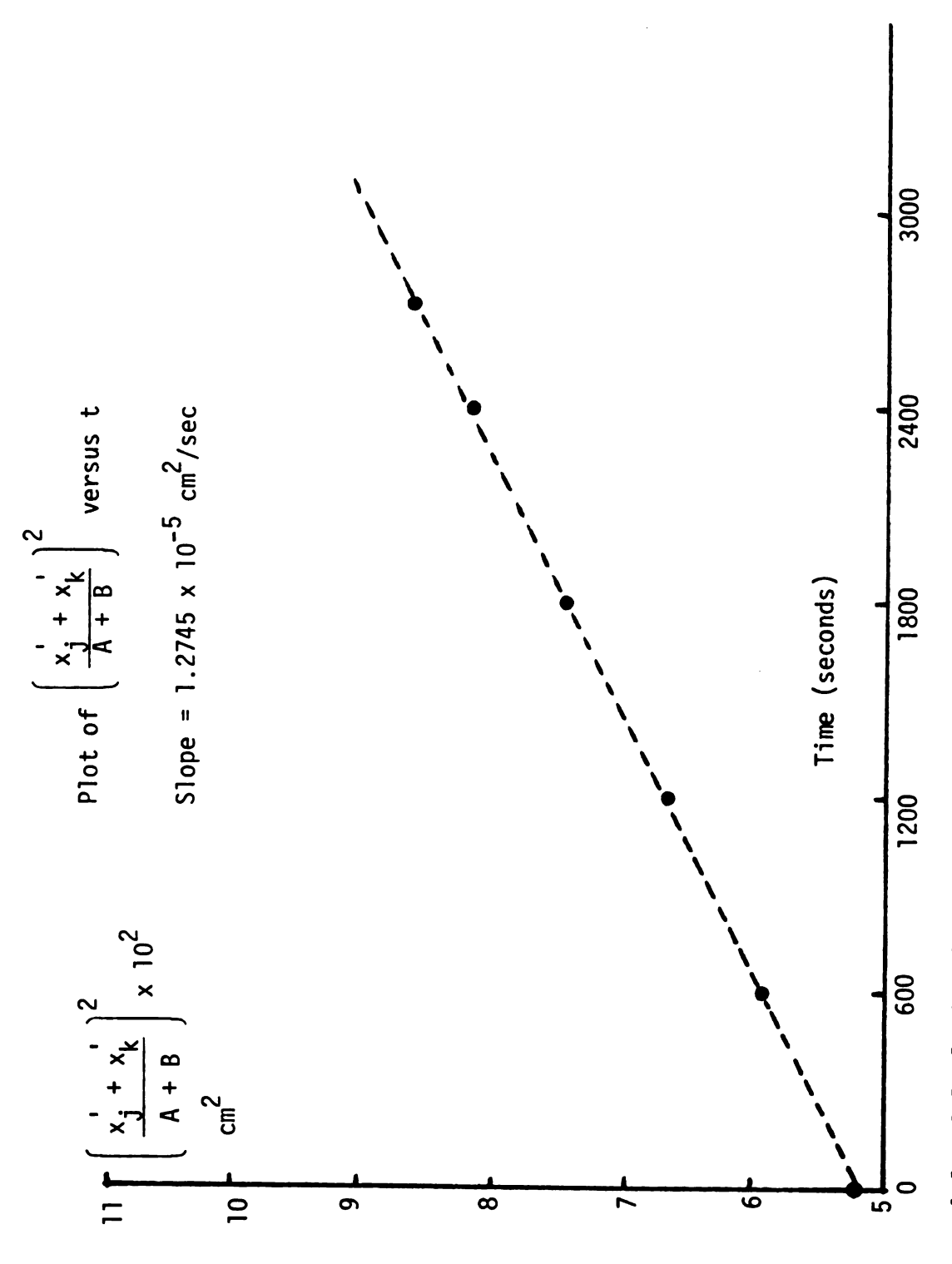


Figure A-1.--Calculation for experimental run R18.

APPENDIX B

MARK-HOUWINK CONSTANTS

The Mark-Houwink relation is

 $[\eta] = K M^a$

Where $[\eta]$ is the intrinsic viscosity, M is the molecular weight of the polymer and K and a are Mark-Houwink constants.

Polymer	Solvent	K, cm ³ /gram	a	Reference
PS	Benzene	11.3 x 10 ⁻³	0.73	AB-1
PS	MEK	39.0×10^{-3}	0.58	AB-2
PS	Toluene	10.5×10^{-3}	0.73	AB-3
PS	Cyclohexane	84.6×10^{-3}	0.5	AB-4
SAN	DMF	16.2×10^{-3}	0.73	7E-1
SAN	MEK	-	0.68	7E-1
SAN	Benzene	-	0.52	3A-22
PS	Decalin	-	0.50	3A-22

Here PS - stands for polystyrene; SAN - for azeotropic styrene-acrylonitrile copolymer; DMF - for dimethyl formamide; and MEK - for methyl ethyl ketone

APPENDIX D

LIGHT BEATING DATA

Polymer	Solvent	Concentration of Polymer gms/100 cm ³	D x 10 ⁷ cm ² /sec	
PS-1	Decalin	2.003 1.001 0.5001 0.1012	1.312 1.454 1.551 1.716	
PS-2	Decalin	1.9987 0.9994 0.4997 0.1050	1.357 1.251 1.209 1.171	
PS-2	Benzene	1.9959 0.9979 0.4989 0.0983	2.714 2.288 2.117 1.955	
PS-1	Benzene	1.9995 0.9975 0.0994 0.0497	3.087 3.297 3.467 3.51	
SAN-1	Dimethyl formamide	1.7044 0.8522 0.4261 0.1031	1.857 1.622 1.495 1.348	
SAN-1	Methyl ethyl ketone	1.7771 0.8886 0.4443 0.1016 0.0508	2.575 2.485 2.447 2.394 2.401	
SAN-1	Benzene	1.9996 0.9998 0.4999 0.1003 0.0502	1.748 1.975 2.138 2.336 2.354	
SAN-2	Dimethyl formamide	1.6031 0.8016 0.4008 0.1063 0.0106	1.774 1.589 1.344 1.252 1.173	

Polymer	Solvent	Concentration of Polymer gms/100 cm ³	D x 10 ⁷ cm ² /sec	
SAN-2	Methyl ethyl ketone	1.6664 0.8332 0.4166 0.1050	2.843 2.632 2.494 2.292	
SAN-2	Benzene	2.0106 1.005 0.0503 0.1072 0.0536	2.016 2.037 2.028 2.115 2.051	
SAN-3	Dimethyl formamide	1.999 0.9995 0.4998 0.4998 0.1074 0.0537	1.476 1.107 1.007 1.007 0.776 0.832	
SAN-3	Methyl ethyl ketone	1.0015 0.5008 0.1067 0.0107	1.994 1.921 1.845 1.693	
SAN-3	Benzene	2.0028 1.0014 0.1005 0.0101	1.545 1.429 1.314 1.301	

APPENDIX E

DATA FROM INTERFEROMETRY

Polymer	Solvent	Concentration of Polymer in gms/100 cm ³	D x 10 ⁷ cm ² /sec	
PS-3 Benzene		0.063 0.1265 0.406 0.701 1.054	5.877 6.528 7.88 7.56 9.441	
PS-4	Benzene	0.0595 0.1192 0.411 0.694 1.0517	1.854 2.546 3.152 4.036 3.818	
PS-5	Benzene	0.065 0.1318 0.405 1.0663	3.869 4.489 5.691 5.558	
PS-6	Benzene	0.0891 0.1782 0.6414	2.972 3.362 4.443	
PS-2	Benzene	0.2113 0.528 0.702 1.001 2.007 5.00 9.93	3.127 3.531 4.126 4.441 5.375 9.503 12.886	
SAN-1	Dimethyl formamide	0.6458 1.09 1.96 5.01	4.075 4.524 5.149 7.489	
SAN-1	Methyl ethyl ketone	1.067 1.98 4.86	8.467 8.561 11.981	
SAN-2	Dimethyl formamide	1.111 1.98 4.85	4.704 5.083 6.353	

Polymer	Solvent	Concentration of Polymer in gms/100 cm ³	D x 10 ⁷ cm ² /sec 6.087 7.704 10.340	
SAN-2	Methyl ethyl ketone	1.04 1.964 4.987		
SAN-3	Dimethyl formamide	1.063 1.989	3.619 4.151	
SAN-3	Methyl ethyl ketone	1.085 1.98	4.831 6.945	

APPENDIX G

CARDS USED IN COMPUTER INTERFACING

I/O PATCH CARD:

This card serves as an input output line from the computer interface buffer box to the computer interface ADD. This is a 32 pin patch card. The card top diagram is shown in Figure AI-1. Pin numbers 1 through 6 are used for device address. In an I/O instruction, the middle six bits of the instruction word are used to identify the device which is to provide or accept data. The pins 1 through 6 give out signals during an I/O instruction corresponding to the middle six bits of the instruction word. These signals are decided by the octal decoder card. Pins 7 to 12 are the IOP pulses. They are the pulses that are available from the computer during an I/O Pins 13 to 24 are the lines instruction. that are connected to the accumulator whenever the skip (SKP) pin (pins 26 or 27) goes low or is grounded momentarily. The data that are

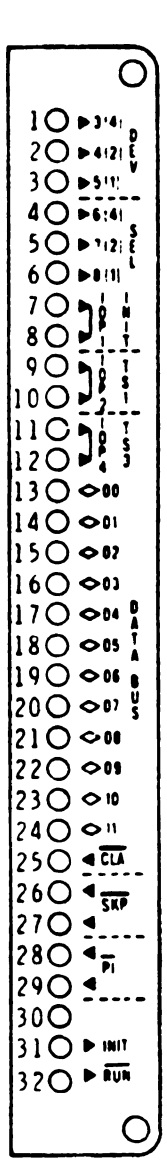


Figure AI-1

available to the pins 13 to 24 will be handed to the computer whenever the SKP line is grounded momentarily. The other pins are not used in this work.

OCTAL DECODER CARD:

The card provides a system for decoding a six bit binary coded input into a two digit octal output from 00 to 77 in octal number base. The outputs of the two independent binary to octal converter circuits can be combined with the two NOR gates included to provide a decoded signal for any given two digit octal number. The card top diagram is shown in Figure AI-2. Pins 1 through 6 are for device address. These six pins receive signals from the pins 1 through 6 on the I/O patch card. During an I/O instruction the computer sends signals to these six pins in binary form corresponding to the middle six bits of the instruction word. Pins 8 through 14 are one octal decoder designated 8¹ and pins 15 to 22 are the other decoder designated 8° , for the two octal digits in the device address number. Pins 24 to 28 are the two NOR gates.

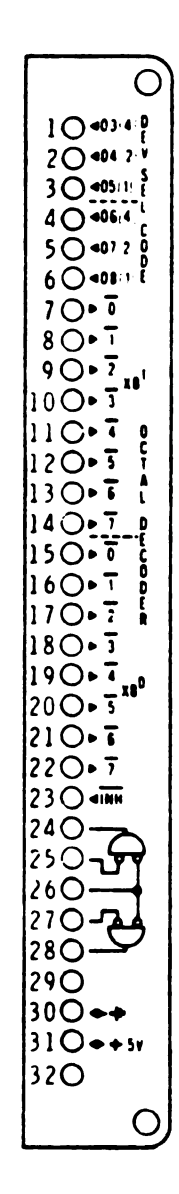


Figure AI-2

As an example say the middle six bits of the instruction word are 45 octal. So when the computer encounters the I/O instruction, it sends binary signals to the I/O patch card pins 1 through 6. If these are connected to pins 1 through 6 of the octal decoder card, then the signals are in the octal decoder. If pins 4×8^{1} and

 5×8^{0} are connected to pins 25 and 26, then pin 24 would go HI when the I/O instruction is executed, the rest of the time it is LO.

GATED DRIVER CARD:

It is necessary that each device output signal be connected to the accumulator 0 - 11 lines only when the data are to be transferred from that device. For this purpose, external data source registers are connected to the accumulator 0 - 11 lines through gates which have outputs that are active only at the appropriate times. The appropriate time is when the device is addressed and an IOP pulse is generated by the execution of an I/O instruction. The card top diagram of the gated driver card is shown in Figure AI-3. Pins 1 - 12 are data inputs and pins 13 - 24 are data outputs from the gated driver. Pins 27 and 28 are called strobe (STR) and select (SEL) signals. These signals control data transfer between the inputs and outputs of the gated driver card. When both the STR and SEL signals are HI, the

When both the STR and SEL signals are HI, the Figure AI-3 signal levels at the inputs determine the signals at the output. When either SEL or STR are low, the data inputs are disconnected from the data outputs.

DUAL FLAG CARD:

The synchronization of the appearance of the data transfer instruction in the program operation with the external devices readiness for that transfer is accomplished with "skips" and "flags." The flag is a circuit that provides a signal which indicates that the I/O device is ready to receive or transfer data. The skip is an externally generated skip instruction that allows a branch in the program depending upon the state of readiness of the external device. The card top diagram of the dual flag is shown in Figure AI-4. The dual flag card consists of two flags. Pins 1-14 are for flag 1 and 15 - 28 are for flag 2. Each flag circuit is usually a flipflop which is set by the falling edge of the ready signal. Each flag also has clear pins, whereby the flag can be cleared. The pins for clearing flag 1 are 10 to 14 and for flag 2 are 24 to 28.

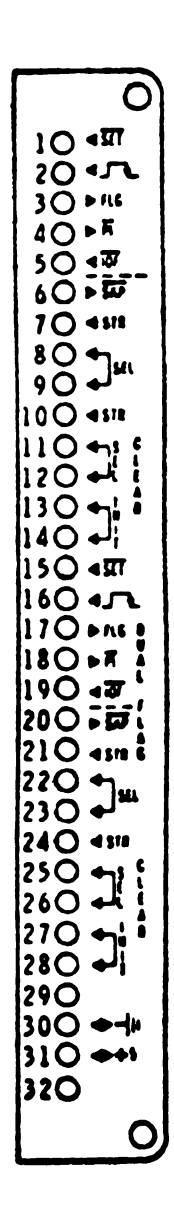


Figure AI-4

As an example suppose we want the computer to know when a particular device 45 is ready to transmit data. We take the signal that indicates the readiness of the device 45 into pin 2. A 6451 instruction will test the state of the flag. A device select of 45 is connected to pin 8 or 9, and the IOP 1 is connected to pin 7.

When the computer encounters the instruction 6451, it gives out an IOP 1 pulse and a device select pulse for 45 through an octal decoder card. At this time if the readiness of the device signal is also HI, then the SKP line (pin 6) will provide a momentary LO signal (ground). If this SKP line is connected to the SKP on the I/O patch card, then the next instruction in the program is skipped. By using a flag card, we can design our software such that the computer loops around checking to see if the device is ready to transmit data; when it finds it is ready it goes out of the loop and reads the data.

Once the flag is set it must be cleared. Flag 1 is cleared by HI signals at pins 10 and 11 or 12, and flag 2 by HI signals at 24 and 25 or 26. When the computer is first turned on, it is desirable to have all the device flags cleared. An initialize pulse is generated (called INIT) when the computer is turned on or when start is pushed. The INIT signal from the I/O patch card is usually wired to pins 13 or 14 for flag 1 and to pins 27 or 28 on flag 2 for clearing the flags.

NAND GATE CARD:

A card top diagram of the NAND gate card is shown in Figure AI-5. One of the NAND gate integrated circuit is a quadruple two input gate, while the other is a dual four input NAND gate. Each of the six gates can be used independently to perform NAND gate functions. The NAND gate is a negative or inverted output AND gate. As such, the NAND gate output is LO only when all inputs are HI. An unused input of a NAND gate acts like a HI input and has no effect on the gate function. If only one input is used the NAND gate output is always the opposite in logic level of the input. Thus a single input NAND gate is a logic level inverter.



Figure AI-5

APPENDIX H

PROGRAM FOR DATA TRANSFER

S		OPDEF	DCAI	3400	/Defining mnemonic code for DCAI
		COMMON	IDATA		
		DIMENSION	IDATA(400)	
S		CLA CLL			/Clear the accumulator and link
S		6214			/Read data field
S		TAD	6201		/Two's complement add 6201 (OCTAL) with contents of accumulator
S		DCA	DCFI		/Deposit the contents of accumulator at DCFI and clear the accumulator
S		6452			/Clear the sweepgate flag
S	В,	6441			/Is the sweepgate HI
S		JMP	В		/No, check it again
S		6452			/Clear the sweepgate flag
S		CLA			/Clear accumulator
S		TAD	(200)		/Two's complement add literal 200 with contents of accumulator
S		DCA	POINT		/Deposit the contents of accumulator at point and clear accumulator
S		6444			/Clear the circulation pulse flag
S	Α,	6451			/Is the circulation pulse HI
S		JMP	Α		/No, check it again
S		6442			/Read data and clear circulation pulse flag
S		6211			/Change to data field l
S		DCAI	POINT		/Deposit the contents of accumulator at point and clear accumulator
S		ISZ	POINT		/Increment point
S		ISZ	COUNT		/Increment count and skip next instruction if count is zero
S		JMP	Α		/Go to A
S	CDFI,	0			/Go to original data field
S		JMP	D		/Go to D
S	COUNT,		-620		/Count initially is 620 (OCTAL) or 400 digital
S	POINT,		0		/Point initially is zero
S	D,	NOP			/No operation

- READ (1, 5) COMNT, SNOIC, THETA
- 5 FORMAT (8H COMNT = ,A6/8HSNOIC = ,F10.8/ 8H THETA = ,F4.1)
 READ (1, 6) FILE
- 6 FORMAT (7H FILE = ,A6)
 CALL OOPEN ('FLP2', FILE)
 WRITE (4, 7) COMNT, SNOIC, THETA
- 7 FORMAT (5X, A6, 5X, F10.8, FX, F4.1) WRITE (4, 8) (IDATA(I), I = 1,400)
- 8 FORMAT (1415) CALL OCLOSE END

APPENDIX J

DERIVATION FOR FUNCTION I (m,n)

Benbast and Bloomfield showed (5A-33) that the I function was

$$I(m,n) = \int_{0}^{\infty} \int_{0}^{\infty} \frac{u^{m}v^{m} e^{-(u+v)}}{(u+v)^{n}} dudv$$
 (J-1)

related to Beta function and are defined in terms of the Gamma function as

$$I(m,n) = \frac{\sqrt{\pi}}{2^{m+1}} \frac{\Gamma(m+1) \Gamma(2m+n+2)}{\Gamma(m+3/2)}$$
 (J-2)

where $\Gamma(x)$ is a Gamma function of x.

They performed numerical calculations from equation J-1 for various values of m and n and tabulated the results. Their results do not correspond to the values obtained from J-2 for the same values of m and n. Therefore the relation between J-1 and J-2 was examined here.

Let
$$u = r \cos^2 \phi$$
, $v = r \sin^2 \phi$

 $dudv = 2 r \sin \phi \cos \phi dr d\phi$

$$\therefore I(m,n)=2\int_{C}^{\pi/2}\int_{C}^{\infty}\frac{(r\cos^2\phi)^m(r\sin^2\phi)^m}{r^n}e^{-r}r\sin\phi\cos\phi\,drd\phi$$

$$I(m,n) = 2 \int_{0}^{\pi/2} (\cos^{2}\phi)^{m} (\sin^{2}\phi)^{m} \sin \phi \cos \phi d \phi \int_{0}^{\infty} r^{2m-n+1} e^{-r} dr$$
(J-3)

The second integral in J-3 is a Gamma function of (2m - n + 1), and the first integral can be related to the Beta function as follows.

The Beta function is defined as (AJ-1)

$$B(m, n) = \int_{0}^{1} t^{m-1} (1-t)^{n-1} dt$$

Let

$$t = \sin^2 \phi$$
, $1-t=\cos^2 \phi$, $dt = 2 \sin \phi \cos \phi d\phi$

...
$$B(m, n) = 2 \int_{0}^{\pi/2} (\sin^2 \phi)^{m-1} (\cos^2 \phi)^{n-1} \sin \phi \cos \phi d \phi$$

...B(m+1,m+1) =
$$2\int_{0}^{\pi/2} (\sin^2 \phi)^m (\cos^2 \phi)^m \sin \phi \cos \phi d \phi$$
 (J-4)

Comparing J-3 and J-4 we obtain

$$I(m, n) = B(m+1, m+1) \Gamma(2m-n+2)$$
 (J-5)

The relation between Beta and Gamma functions is (AJ-1)

B(m+1, m+1) =
$$\frac{\Gamma(m+1) \Gamma(m+1)}{\Gamma(2m+2)}$$

Using the above relation and J-5 it is found

$$I(m, n) = \frac{\Gamma(m+1) \Gamma(m+1) \Gamma(2m-n+2)}{\Gamma(2m+2)}$$

This relation gives identical values corresponding to m and n in the tables of Benbast and Bloomfield. This relation for I(m, n) is therefore the correct one and was used in this work.

BIBLIOGRAPHY

- 1A-1 Secor, Robert M. A. I. Ch. E. Journal 11 (1965):452.
- 2A-1 Flory, P. J. <u>Principles of Polymer Chemistry</u>. New York: Cornell University Press, 1953, ch. XIII.
- 2A-2 Morawetz, H. <u>Macromolecules in Solution</u>. New York: John Wiley & Sons, 1966, (a) p. 276.
- 2E-1 Bird, R. B.; Stewart, W. E.; and Lightfoot, E. L. <u>Transport</u> Phenomenon. New York: John Wiley & Sons, 1960.
- 3A-1 Einstein, A. Ann Physik 17 (1905):549.
- 3A-2 Kirkwood, J. G., and Riseman, J. J. Chem. Phys. 16 (1948):565.
- 3A-3 Mandelkern, L., and Flory, Paul J. <u>J. Chem. Phys.</u> 20 (1952): 212.
- 3A-4 Johnston, H. K., and Rudin, A. Polymer Letters 9 (1971):55.
- 3A-5 Yamakawa, H. Modern Theory of Polymer Solutions. New York: Harper & Row, 1971, (a) ch. 3; (b) ch. 4; (c) ch. 5; (d) ch. 6; (e) ch. 7.
- 3A-6 Vrentas, J. S., and Duda, J. L. <u>J. App. Poly. Sci.</u> 20 (1976): 1125.
- 3A-7 King, T. A.; Knox, A.; Lee, W. I.; and Adam, J. D. G. Polymer 14 (1973):151.
- 3A-8 Cowie, J. M. G., and Cussler, E. L., <u>J. Chem. Phys.</u> 46 (1967): 4886.
- 3A-9 Brandrup, J., and Immergut, E. H., eds. <u>Polymer Handbook</u>, 2nd ed. New York: John Wiley & Sons, 1975.
- 3A-10 Jacob, M.; Varoqui, R.; Kenine, S.; and Danue, M. <u>J. Chem.</u> <u>Phys.</u> 59 (1962):865.
- 3A-11 Matsuda, H.; Aonuma, H.; and Kuroiwa, S. <u>J. Appl Polymer Sci.</u> 14 (1970):335.
- 3A-12 _____. Rept. Prog. in Polymer Sci. (Japan) 11 (1968):25.
- 3A-13 Meyerhoff, G., Makromol Chem. 37 (1960):97.

- 3A-14 King, T. A.; Knox, A.; and McAdam, J. D. G. <u>Polymer</u> 14 (1973):293.
- 3A-15 Ford, N. C.; Karasaz, F. E.; Owen, J. E. M. <u>Disc Faraday Soc.</u> 49 (1970):228.
- 3A-16 Nachtigall, and Meyerhoff, G. Phys. Chem. 30 (1961):35.
- 3A-17 Elias, H. G. Macromol Chem. 50 (1961):1.
- 3A-18 Auer, R. L., and Gardner, C. S. J. Chem. Phys. 23 (1955):1546.
- 3A-19 Ptitsyn, O. B., and Eizner, Yu. E. Soviet Phys. Tech. Phys. 4 (1960):1020.
- 3A-20 Zimm, B. H. <u>J. Chem. Phys.</u> 24 (1956):269.
- 3A-21 Einstein, A. <u>Theory of Brownian Motion</u>. New York: Dover, 1956.
- 3A-22 VanKrevelen, D. W. <u>Properties of Polymers, Correlations with Chemical Structure</u>. New York: Elsevier Publishing Co., 1972.
- 3B-1 Tsvetkov, V. N., and Klenin, S. I. <u>J. Polymer Sci.</u> 30 (1958): 187.
- 3B-2 Duda, J. L., and Vrentas, J. S. <u>J. App. Polymer Sci.</u> 20 (1976): 2569.
- 3B-3 _____. <u>J. Polymer Sci.; Polymer Phys. ed.</u> 14 (1976):101.
- 3B-4 Pyun, C. W., and Fixman, M. <u>J. Chem. Phys.</u> 41 (1964):937.
- 3B-5 Refer to 3A-5.
- 3B-6 Yamakawa, H., and Tanaka, G. J. Chem. Phys. 47 (1967):3991.
- 3B-7 Kurata, M.; Fukatsu, M.; Sotobayashi, H.; and Yamakawa, H. J. Chem. Phys. 41 (1964):139.
- 3B-8 Yamakawa, H. <u>J. Chem. Phys.</u> 48 (1968):2103.
- 3B-9 Paul, D. R.; Mavichak, V.; and Kemp, D. R. <u>J. App. Polymer Sci.</u> 15 (1971):1553.
- 3B-10 McDonnell, M. E., and Jamieson, A. M. <u>J. Macromol Sci. Phys.</u> B13 (1977):67.
- 3B-11 Mandema, W., and Zeldenrust, H. <u>Polymer</u> 8 (1977):835.

- 3B-12 Berry, G. C., and Casassa, E. F. Macromol Rev. 4 (1970):1.
- 3C-1 Hayes, M. J., and Park, G. S. <u>Trans Faraday Soc.</u> 52 (1956): 949.
- 3C-2 Chalykh, A. Ye., and Vasenin, R. M. Polymer Science U.S.S.R. 8 (1966):2107.
- 4A-1 Odian, George. <u>Principles of Polymerization</u>. New York: McGraw-Hill, 1970, ch. 6, (a) pp. 20-21.
- 4A-2 Atherton, J. N., and North, A. M. <u>Trans Farad Soc.</u> 58 (1962): 2049.
- 4A-3 Blanks, Robert F., and Shah, B. N. <u>J. Polymer Sci., Polymer Chem. ed. 14 (1976):2589.</u>
- 4A-4 Shah, B. N. Ph.D. thesis, Michigan State University, 1975.
- 4C-1 Shimura, Y.; Mita, I.; and Kambe, H. <u>J. Polymer Sci.</u> B,2 (1964):403.
- 4C-2 Mino, G. <u>J. Polymer Sci.</u> 22 (1956):369.
- 4C-3 Ljerka, Lovric. <u>J. Polymer Sci.</u> A2,7 (1969):1357.
- 4C-4 Private communication from Dr. J. B. Kinsinger, Chemistry Dept., Michigan State University, East Lansing.
- 5A-3 Vrancken, E. Ph. D. thesis, University of Akron, 1975.
- 5A-4 Gyesezly, S. W. Ph.D. thesis, Michigan State University, 1974.
- 5A-5 Gross, E. <u>Nature</u> 126 (1930):201, 400, 603.
- 5A-6 Pecora, R. <u>J. Chem. Phys.</u> 43 (1965):1562.
- 5A-7 _____. <u>J. Chem. Phys.</u> 48 (1968):4126
- 5A-8 _____. <u>J. Chem. Phys.</u> 49 (1968):1032.
- 5A-9 _____. <u>J. Chem. Phys.</u> 49 (1968):1036.
- 5A-10 Pecora, R. and Tagami, Y. J. Chem. Phys. 51 (1969):3293.
- 5A-11 J. Chem. Phys. 51 (1969):3298.
- 5A-12 Pecora, R. Macromolecules 2 (1969):31.
- 5A-13 Forrester, A. T.; Parkins, W. E.; and Gerjuoy, E. <u>Phys. Rev.</u> 72 (1947):728.

- 5A-14 Cummins, H. Z.; Knable, N.; and Yeh, Y. Phys. Rev. Lett. 12 (1964):150.
- 5A-15 Ford, N. C., and Benedek, G. B. <u>Phys. Rev. Lett.</u> 15 (1965): 649.
- 5A-16 Sheperd, I. W. Rep. Prog. Phys. 38 (1975):565.
- 5A-17 Ford, N. C.; Gabler, R.; Karasz, F. E. <u>Adv. in Chem. Ser</u> 125 (1974):25.
- 5A-18 Cummins, H. G., and Swinney, H. L. <u>Progress in Optics</u> 8, ed. Wolf. Amsterdam: North Holland Publishing Co., 1970.
- 5A-19 Chu, B. <u>Laser Light Scattering</u>. New York: Academic Press, 1974.
- 5A-20 Jamieson, A. M., and Maret, A. R. <u>Chem. Soc. Rev.</u> 2 (1973): 325.
- 5A-21 Frederick, J. E., and Reed, T. F. Macromolecules 4 (1971):72.
- 5A-22 Brown, J. C., and Pusey, P. N. J. Chem. Phys. 62 (1975):1136.
- 5A-25 Frederick, J. E.; Reed, T. F.; and Kramer, O. <u>Macromolecules</u> 4 (1971):242.
- 5A-27 Adam, M.; and Delsanti, M. J. de Physique 37 (1976):1045.
- 5A-28 Fujime, Satoru. J. Phy. Soc. Japan 29 (1970):416.
- 5A-29 Stutesman, W. D. M.S. thesis, Michigan State University, 1972.
- 5A-30 Thompson, D. S. Rev. Sci. Instr. 41 (1970):1228.
- 5A-31 _____. <u>J. Chem. Phys.</u> 54 (1971):1411.
- 5A-32 _____. <u>J. Phys. Chem.</u> 75 (1971):789.
- 5A-33 Benbast, J.A., and Bloomfield, V. A. <u>J. Polymer Sci., Polymer Phys. ed.</u> 10 (1972):2475.
- 5A-34 Nelson, T. J. M.S. thesis, Michigan State University, 1974.
- 5A-35 McQuarrie, D. A. <u>Statistical Mechanics</u>. New York: Harper & Row, 1976, ch. 20.
- 5A-36 Gulari, E.; Brown, R. J.; and Pinas, C. J. <u>A. I. Ch. E.</u> Journal 19 (1973):1196.

- 5A-37 Mountain, R. D. Rev. of Modern Physics 38 (1966):205.
- 5A-38 _____. <u>J. Chem. Phys.</u> 50 (1969):1103.
- 5B-1 Weissberger and Rossiter, eds. <u>Physical Methods of Chemistry</u>, Part IV. New York: Wiley Interscience, 1972, ch. 4.
- 5B-2 Paul, D. R.; Mavichak, V.; and Kemp, D. R. <u>J. App. Polymer</u> Sci. 15 (1971):1553.
- 5B-3 Duda, J. L.; Sigelko, W. L.; and Vrentas, J. S. <u>J. Phys. Chem.</u> 73 (1969):141.
- 5B-4 Paul, D. R. I. and E. C. Fundm. 6 (1967):217.
- 5B-5 Secor, R. M. A. I. Ch. E. Journal 11 (1965):452.
- 5B-6 Rehage, G., and Ernst, O. <u>Disc Faraday Soc.</u> 49 (1970):208.
- 5B-7 Zehnder, L. Z. Instrumentenk 11 (1891):275.
- 5B-8 Caldwell, C. S.; Hall, J. R.; and Babb, A. L. <u>Rev. Sci. Instr.</u> 28 (1957):816.
- 5B-9 Bidlack, D. L. Ph.D. thesis, Michigan State University, 1964.
- 5B-11 Shimura, Y. J. Polymer Sci., Part A2 4 (1966):423.
- 5B-12 Sundelof, L. O. Arkiv for Kemi. 25 (1965):1.
- 5B-13 Schulz, G. V. Z. Physik Chem. B43 (1939):25.
- 5B-14 Gosting, L. J., and Morris, M. S. <u>J. Am. Chem. Soc.</u> 71 (1949):1998.
- 5B-15 Akeley, D. F., and Gosting, J. L. <u>J. Am. Chem. Soc.</u> 75 (1953): 5685.
- 5B-16 Creeth, J. M. <u>J. Am. Chem. Soc.</u> 77 (1955):6428.
- 5B-17 Cussler, E. L., and Dunlop, P. J. <u>J. Phys. Chem.</u> 70 (1966): 1880.
- 7B-1 Coleman, M. F., and Fuller, R. E. <u>J. Macromol Sci., Phy. ed.</u> 14 (1976):101.
- 7C-3 Chitrangad. Ph. D. thesis, University of Rochester, 1973.
- 7D-4 Pusey, P. N.; Vaughan, M. J.; and Williams, G. J. <u>J. Chem. Soc. London, Faraday trans.</u> 70 (1974):1696.

- 7D-6 Berry, G. C. J. Chem. Phys. 44 (1966):4540.
- 7E-1 Rami Reddy, G., and Kalpagam, V. <u>J. Polymer Sci., Polymer Phys. ed.</u> 14 (1976):759.
- 7F-1 Noda, I.; Kitano, T.; and Nagasawa, M. J. Polymer Sci., Polymer Phys. ed. 15 (1977):1129.
- AB-1 Bawn, C. E. H.; Freeman, C.; and Kamaliddin, A. <u>Trans. Faraday</u> Soc. 46 (1950):1107.
- AB-2 Outer, P.; Carr, C. I.; and Zimm, B. H. <u>J. Chem. Phys.</u> 18 (1950):830.
- AB-3 Breitenbach, J. W.; Gabler, H.; and Olaj, O. F. Macromol Chem. 81 (1964):32.
- AB-4 Inagaki, H.; Suzuk, H.; Fuiji, M.; and Matsuo, T., <u>J. Phys.</u> Chem. 70 (1966):1718.
- AJ-1 Spiegel, Murray R. <u>Mathematical Handbook</u>. New York: McGraw-Hill, 1968.

